Assessment of Paint Appearance Quality in the Automotive Industry

A thesis submitted for the degree of Doctor of Philosophy

Hai-zhuang Kang (BSc, MSc)

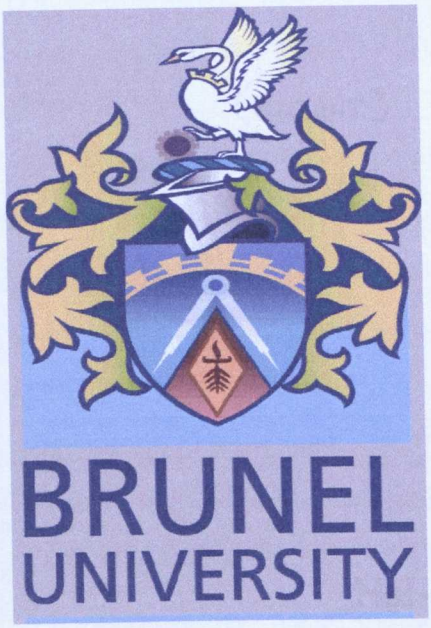

Department of Systems Engineering, Brunel University

May 2000

To my wife and daughter:

Judith Qunhun Nie

Connie Yue Kang

Abstract

In the modern automotive industry, more and more manufacturers recognise that vehicle paint appearance makes an important contribution to customer satisfaction. Attractive appearance has become one of the important factors for customers in making a decision to purchase a car. Objective measurement of the quality of autobody paint appearance, as perceived by the customer, in a repeatable, reproducible, continuous scale manner is an important requirement for improving the paint appearance. It can provide car manufacturers a standard reference to evaluate the quality of the paint appearance.

This thesis mainly deals with the measurement of paint appearance quality in the automotive industry by investigating, identifying and developing measurement methods in this area. First of all, the 'state of the art' in the area of paint appearance measurement was presented, which summarised the concept of appearance, models, attributes and definitions. To further identify the parameters and instruments used in the automotive industry, a round robin test was launched to perform visual assessment and instrument measurements on a set of panels in some European car manufacturers. A summary of the correlation found between measurable parameters and visual assessment provided the basis of the further work. Based on the literature survey and round robin test results, the next work is mainly concentrated on the two most important parameters, 'orange peel' and 'metal texture effect', how to separate and evaluate them. Digital signal processing technique, FFT and Filtering, have been employed to separate them and a set of measures have been provided for evaluation. At the same time, The technique for texture pattern recognition was introduced to evaluate the texture effect when a fine texture comparison was needed. A set of computable textural parameters based on grey-tone spatial-dependence matrices gives good correlation directly corresponding to visual perception.

To resolve the overall appearance modelling problem, two novel and more powerful modelling tools, artificial neural networks and fuzzy logic, are introduced to model the overall appearance. The test results showed that both of them are able to reflect the

correlation between overall appearance and the major parameters measured from a painted surface.

Finally, an integrated measurement system, 'Smart Appearance', was developed using the image processing techniques and the artificial neural network model. The implement results show that this system can measure the major attributes of paint appearance and provide an overall appearance index corresponding to human visual perception. This system is helpful to product quality control on car body paint. It also could be used on the paint production line for dynamic measurement.

Acknowledgements

I am most indebted to my research supervisor, ***Prof. Clive Butler***, Director of the Postgraduate Programmes in Advanced Manufacturing Systems at the Department of System Engineering of Brunel University, for his continuous guidance, support and encouragement. His sincere personal concern and invaluable advice have motivated me throughout the research period. With his help the research was completed on time. I am very grateful to him for taking the pain to read, refine and polish this thesis.

I would also like to express my thanks and appreciation to my second supervisor, ***Dr. Qingping Yang***, Lecturer at the Department of System Engineering of Brunel University, for his help, encouragement, and invaluable advice on this research. His constant concern and encouragement helped me throughout my PhD studies.

The research work is founded by the EU project, BRITE EURAM Project n^0 BE-97-4140 AUTOSURF (Surface Texture Optimisation for Automotive Industry). Our industrial partners provided their instruments, Round Robin Test results, painted steel panels and invaluable experience. Their requirements inspired me to develop an advanced measurement system for paint appearance quality control. Their advice and help made this research work more valuable. Here I would like to express my genuine thanks to: ***Delpine Eyquem, Magali Touze*** (Renault), ***Katrien Meseure, Jan Scheers*** (OCAS), ***Claudoi Prelini*** (IVECO), ***John Davies*** (PPG UK), ***Clive Challinor, Michelle Lewis*** (British Steel), ***Marie Louise*** (VOLVO), ***Stefano Gatti*** (Qualitech Research Co.).

I would also like to thank the other members of the Autosurf Brunel team, ***Franco Sacerdotti, Fabrizio Benati and Alessandro Porrino***. We had a very good work and collaboration environment. I benefited from our talks, discussions or even disputes. Teamwork also made a valuable contribution to the success of the project 'Autosurf'.

Finally, I would like to thank to my wife, ***Qunhun Nie***, and daughter, ***Connie*** for their tolerance, continuous support and understanding.

My PhD study has been supported by the Overseas Research Students Awards Scheme (ORS) founded by the British Council.

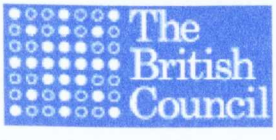

Table of Contents

Chapter 3. Visual Assessment on Paint Appearance

Chapter 4. Round Robin Test and Statistical Analysis

Chapter 5. Evaluation of Orange Peel on Paint Appearance

Chapter 6. Evaluation of Metal Texture Effect on Paint Appearance

Chapter 7. Modelling of Overall Appearance using Artificial Neural Network

Chapter 8. Modelling of Overall Appearance Using Fuzzy Logic

Chapter 1
Introduction

1.1. Research Problem Statement

The appearance (colour, gloss, texture) of an object greatly influences a customer's appreciation of the quality of that object, especially in the automotive industry. Further, as manufacturers want to demonstrate their ability to provide their products with improved appearance properties, as well as exciting new ones, customer expectations for appearance quality increase. To enhance the development and implementation of new products and processes, it is essential that industries have the physical tools to quantify accurately the appearance of their products. Also they require the modelling capabilities to predict the appearance of objects based on paint formulation and manufacturing processes.

To measure appearance, it is first necessary to know what constitutes appearance and its attributes. Appearance is often described as the total quality of what is visually perceived. Colour, texture, lustre, gloss, haze, sparkle, and roughness are examples of appearance attributes. With the human environment increasingly becoming colourful, the language of appearance is becoming abundant as well. New terms are being used to describe paint products, such as dazzle, vivid, glitter, and sparkle. Table 1-1 illustrates a group of words to describe appearance properties. In fact the appearance properties of most manufactured objects depend on the pigments used in paint. The requirements of pigments include optical characteristics, safety, durability, and affordability. Extreme optical characteristics are required. For example, of the billions of chemical compounds, only a few have a refractive index high enough to serve as a white

pigment. Coloured pigments must have a wavelength-specific light absorption. A black pigment must have total light absorption. Safety during manufacture, application, and use is an additional concern. Pigments may be required to withstand the effects of UV radiation, water, oxygen, elevated temperatures, and environmental assaults by acids and alkalis. Cost is also an issue. Pigment prices vary over a wide range.

Table 1-1. Terms Describing Appearance

The Words of Appearance			
sheen	shine	dull	grey
polish	lustre	drab	dark
bright	shimmer	lack-lustre	bleak
light	bright	dingy	leaden
vivid	radiant	sombre	hazy
glamorous	gleam	sooty	muddy
glitter	dazzle	cloudy	dusky
gloss	colourful		
sparkle	brilliant		

Among so many terms used to describe paint appearance, it is necessary to decide which of them are essential properties, which can characterize paint appearance well as perceived by human eye and be measurable with an instrument. This thesis is mainly concerned with appearance measurement.

In the modern automotive industry, more and more manufacturers recognise that the paint appearance of vehicles (Fig. 1-1) makes an important contribution to customer product satisfaction. Attractive appearance has become one of the important factors for customers to make a decision when purchasing a car. So objective measurement of the quality of autobody paint appearance, as perceived by the customer, in a repeatable, reproducible, continuous scale manner is significant for improving the paint

appearance. It can provide car manufacturers a standard reference to evaluate the quality of the paint appearance.

Figure 1-1 Paint Appearance on automotive bodies

The measurement of paint appearance has been studied for many years. Current appearance metrology is almost exclusively based on specular and colorimetric measurements. It is a complex issue for the following reasons:

(1) As the measurement is performed on the painted surface, only non-contact measurement methods can be used.

(2) As the modern automotive coating composes of four or five layers, the interference between each layer and the substrate itself makes the reflected images from these paint surfaces complex from the point of view of human visual perception.

(3) What we measure is expected to correspond to human visual perception. What we measure is what we can see, not what we 'feel' about the surface. It is a visual phenomenon, not a straightforward measurement of a real surface. It is also sensitive to change with the angle of view and the illumination system.

(4) The complex nature of the coating structure results in the need for many parameters to quantify the various appearance characteristics. It is a multiple-

dimension problem to link the measured parameters to the overall appearance. A multiple input, non-linear system is needed to model it.

(5) As the measurement result is expected to be same as human visual perception, this means that the measurement reference must be based on human visual assessment. Such a measurement standard is difficult to obtain and is not stable in some circumstances.

Nowadays there are many parameters being used in the automotive industry to characterize paint appearance. The spectral properties include gloss, haze, DOI (distinctness of image). The spatial properties include orange peel, separated by longwave and shortwave characteristics, tension, etc. The measurement methods vary with different instruments. The existing problems in this area are:

- There is no international standard to specify the parameters and methods to measure paint appearance.
- The existing parameters are not optimised. There is still redundancy.
- Relations between individual parameters and overall appearance are not established.
- Some features of paint appearance are not determined by existing parameters. New parameters need to be introduced.
- A measurement framework needs to be established to guide the daily measurement of paint appearance for automotive painting work.

The need for new or improved measurable parameters, standards, and measurement tools has been recognised by the industry for some time. The improvements in appearance understanding, measurement, and control can provide them with significant

competitive advantage. This study will develop an intelligent measurement system with advanced image processing, artificial neural network and fuzzy logic to advance the science of appearance measurements.

1.2. Research Objective

The objective of this research is:

To investigate, identify and develop measurement methods to measure objectively the quality of the autobody paint finish visual appearance, as perceived by the customer, in a repeatable and reproducible, continuous scale manner and establish a measurement framework to guide the measurement of paint appearance in the automotive industry.

To fulfil our objective the following is required:

- To investigate and identify the existing parameters.
- To investigate and identify the existing measurement methods.
- To optimise the existing parameters and reduce the redundant parameters.
- To develop new parameters to characterise the new features of paint appearance.
- To model the individual parameters and overall appearance.
- To set up the measurement framework.
- To develop a new instrument which integrates new measurement methods to permit the measurements to be made.

1.3. Research Significance

Research into paint appearance measurement is significant for the following reasons:

a) Paint appearance measurement can clarify various aspects of paint quality. Using the new measurement framework the paint appearance can be measured objectively. The paint quality can then be guaranteed.

b) Paint appearance measurement is also the basis of other requirements. In the automotive industry, due to the increasing demands to minimise environmental impact from the painting process and the need to minimise the cost, the paint thickness must be decreased. The paint appearance then becomes more sensitive to substrate surface irregularities. The paint appearance is generally better when the sheet material is smooth, but this introduces upstream problems including poor forming behaviour during panel manufacture and a high sensitivity to surface damage during handling. A certain roughness or surface texture is needed. So optimisation of steel sheet surface properties and the painting procedure to achieve the best paint appearance is required. A reliable paint appearance measurement system provides the basis for such optimisation.

c) In the coating industry, when the paint formula is changed, the painted panels are often assessed by the human eye, which is very time-consuming. With the paint appearance measurement system, which simulates the response achieved with the human eye, the time to produce new products can be reduced.

d). Applying neural networks and fuzzy logic into the paint appearance measurement system makes it appear to have aspects of intelligence like the human. The paint appearance can be increasingly improved to satisfy customers' higher expectations. This can enhance the car manufacturers' competitive ability to win more world market share.

1.4. Knowledge Requirement

The quantification of appearance involves a high degree of connectivity among the many subfields of science and technology. The degree of complexity and the specific disciplines that are required for appearance solutions are illustrated in Figure 1-2. A partial listing of candidate appearance attributes is at the core of the diagram. Associated disciplines and applications are included as the outer shell.

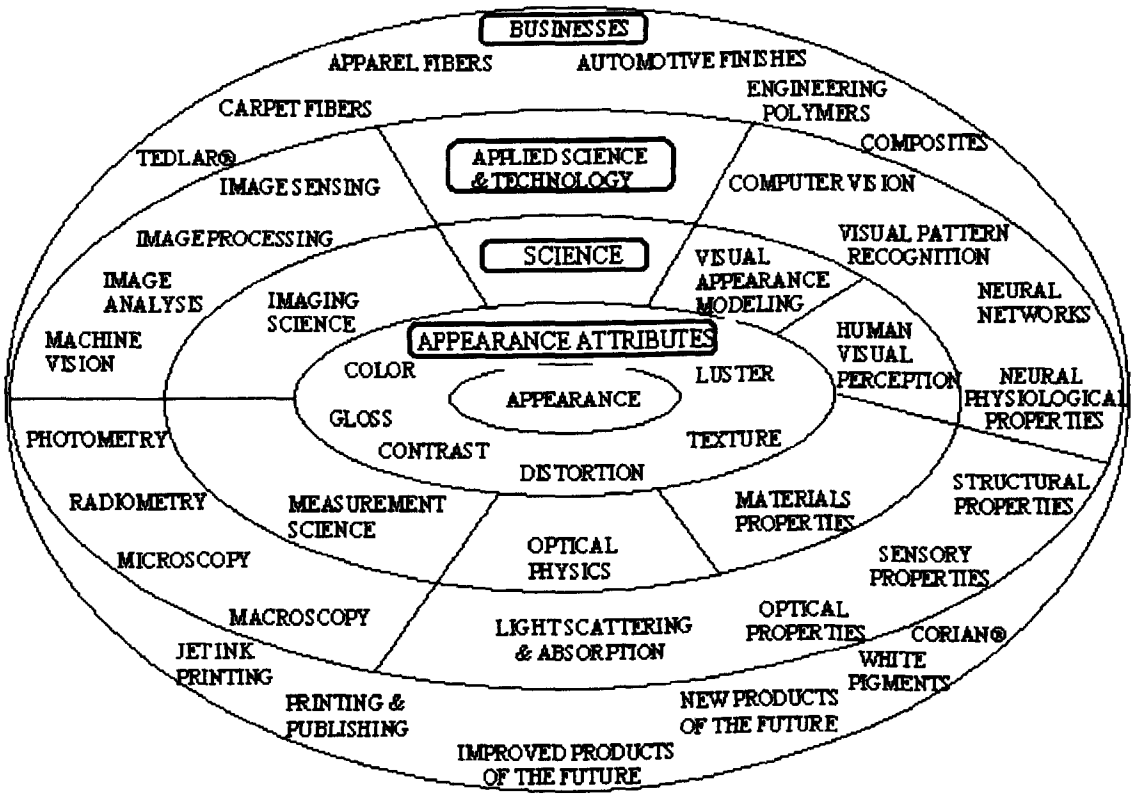

Figure 1-2. Connectivity of disciplines and applications involved in appearance measurements

As complex as paint appearance itself, the paint appearance measurement system is correspondingly a complex system as well. As both optical and spatial characteristics need to be represented, knowledge on the following is required to develop an intelligent measurement system for paint appearance.

- Human visual perception and statistical methods.
- Optical physics
- Image science
- Measurement science
- Digital Signal Processing (DSP) including filter design, FFT and power spectrum analysis.
- Modelling using neural networks and fuzzy logic

1.5. Theme of the Research

The main theme of this thesis is to design and develop an intelligent appearance measurement system for painted appearance especially for use in the automotive industry. This system is based on an image processing system and artificial neural networks.

Figure 1-2 shows the three main aspects involved in this study.

The first aspect is human visual assessment since it must be the reference for any instruments. As human visual assessment is an apparently subjective procedure, to obtain objective results, we need to study the visual assessment process and apply statistical techniques.

The second aspect is the appearance measurement with existing instruments. This part provides the evidence to identify the existing parameters, measurement methods, and problems. It also serves as a reference to compare with our new measurement method.

The third part is the main theme of this study. An image processing system will be set up to measure paint appearance. The main parameters like orange peel, metal texture, gloss, and DOI can be measured with this system. Furthermore, neural networks and fuzzy logic models will be applied to this system. The relationship between individual

parameters and overall appearance can then be established. With the use of intelligent networks, the measurement can be performed more like human beings do.

At the end, an integrated measurement system prototype is expected to be developed to combine all the advantages discovered.

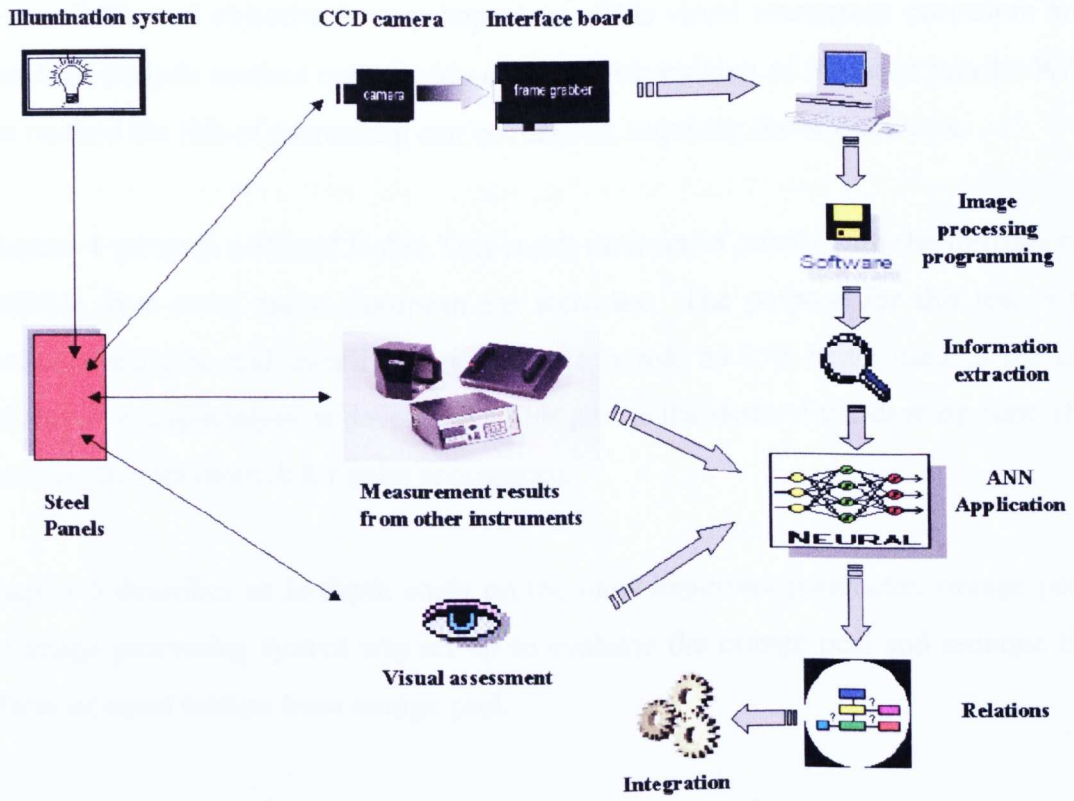

Figure 1-3. Framework for studying appearance measurement

6. Organisation of the Thesis

This thesis is organised in the following manner:

Chapter 2 gives us an overview in the appearance measurement area. First of all the general concept of appearance and the development history are introduced. Then the most frequently used parameters and the measurement principles of some popular

instruments have been reviewed. Finally, the analysis methods to link the individual parameter and overall appearance are presented.

Chapter 3 introduces an effective method for the visual assessment of painted panels. As human visual assessment is a subjective procedure and its results will be the final reference to assess the instrument's performance, making the visual assessment results more reliable and objective is very important. This visual assessment procedure and statistical analysis method can provide more reliable ranking of the paint panels. With this method the risk of misranking can be reduced, requiring fewer observers.

Chapter 4 presents a Round Robin Test result on a set of panels with the instruments available from some major European car factories. The purpose for this test is to further investigate and identify each parameter's role as it is being used in the car industry. A gap-analysis is developed. This part is the basis of the development of a measurement framework for paint appearance.

Chapter 5 describes an in-depth study on the most important parameter, orange peel. An image processing system was set up to evaluate the orange peel and separate the effects of metal texture from orange peel.

Chapter 6 introduces a new parameter, the metal texture effect in the characterisation of paint appearance. Some traditional texture analysis models and methods are employed to evaluate the metal texture effect on paint appearance.

Chapter 7 uses neural networks to model overall appearance. The procedure for how to use neural networks to predict the overall appearance is demonstrated in a step-by-step manner. The neural networks can present well the correlation between overall appearance and the individual parameters used in visual perception. The introduction of neural networks to the paint appearance measurement system makes the measurement system appear more intelligent to deal with variable situations.

Chapter 8 provides another modelling technique, fuzzy logic, as an alternative for paint appearance modelling. With the human understanding and expertise being built into the fuzzy logic model, the measurement system can also present a good overall appearance result corresponding to human visual perception. The comparison between fuzzy logic and neural networks indicates that fuzzy logic can provide us with more details inside the model.

Chapter 9 introduces an integrated measurement system, called 'Smart Appearance'. It consists an image processing system and a built-in neural network, which can provide most used parameters, like orange peel, metal texture effect, gloss contrast and so on, it can also provide an overall appearance index with the trained neural network.

Chapter 10 is a summary of the whole research work which has been done and the main points of the contributions to this area. At the end, the further work has been indicated.

Chapter 2

An Overview of Paint Appearance Measurement in the Automotive Industry

2.1. Introduction

Since Hunter invented the first glossmeter in the 1930's, development in the area of appearance measurement has never stopped. With the improvement of understanding on paint appearance and the rapid growth of new techniques in measurement and the computer area, appearance measurement has become more sophisticated. More measurement methods have been developed to meet the increasing needs for appearance measurement. In this chapter, an overview on paint appearance measurements in the automotive industry will be presented. Firstly, the concept of appearance will be reviewed including the definition of appearance, appearance models, and their attributes. Further, the sub-model which suits autobody appearance can be derived. Then the definitions of some measurable attributes are presented. The current developments in instrument design, including principles, method and measurable parameters are introduced. Finally, two methods for linking the individual parameters and overall appearance are introduced.

2.2. Concept of Appearance

Appearance is a very general concept. Different models could have different attributes. Initially, the definition, model, and attributes, which suit autobody paint appearance, are considered.

The following two definitions of appearance are taken from the ASTM (American Society for Testing and Materials) E284 [ASTM E284 1995]:

[1] The aspect of visual experience by which things are recognised. (1990)

[2] In psychophysical studies, visual perception in which the spectral and geometric aspects of a visual stimulus are integrated with its illuminating and viewing environment. (1993)

The first definition is quite abstract. The second one gives more detail about the appearance, which indicates that the visual perception can be divided into the spectral and geometric aspects and is related to the illuminating and viewing environment. Bearing these two definitions in mind, the appearance models need to be considered. Dr. Deane B. Judd at the National Bureau of Standard (NBS, USA) in 1934 proposed a classification of the optical attributes which combine to identify the appearances of objects and materials. The three principal modes of appearance related to the geometric conditions of illumination and view are illustrated in Fig. 2-1 [Judd 1961].

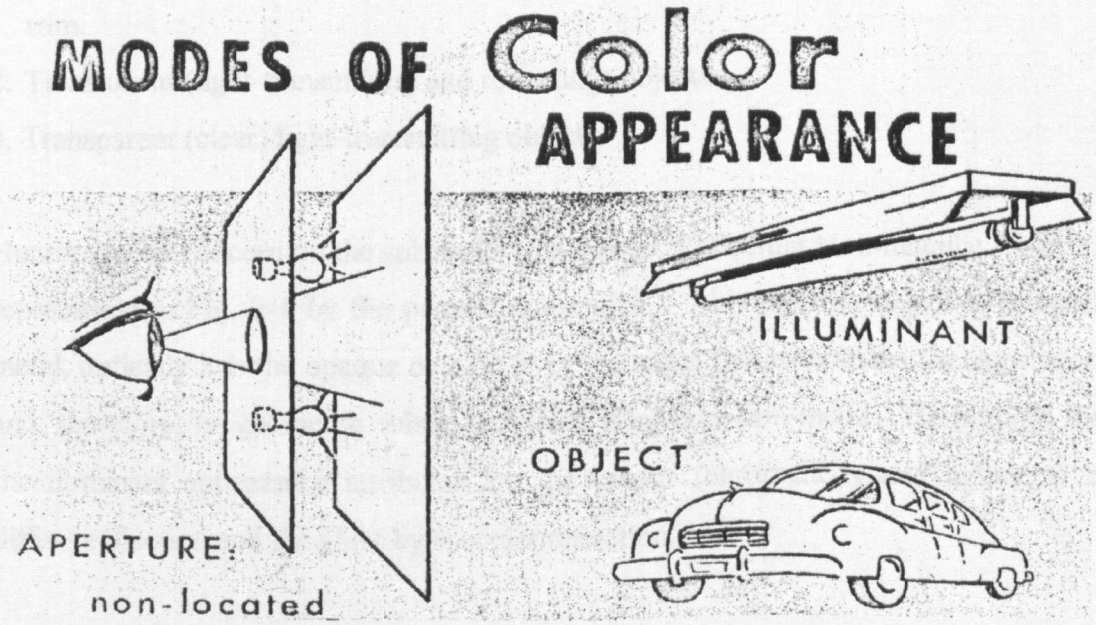

Figure 2-1. The three modes of colour appearance

Mode-1 Aperture

The colour is seen through a hole so that the observer is unable to identify the illuminant or objects involved or both. He can measure only the distribution of energy passing through the aperture.

Mode-2 Illuminant

For lights and other self-luminous objects, spectral and geometric distributions of light can be measured.

Mode-3 Object

The observer is conscious of both the object seen and its environment.

Our primary concern is with Mode-3, the object mode. Based on Mode 3, Richard S. Hunter presented four submodes of the object mode [Hunter 1985]:

1. Opaque, reflecting nonmetallic objects: paint films, moulded plastic objects, thick textile fabrics, papers, and so forth (Fig. 2-2).
2. Opaque metallic objects (bare metal surfaces): automobile bumpers and metallic trim.
2. Translucent (light-transmitting and reflecting) objects.
4. Transparent (clear) light-transmitting objects.

Hunter placed concern on the submode-1, "Opaque, Reflecting Non-metallic Objects," represented in Fig. 2-1 by the painted automobile. Although the object is primarily metal, optically it is the opaque coating over the metal that establishes the appearance and, therefore, its geometric submode, which is opaque non-metal. He thought that the dominant appearance attributes are the colour (chromaticity and lightness) by diffuse reflection and the gloss by specular reflection.

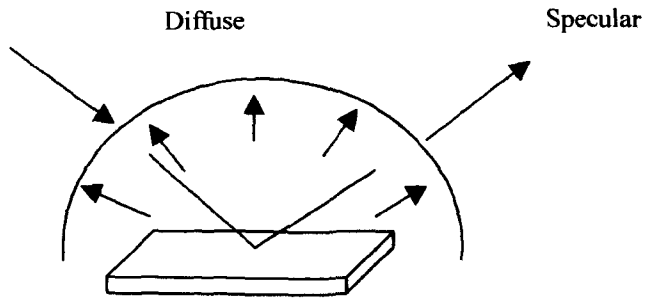

Figure 2-2. Submode-1 Opaque non-metals, painted

For the gloss attribute, it can be further identified into approximately six types [O'Donnell 1986].

1. Specular Gloss. Perceived surface brightness associated with the luminous specular (regular) reflection from a surface. Because the eye cannot readily judge brightness in an absolute sense, specular gloss is usually judged by comparison between the brightness of the surface of interest and that of a reference surface, present either deliberately or fortuitously.

2. Sheen. Perceived shininess at a large angle of incidence seen in otherwise matte specimens.

3. Distinctness-of-Image Gloss. The sharpness with which images are perceived after reflection from a surface. The conditions of illumination require a well-defined source with a black background, for example, a black-velvet-backed fluorescent lamp with a coarse wire screen.

4. Contrast Gloss (Lustre). Perceived relative brightness of brighter and less-bright adjacent areas of the surface of an object, resulting from selective reflection in directions relatively far from those of specular reflection.

5. Reflection Haze. Perceived scattering of light reflected from a surface in directions near those of specular reflection. Reflection haze is observed in specimens with

high specular gloss and, generally, high distinctness-of-image gloss. Often the haze appears bluish and the image reddish in comparison to similar areas of a haze –free specimen.

6. Macroscopic Surface Properties. Grouped under the aid of this heading are all the properties of a surface that can easily be seen without the aid of a high-power microscope. Surface properties, such as 'orange peel', directionality, and texture, are some examples of this type of phenomenon.

Based on the above description, the model and its attributes of the paint appearance on car body can be summarised in Figure 2-3.

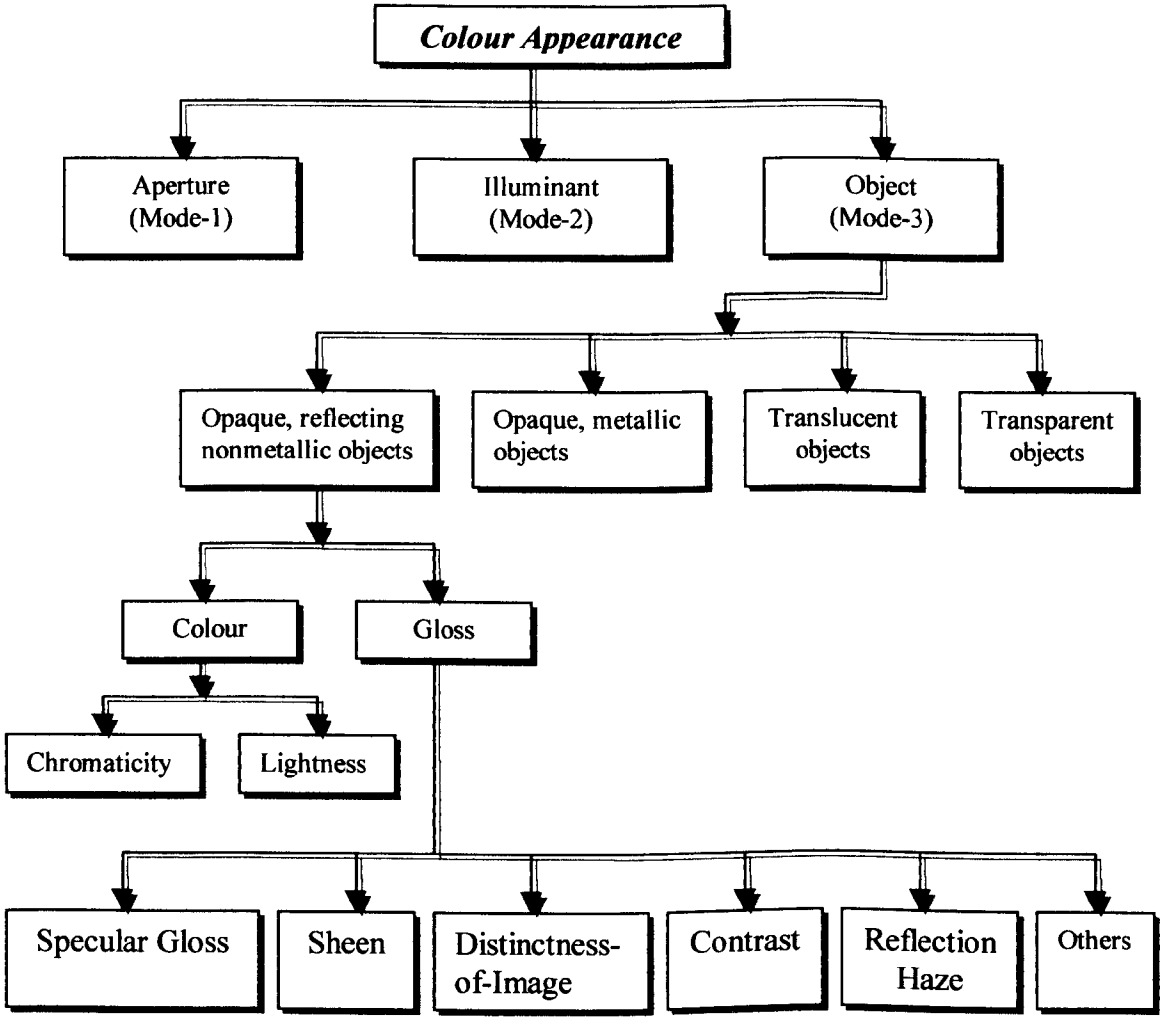

Figure 2-3 Colour Appearance mode and its properties

2.3. Appearance measurement

2.3.1. Introduction

From the introduction described above, it can be seen that the surface appearance is dominated by the colour and the gloss. The gloss can be further divided into many different types. Considering the circumstances in the automotive industry, Gabriele Kigle-Boeckler presented a diagram (Figure 2-4) to give an overview of the different types of surface appearance phenomena [Kigle 1996].

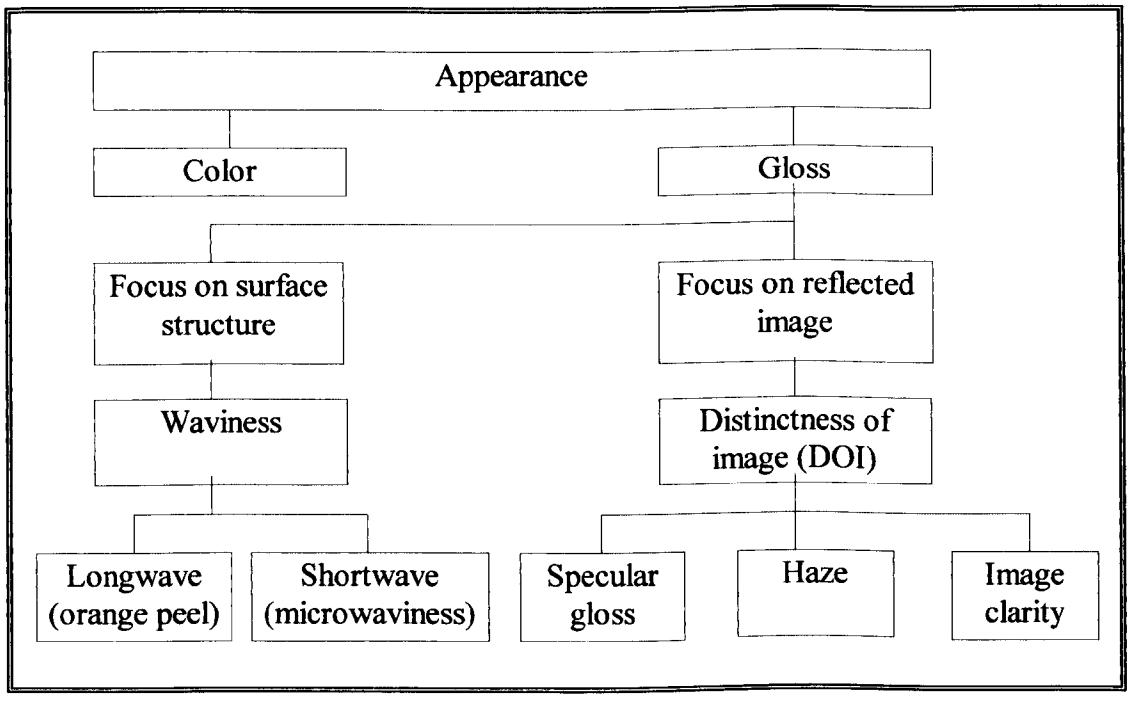

Figure 2-4 Surface appearance phenomena

In this diagram, appearance measurement is still divided into two parts, colour and gloss. The colour measurement is only mentioned. But the gloss measurement has been subdivided into details, which are more related to customer's visual perception and easier to measure in the automotive environment. Here an important comment should be made that, in the automotive industry, when we compare the quality of paint appearance, normally we only compare its gloss attributes. In this case the colour is

not taken into account. But it does not mean that the colour is not important. The reason is that the colour comparison is a further complex issue, which is usually studied separately.

The colour appearance of an object changes according to different viewing parameters such as media, light sources, background colours, and luminance levels. This phenomenon makes colour appearance assessment more difficult. To compare a panel with a given shade or another panel across a wide range of illumination conditions is the main task for colour appearance assessment. The development of colorimetry can be divided into three phases [Luo 1996][McCamy 1996]: matching, differences and appearance. Measures used to indicate whether two stimuli match each other include tristimulus values, chromaticity coordinates, dominant wavelength, and excitation purity. Methods used to quantify colour differences (e.g. in lightness, chroma or hue) have been devised so that equal scale intervals represent approximately equally perceived differences in the attributes considered.

In the automotive industry, colour is separately considered from appearance measurement due to the following:

- For car manufacturers, the colour is a very important property of surface appearance. They always endeavour to match the surface colour of a car body to a given reference shade or minimise the degree of the mismatch across a wide range of illumination conditions. Normally colour assessment requires visual judgement by very experienced workers or measurement by specialised instruments.

- For customers (car buyers), when they choose a car, colour is more likely to be dominated by the customer's psychology. Different people have different favourite colours. They choose the colour that they like rather than assess the colour as an aspect of quality. They are more likely to concentrate on another surface attribute, the gloss, when assessing quality.

- Since the appearance assessment is a complicated procedure, if the colour is excluded, the appearance measurement becomes easier, although far from simple.

Due to the customer's psychology, the difficulty of the colour assessment, and the complication of appearance measurement, the colour property is not taken into account in this study when we assess the quality of paint appearance. Assuming that the colour quality is good enough to meet customer's satisfaction, the quality of paint appearance is only represented by the optical attributes and the topographical properties.

In Figure 2-4, to simulate human visual assessment procedure, the gloss measurement procedure is also divided into two parts, focusing on the surface to obtain the topography information of the surface and focusing on the reflected image of an object to obtain the optical attributes of the surface (Fig. 2-5).

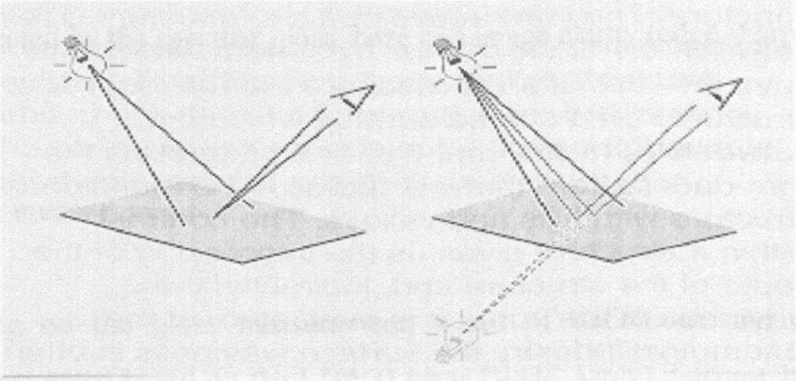

Figure 2-5 Focus on the surface or the reflected image of an object

(a). Focus on the surface

When focusing on the surface, the surface structure can be assessed according to the contrast between highlighted and non-highlighted areas in the reflected image. This type of evaluation provides us with a multitude of information about structure size and form. Structures between 0.1 and 10 mm can be seen as a wavy, light-dark pattern. In

the automotive industry this wavy pattern is often referred to as 'orange peel' (see Figure 2-6).

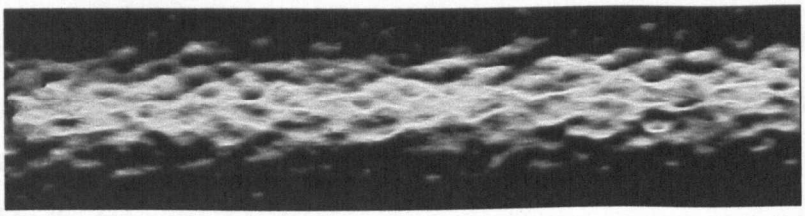

Figure 2-6 Orange peel phenomenon on paint appearance

(b). Focus on the reflected image of an object

By focusing on the reflected image of a light source, the distinctness of image (DOI) can be evaluated. There are the following situations: the reflected image may appear brilliant or dull (specular gloss measurement); the outlines of the image may be distinct or blurred (image clarity), or a halo could surround the image (haze). So DOI is normally affected by the specular gloss, haze and image clarity (edge sharpness).

2.3.2. Gloss measurement

Concentrating on the gloss measurement, a set of definitions and measurement methods is presented based on the LDA (Linear Diode Array) detector [Smith 1997]. They are easier to understand from the measurement point, which fully agree with the ASTM D523; BS 3900 D5; ISO 2813 etc.

Standard specular gloss

The gloss describes the perception of the shiny appearance of a surface when light is reflected from that surface. When viewing a glossy surface it is found that a sudden

increase in brightness occurs when the angle of observation is equal to the angle of incidence of the illuminating light. This condition is termed specular reflection.

ISO 2813 [ISO 2813 1994] gives a standard definition of specular gloss: *The ratio of the luminous flux reflected from an object in the specular direction for a specified source and receptor angle to the luminous flux reflected from glass with a refractive index of 1.567 in the specular direction.*

Note: To define the specular gloss scale, polished black glass with a refractive index of 1.567 is assigned the value of 100 for geometries of 20°, 60° and 85°.

Based upon the ISO 2813 configuration, the standard methods for measuring gloss have an angle of acceptance at the detector of ± 0.9° either side of the specular angle in the plane of measurement. In the case of a specular angle of 20°.

$$Gloss = \frac{Sum of\ Ir\ 20° \pm 0.9°\ sample}{Sum\ of\ Ir\ between\ 20° \pm 0.9°\ standard} \qquad (2\text{-}1)$$

Where, the Ir is the intensity of reflected light.

A method for measuring specular reflection with the basic illuminating and detecting geometry is shown in Fig. 2-7. A light source and lens consist of parallel or slightly convergent light on the surface under test. A lens field stop and photodetector are in a position so that their axis coincides with the direction of specular reflection of the incident beam.

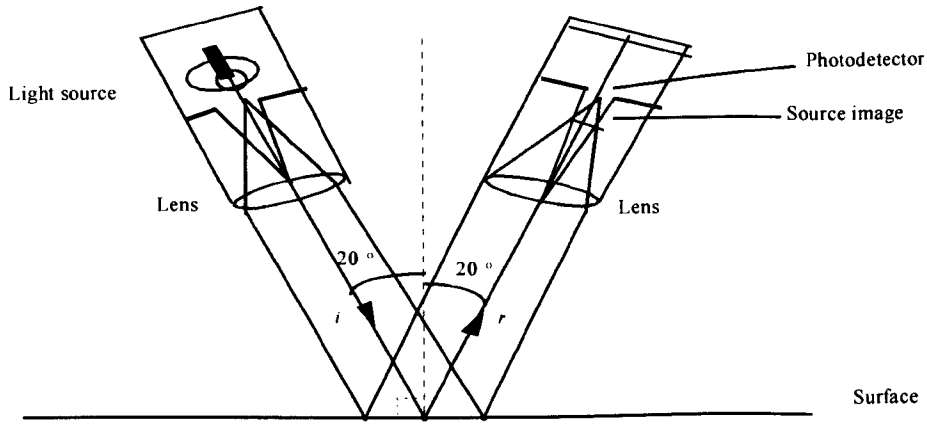

Figure 2-7 Schematic Layout of a 20° Glossmeter

Haze

Method B in the Standard ASTM E 430-91 was considered as a guide to the measurement of haze and it was decided to collect the 'haze' signal between 1°–2 ° either side of the specular angle.

$$Haze = \frac{Sum\ of\ Ir[(18.0°to19.0°) + (21.0°to22.0°)]}{Specular\ Gloss\ for\ Standard\ (BlackGlass)} \times 100 \quad (2\text{-}2)$$

Distinctness of Image (DOI)

Hunter defined distinctness of image (DOI) as the rate of change in intensity of the reflected light as a function of small changes in the angle of reflection.

Therefore DOI can be related to the gradient of a light intensity distribution curve and a reasonable approximation is given by the peak width at 1/2 peak height.

ASTM E430 method 'A' measures the light at fine apertures placed at 0.3° off specular and ratios this to the specular gloss for the standard (Black glass in the case of paints).

The problem with this index for DOI is that it will vary according to the specular gloss of the sample.

However, if the 'constant' denominator in ASTM E430 is replaced by the sum of the reflectance about the specular of the sample a much more variable and sensitive index results. Considering DOI at 0.5° ±1° either side of the specular (20°) then:

$$DOI = \left[1 - \frac{Sum\ of\ Ir\ [(20.4°\ to\ 20.6°) + (19.4°\ to\ 19.6°)]}{2 \times Sum\ of\ Ir\ between\ 20° \pm 0.1°\ sample}\right] \times 100 \quad (2\text{-}3)$$

Furthermore this index tends to 0% for matt surfaces, which is not the case for the index in ASTM E430.

Orange Peel

Hunter does not describe any methods for measuring coarse surface texture, and does not even mention orange-peel in the index of his treatise [Hunter 1975]. The protocols of the American Society for Testing and Materials (ASTM), published in 1984 as a compilation of methods for the measurement of colour and appearance, defined orange peel. But no quantitative method for the measurement of orange-peel was given [ASTM E12 1984].

As introduced before, orange peel is a special optical phenomenon on paint appearance due to the irregularity of the surface and interference between coating layers and substrate. When focusing on the surface, the contrast between highlighted and non-lighted areas can be observed with a large amount of information about structure size and structure form. As the human eye can see structure sizes between 0.1mm and 10 mm. our triangulation system does not have the resolution to measure the real depths

of structure on topcoat surface, which are between 1 μm and 2 μm. In Fig. 2-8, when the light beam hits a peak or a valley of the surface, the maximum signal was detected (the light pattern); on the slopes a minimum signal is registered. In the automotive industry this kind of phenomena is referred to as orange peel.

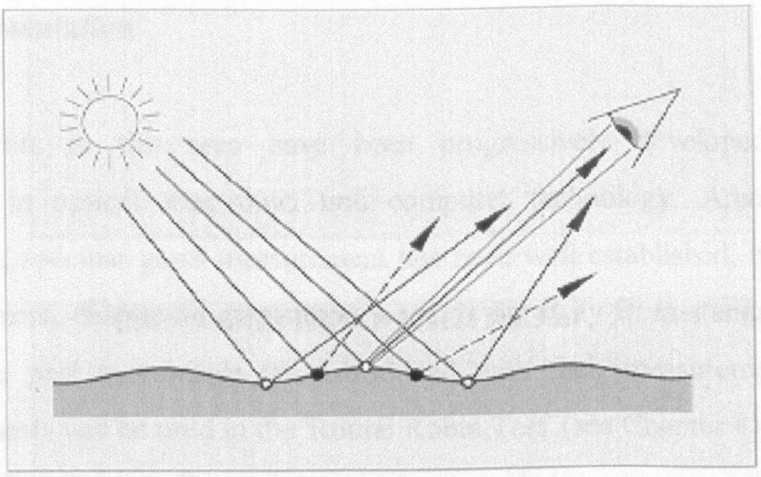

Figure 2-8. Visual orange peel assessment

The signal frequency perceived by the human eye is equal to double the spatial frequency of the topography (see Fig. 2-9). Thus the optical profile reflects " what you see ", the mechanical profile measures " what you feel ".

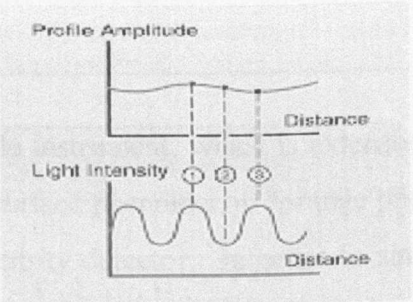

Figure 2-9 Optical Profile versus Mechanical Profile

In fact, in the modern automotive industry, as a high quality of paint appearance can be achieved, the gloss is high enough to meet the customer's satisfaction. In this case, the orange peel is more obvious. So the orange peel has become an important parameter which is driving the quality of paint appearance.

So far there is no standard definition for orange peel, nor a standard measurement method. The different instruments use different ways to measure it. The methods for orange peel measurement will be introduced in the next section.

2.3.3. Instrumentation

The instruments in this area have been progressively developed with rapid improvement in optical, electronic, and computer technology. Among the gloss measurements, specular gloss measurement has been well established, but the orange peel measurement, despite its great importance, is far away from standard. Here two typical orange peel instruments are introduced with their measurement principles. These instruments will be used in the 'Round Robin Test' (see Chapter 4). An empirical formula regarding the overall appearance is also provided.

2.3.3.1. Wavescan (BYK)

The 'Wavescan' is a portable instrument, which is extensively used in the automotive industry for measuring the surface phenomenon "orange peel". It is made up of a laser light source and a light intensity detector. In order to simulate the resolution of the human eye, the waviness of the paint surface was divided into long term and short term waviness. Human eye resolution is illustrated in Figure 2-10. Being 50 cm away, the human eye can see 35 separate lines, which have a width of 0.1mm as well as a distance between each other of 0.1 mm. At a distance of 2.5m we can see 35 separate lines which have a width of 0.6 mm as well as a distance between each other of 0.6mm.

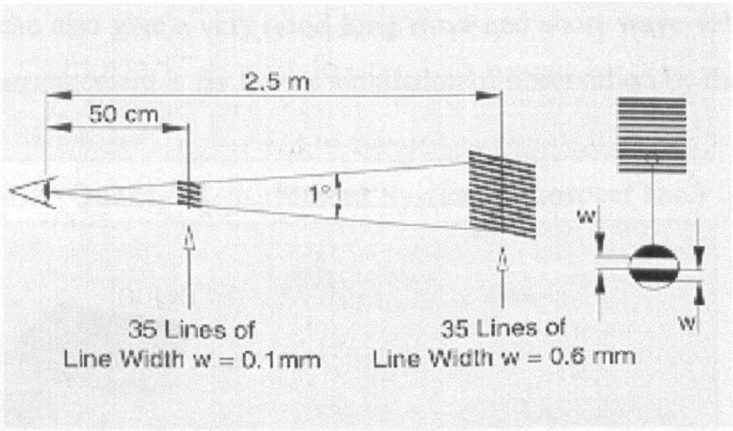

Figure 2-10 Resolution of the human eye

To simulate this situation, the detected signal is divided into longwave (structure size > 0.6 mm) and shortwave (structure size < 0.6 mm) signals by using a mathematical filter function. **The long-term waviness represents the variance of the long wave signal amplitude and the short-term waviness represents the variance of the shortwave signal amplitude** [Wave-scan 1992]. The longwave and shortwave are all normalised to 0 – 100 (100 is the worst). There is no unit for them. The output value is only a relative level regarding the amplitude of longwave or shortwave.

The Wavescan scans the wavy light-dark pattern of the surface with a laser point source illumination system at 60 degrees incidence angle. The sample surface is scanned by moving the instrument over a distance of 10 cm and the reflected light intensity is detected every 0.08 mm. At a close distance, the light-dark pattern can be interpreted visually as a micro-waviness (structure sizes smaller than 0.6mm). At a greater distance, the phenomenon of orange peel (structure sizes larger than 0.6mm) can be seen.

Advantage: portable, easy-to-use, long wave and short wave.

Disadvantage: Surface defects such as dust enclosures, scratches or fingerprints can falsify the readings up to 50-200%. There is no gloss measurement, as it is fully based on the reflected light intensity. The low gloss surface

can also give a very good long wave and short wave value. The optical arrangement is far from a simulation of observation by the human eye.

2.3.3.2. QMS-BP (Quality Measurement System, Autospect Inc.)

The QMS-BP is a measurement system that provides four parameters, gloss, distinctness of reflected image, orange peel, and overall appearance. The QMS-BP is made up of a white light source, an electronic camera, and computer. Its working principle is shown in Figure 2-11 [QMS-BP, 1996].

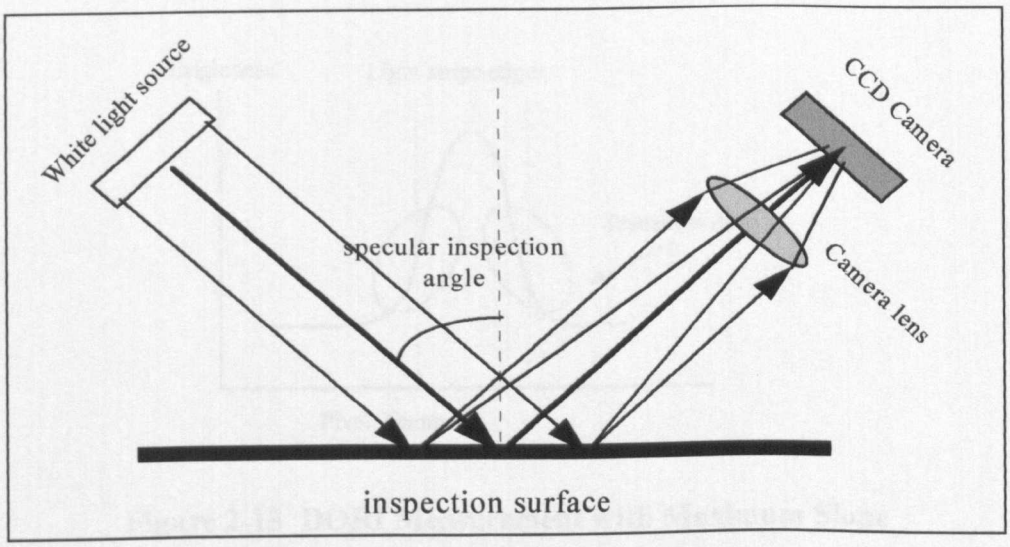

Figure 2-11 Optical system of QMS-BP

The gloss is determined by measuring the average difference between the brightness of the reflected image and the brightness of the surrounding area. This produces a figure, which is similar to, but not identical to specular gloss measurements, Figure 2-12.

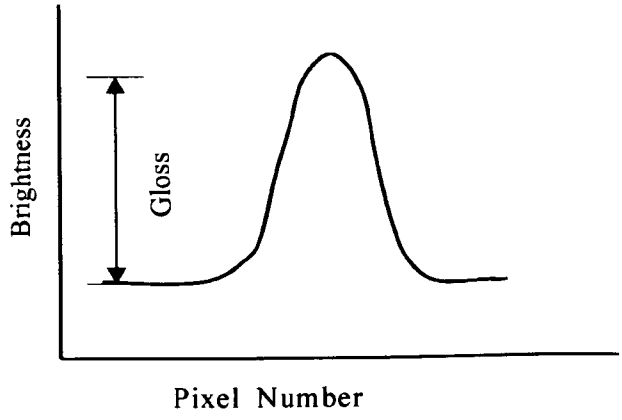

Figure 2-12 Gloss Measurement with QMS-BP

The distinctness of reflected image (DORI) is determined by measuring the rate at which the image changes from dark to bright at the edge of the reflected image. It is, therefore, a measure of haze or smokiness. There are two ways to measure the DORI. One is the measurement of the maximum slope of the brightness graph in the transition areas (Figure. 2-13); another one is the comparison of the sharpness of the image (Figure 2-14).

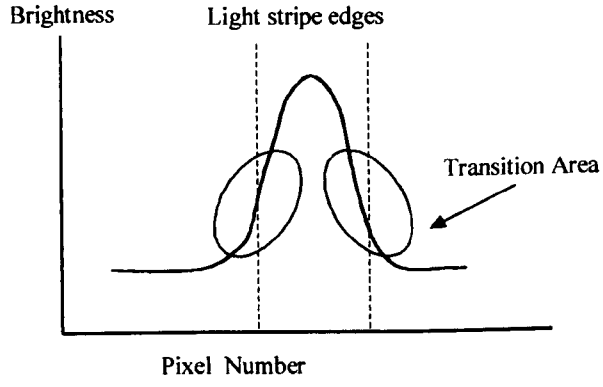

Figure 2-13 DORI Measurement with Maximum Slope

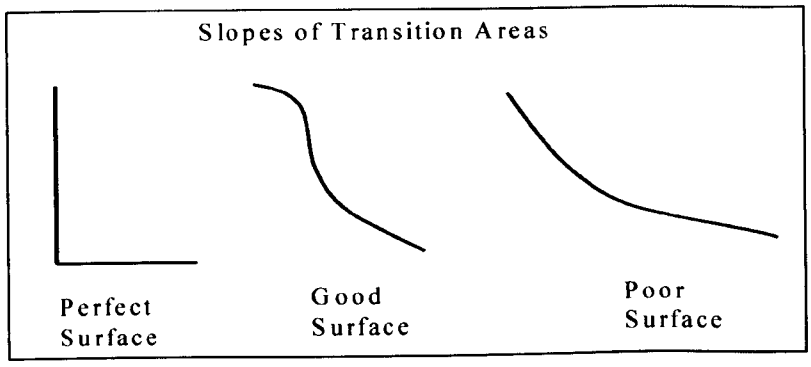

Figure 2-14 DORI Measurement with comparing Slopes of Brightness Vs Length (Pixel)

Orange Peel is calculated by measuring the waviness of the edge of the reflected image longitudinally along the image (Fig. 2-15). Noise is removed using a high-pass frequency filter. The algorithm used has been developed to measure the waviness in the wavelength range from 1.25 mm to 5 mm.

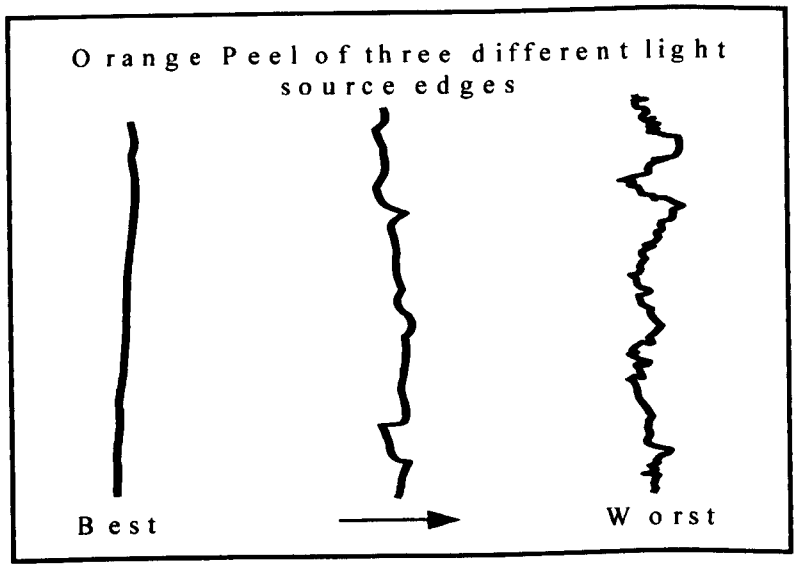

Figure 2-15 Orange Peel Measurement

The Overall appearance is based on the following empirical formula, which assigns an index to each individual parameter.

$$Overall\ Appearance = 0.15 \times Gloss + 0.35 \times DORI + 0.50 \times Orange\ Peel \quad (2\text{-}4)$$

2.4. Links between the visual assessment and individual parameters

People are always seeking an effective way to link the visual assessment with the individual parameters obtained from instruments, because our objective is to have an overall assessment on the quality of paint appearance by measuring its gloss attributes. Two major methods were found for the overall appearance model in the literature survey.

2.4.1. Empirical Formula

Empirical formula is one of the common ways found in connecting the overall appearance and measurable parameters in the automotive industry. An empirical formula is given in the last section (Equation 2-4) in which each parameter has been assigned an index according to its importance to overall appearance. It is apparently a linear model to build up the relationship between overall appearance and individual parameters. This formula will be verified and compared in Chapter 4 and Chapter 7.

Another similar formula was found in [Scheers 1997], in which the appearance index (A.I.) was defined as a weighted average of gloss, distinctness of image (DOI), image distortion (NSIC) and loss of contrast (NSIC*).

$$A.I. = 0.15\,Gloss(20°) + 0.35\,DOI + 0.25\,NSIC + 0.25\,NSIC^{*} \qquad (2\text{-}5)$$

2.4.2. Regression Analysis

Another way for linking the overall appearance and individual parameters is regression analysis, which is a mathematical technique that fits a set of data with an equation of the form:

$$y = b_0 + b_1 x_1 + b_2 x_2 + \cdots + b_n x_n \qquad (2\text{-}6)$$

Where y is the dependent variable, or response, x_1, x_2, ... x_n are the independent variables, or input variables and b_0, b_1, b_2, ... b_n are constants.

An example can be found in reference [Guthrie 1996], in which J. Guthrie and A. Weakley conducted an experiment to find the relationship between visual assessment and orange peel (with instrument QMS) and gloss. He found that the gloss levels of the paint appearance influence the perceived orange-peel on higher gloss surfaces. The more gloss level increases, the greater the orange-peel could be perceived. A regressed formula was given as below according to the experimental data.

Average Visual Ranking = 26.65 – 0.26 (QMS orange-peel rating) + 0.02 (20° gloss) (2-7)

This formula works in the same way as the overall appearance in Equation 2-4. It is still working on the level of a linear model.

2.5. Conclusion

In this chapter, we reviewed the concept of appearance, gloss measurement, and overall appearance formulae. The following conclusions can be drawn from the literature survey:

- The measurement of paint appearance is a complicated issue, which combines the optical and geometric properties of the paint surface. With rapid development in the automotive industry, paint industry and instrument industry, human understanding of appearance measurement is going deeper. More and more measurable parameters are required to characterise the paint appearance. Apart from specular gloss, some new parameters like orange peel, metal texture are far from standard. No standard definitions and measurement methods can be found for them in the literature survey.

- As the various definitions and measurement methods existing for some parameters, the measurement results may be quite different from instrument to instrument, even though the parameter's name is the same. A most obvious example is the gloss measurement with QSM-PB and traditional methods.

- The overall appearance measurement is still staying at the level of empirical formulae and linear regression. It is proposed that multiple input and non-linear systems are needed to model overall appearance.

- A standard measurement framework is needed to be set up to measure objectively the quality of paint appearance in the automotive industry. This involves visual assessment, measurable parameters, and overall appearance models. The quality of paint appearance should be measured in a repeatable and reproducible, continuous scale manner as perceived by the customer.

Chapter 3

Visual Assessment of Paint Appearance

3.1. Introduction

The customers' perception is an important reference point for paint appearance measurement in this study. The experimental work on visual assessment in accordance with customers' opinion is useful to compare with instrumental results and ultimately to ensure paint quality. Although visual assessment is a subjective procedure, it is important to obtain accuracy and reliability in the statistical interpretation of the results on paint quality. In this chapter, we will introduce the procedure for visual assessment and the statistical methods employed to obtain objective results.

From the introduction in the last chapter, it is clear that, for visual assessment, it is necessary to concentrate on the gloss attributes. Gloss has many attributes as follows: - specular gloss, sheen, distinctness-of-image, contrast gloss, reflection haze, and macroscopic surface properties, such as orange peel, directionality, and texture. For the customer, there is generally no understanding of all of these attributes, but they can directly compare two panels and form a firm opinion on which one is better.

As the surface appearance has several properties, the judgment can be influenced by the different parameters. This type of problem is called 'multidimensional'. However, it is difficult for a customer to give direct ranking on a scale of 1 to 100, say. Therefore, the experiment is based on paired comparisons.

3.2. Visual assessment

It is well known that direct comparison between two items is far more sensitive and discerning than actual measurement on a scale of values. Visual assessment was conducted by customers by comparing every possible combination of the panels.

If there are n = 10 panels labeled from A to J, the total number of combinations is $nC2 = \frac{n(n-1)}{2} = 45$, n being the number of panels. All the possible pairs of panels are listed in Table 3-1.

Table 3-1. All the combination of panels

AB	AC	AD	AE	AF	AG	AH	AI	AJ
	BC	BD	BE	BF	BG	BH	BI	BJ
		CD	CE	CF	CG	CH	CI	CJ
			DE	DF	DG	DH	DI	DJ
				EF	EG	EH	EI	EJ
					FG	FH	FI	FJ
						GH	GI	GJ
							HI	HJ
								IJ

Procedure for visual assessment:

According to the measurement framework described in Figure 2-4. The visual assessment is also divided into two procedures. Focus on the surface to evaluate the surface topography effect. Focus on the reflected image to evaluate its optical properties.

a). In a room illuminated by a warm fluorescent tube, hold the panels as a pair at an arms-length distance.

b). Focus on the surface to observe the surface structure. Focus on the image of reflected fluorescent tube to compare the optical properties of the panels.

c). Comparing two panels in terms of overall appearance, answer the question: - which one is better?

d). Compare panel A with B, A with C etc. until all the combinations are completed.

3.3. Statistical Methods

Effective statistical methods can improve the accuracy and reliability of such test results to reflect objectively the quality of paint appearance. Here two statistical methods, score based and ranking based, are introduced to obtain statistical results.

3.3.1. Score Based

For the individual observer, the score can be distributed by comparing all the possible pairs of panels (see Table 3-1). Each time only one score can be assigned to either panel. In this case, two panels must be discriminated to decide which one is better, even if they are quite close. In Table 3-2, the right of the diagonal is the test result, where 1 stands for that the panel in the row is better than the panel in the column, 0 stands for that the panel in the row is worse than the panel in the column. The left of the diagonal is the reversed result of the right of the diagonal. The last column is the total score for each panel by summing all the scores in one row.

For several observers, the final results are obtained by simply summing all the individual results as Table 3-3 shows with 10 observers. The number in each cell is the number of agreements for panels in rows against those in the columns.

Table 3-2. Individual test result

Panel code	A	B	C	D	E	F	G	H	I	J	Sum
A		0	1	1	1	1	1	1	1	1	8
B	1		1	1	1	1	1	1	1	1	9
C	0	0		0	0	0	0	1	0	1	2
D	0	0	1		0	1	1	0	1	1	5
E	0	0	1	1		1	1	1	0	1	6
F	0	0	1	0	0		1	1	0	1	4
G	0	0	1	0	0	0		1	0	1	3
H	0	0	0	1	0	0	0		1	1	3
I	0	0	1	0	1	1	1	0		1	5
J	0	0	0	0	0	0	0	0	0		0

Table 3-3. Test result for 10 observers

Panel code	A	B	C	D	E	F	G	H	I	J	Sum	Rank
A		8	10	8	7	9	10	9	7	10	78	1
B	2		10	8	10	8	10	9	9	9	75	2
C	0	0		2	0	3	3	2	1	5	16	10
D	2	2	8		3	8	9	6	5	10	53	4
E	3	0	10	7		9	10	8	5	9	61	3
F	1	2	7	2	1		9	5	2	9	38	7
G	0	0	7	1	0	1		2	2	4	17	9
H	1	1	8	4	2	5	8		5	7	41	6
I	3	1	9	5	5	8	8	5		8	52	5
J	0	1	5	0	1	1	6	3	2		19	8

In this way the panels can be ranked with the opinions of 10 judges. This statistical result can be confirmed with the coefficient of agreement to see if the judges have similar opinions.

Coefficient of Agreement [Moroney 1990]

$$A = \frac{2J}{mC\ 2 * nC\ 2} - 1$$

Where, m is the number of observers, n is the number of panels, J is defined as $J = \sum jC2$, j is the number of agreements for the panel in the row against the panel in the column (the number in each cell of Table 3-3). $-1 \le A \le 1$, Table 3-4 gives the value of $jC2$ in each cell which is the number of possible combinations for agreement. J is the sum of all the cells in Table 3-4.

Table 3-4. Possible combination for agreement in each cell

Panel code	A	B	C	D	E	F	G	H	I	J
A		28	45	28	21	36	45	36	21	45
B	1		45	28	45	28	45	36	36	36
C	0	0		1	0	3	3	1	0	10
D	1	1	28		3	28	36	15	10	45
E	3	0	45	21		36	45	28	10	36
F	0	1	21	1	0		36	10	1	36
G	0	0	21	0	0	0		1	1	6
H	0	0	28	6	1	10	28		10	21
I	3	0	36	10	10	28	28	10		28
J	0	0	10	0	0	0	15	3	1	

$$J = \sum jC2 = 1435$$

$$A = \frac{2\ J}{mC\ \ 2 \times nC\ \ 2} - 1 = \frac{2 \times 1435}{10\ C\ 2 \times 10\ C\ 2} - 1 = 0.42$$

The coefficient of agreement shows that the agreement between 10 judges on these 10 panels is high, which means the result is consistent between 10 judges. So the result is reliable. It is now necessary to consider whether this value of the coefficient of agreement could have arisen by chance with fair probability. The answer depends on the number of panels being judged and the number of judges expressing an opinion. For the small values of m and n, the result can be directly found in the tables in reference [Kendall 1994]. But for m=10 and n=10, it is outside the range of the published tables. In such cases, it can also be tested with a significance measure, Z.

Significance Z [Moroney 1990]

$Z = [(\frac{4J}{m-2}) - \frac{m(m-1)(m-3)n(n-1)}{2(m-2)^2}]$ is distributed as a χ^2 distribution with degrees of freedom equal to

$$V = \frac{m(m-1)n(n-1)}{2(m-2)^2}$$

So, $Z = 274.53$, $V = 63.28$. The table for χ^2 is not beyond 30 degrees of freedom. In this case, we know that the $\alpha = \sqrt{2\chi^2} = \sqrt{2Z}$ is distributed about a mean value $\beta = \sqrt{2V-1}$ with unit standard deviation. So

$\alpha = \sqrt{2\chi^2} = \sqrt{2Z} = 23.43$; $\beta = \sqrt{2V-1} = 11.20$

The standard error is $\alpha - \beta = 12.23$, which represents a significantly high degree of agreement.

3.3.2. Rank Based

The test result can also be counted using an individual panel's ranking position. Each panel's position in the ranking can be decided by the score it earned (see Table 3-2). In Table 3-5, it is found that the panels D and I, G and H have the same scores, no preference can be expressed between them. These members are called 'tied'. In general, if ties occur in the ranking for the *i*th to *k*th inclusive members, the mid-rank, $(i + k)/2$, is allotted for *i*th to *k*th. Table 3-5 shows the rank result for individual results.

Table 3-5 Individual rank results

Panel code	A	B	C	D	E	F	G	H	I	J	Sum	Rank
A		0	1	1	1	1	1	1	1	1	8	2
B	1		1	1	1	1	1	1	1	1	9	1
C	0	0		0	0	0	0	1	0	1	2	9
D	0	0	1		0	1	1	0	1	1	5	4.5
E	0	0	1	1		1	1	1	0	1	6	3
F	0	0	1	0	0		1	1	0	1	4	6
G	0	0	1	0	0	0		1	0	1	3	7.5
H	0	0	0	1	0	0	0		1	1	3	7.5
I	0	0	1	0	1	1	1	0		1	5	4.5
J	0	0	0	0	0	0	0	0	0		0	10

For more observers, the ranks for each panel can be summed together. Table 3-6 shows the result of summed rankings with 10 observers for each panel. The final ranking can be obtained from the sum of the rankings in each column.

The Kendall coefficient of concordance [Kendall 1990] can be used as a measure of the degree of agreement between all observers. As there are tied members.

$$W = \frac{S}{\frac{1}{12}m^2(n^3 - n) - m\sum U'}$$

Where S is the sum of squared differences between observed and mean rank, m is the number of observers, and n is the number of panels. Average rank is m(n+1)/2. U' is defined as: $U'=\frac{1}{12}\sum(u^3-u)$, u is the number of tied members.

Table 3-6 Rank results with 10 observers

Observer	A	B	C	D	E	F	G	H	I	J
1	1	2	5.5	5.5	3	9	8	7	4	10
2	6	1.5	10	1.5	4	7	9	5	3	8
3	2.5	6	10	6	8	4	9	1	2.5	6
4	3	1.5	10	4.5	1.5	4.5	6	7	9	8
5	1	2.5	8.5	2.5	4	7	10	5	6	8.5
6	2.5	1	6	4.5	2.5	8	9.5	7	4.5	9.5
7	2	1	9	4.5	3	6	7.5	7.5	4.5	10
8	1	2	4	6.5	3	6.5	8.5	8.5	5	10
9	2	2	10	6.5	4	6.5	8	5	2	9
10	1	3.5	10	6	5	3.5	9	7.5	2	7.5
SUM	22	23	83	48	38	62	84.5	60.5	42.5	86.5
Rank	1	2	8	5	3	7	9	6	4	10

In this case, average rank = $\frac{10\times(10+1)}{2}$ = 55,

$$S = (22-55)^2 + (23-55)^2 + (83-55)^2 + (48-55)^2 + (38-55)^2 + (62-55)^2 + (84.5-55)^2 + (60.5-55)^2 + (42.5-55)^2 + (86.5-55)^2$$
$$= 5333$$

$$U' = \frac{1}{12}(2^3-2) + \frac{1}{12}(2^3-2) + \frac{1}{12}[(3^3-3)+(2^3-2)] + \ldots = 12.5$$

$$W = 0.66$$

This value means these ranks have a good correlation. The significance can be verified with Snedecor's distribution for F [Moroney 1990].

As the rank based method stemmed from the score based method, the correlation coefficient between these two summed results (Table 3-3 and Table 3-6) is nearly 1. These two results can be also compared with Spearman's Rank Correlation Coefficient:

$$R = 1 - \frac{6 \times \sum d^2}{n^3 - n} \qquad (3\text{-}1)$$

Where, d^2 represents the squares of the rank differences

n is the number of samples ranked.

The Spearman's Rank correlation Coefficient between these two final ranks (Table 3-3, last column, Table 3-6, last row) is 0.93.

3.4. Improved methods

As the visual assessment results are preferred to be a reference over the instrumental results, to obtain an objective result is of great importance. We need to rank not only panels, but also the quantified evaluation for each panel. If the number of observers is large enough, any inconsistent judgments can be obscured. Otherwise, inconsistent judgments may affect the final result. Here two methods are described for the circumstance of a small number of observers.

3.4.1. Half Score

To minimize the risk of misjudgment effect, first of all the score awarded can be reduced to 0.5, e.g. if A is better than B, A gets 1 score. If A is equal with B, each one has 0.5 score. There are reasons to support this point, one is that this can reduce the misjudgment effect; another is that this status does exist if the objects are genuinely indistinguishable.

Several observers were asked to evaluate the panels using the previous criterion that one must be chosen even if two panels are every close. At the same time, if two panels were difficult to choose, this pair of panels was marked. Table 3-7 gives the first situation; Table 3-8 shows the result with marks '1', '0', and '0.5', where '1' stands for that the panel in the row is better than the panel in the column, '0' stands for that the panel in the row is worse than the panel in the column, '0.5' stands for the case where there is no discrimination between the panels in the row and the column.

Taking the previous result (Table 3-3, sum column) as the reference, the correlation coefficients between these results (last column in Tables 3-7 and 3-8) and the reference can be calculated.

R1 = 0.87, correlation coefficient between Sum columns in Table 3-3 and Table 3-7.
R2 = 0.91, correlation coefficient between Sum columns in Table 3-3 and Table 3-8.

A small improvement was found comparing the reference results and those in Table 3-7 and Table 3-8.

Table 3-7 Individual test result with marks '1' and '0'

Panel code	A	B	C	D	E	F	G	H	I	J	Sum
A		0	1	1	1	1	1	1	0	1	7
B	1		1	1	1	1	1	1	0	1	8
C	0	0		0	0	0	1	0	0	0	1
D	0	0	1		1	1	1	1	0	1	6
E	0	0	1	0		1	1	0	0	1	4
F	0	0	1	0	0		1	1	0	1	4
G	0	0	0	0	0	0		0	0	0	0
H	0	0	1	0	1	0	1		1	1	5
I	1	1	1	1	1	1	1	0		1	8
J	0	0	1	0	0	0	1	0	0		2

Table 3-8 Individual test result with marks '1', '0' and '0.5'

Panel code	BA	BB	BC	BD	BE	BF	BG	BH	BI	BJ	Sum
BA		0	1	1	1	1	1	1	0.5	1	7.5
BB	1		1	1	0.5	1	1	1	0.5	1	8
BC	0	0		0	0	0	0.5	0	0	0	0.5
BD	0	0	1		1	1	1	1	0.5	1	6.5
BE	0	0.5	1	0		1	1	0	0	1	4.5
BF	0	0	1	0	0		1	0.5	0	0.5	3
BG	0	0	0.5	0	0	0		0	0	0	0.5
BH	0	0	1	0	1	0.5	1		0.5	1	5
BI	0.5	0.5	1	0.5	1	1	1	0.5		1	7
BJ	0	0	1	0	0	0.5	1	0	0		2.5

3.4.2. Full Comparison

In the previous visual assessment, all the panels only meet each other once (right part of diagonal in Table 3-1). In this case, the result of A compared with B was assumed to be same with the result of B compared with A. Actually as there is similarity of the panels, people often change their mind during the test. For example, when an observer compared panel A and B, if A was preferred to B, this result can be denoted by the notation A→B, the direction of the arrow indicates the direction of decreasing preference. When comparing B and A, the result may be B→A.

To reflect the observer's true perception and minimize the effect of misjudgment, a full comparison between all the panels is desirable (see Table 3-9). For the sum of each row (last column), the total score for each panel is calculated with '1' and '0.5'. For the sum of each column (last row), the total score for each panel is calculated with '0' and '0.5', '0' represents 1 score, '0.5' represents 0.5 score.

Table 3-9 Full comparison on all panels

Panel code	A	B	C	D	E	F	G	H	I	J	Sum
A		0	1	0	0	0.5	1	1	0	1	4.5
B	1		1	0	1	1	1	1	0.5	1	7.5
C	0	0		0	0	0	0	0	0	0	0
D	0	0	1		0.5	1	1	0.5	0.5	1	5.5
E	0	0.5	1	0		1	1	0	0.5	1	5
F	0	0	1	0	0		1	0.5	0	0.5	3
G	0	0	0.5	0	0	0		0	0	0	0.5
H	0	0	1	0	1	0.5	1		0.5	1	5
I	0.5	0.5	1	0.5	1	1	1	0.5		1	7
J	0	0	1	0	0	0.5	1	0	0		2.5
Sum	7.5	8	0.5	8.5	5.5	3.5	1	5.5	7	2.5	90

Actually, Table 3-9 contains two sets of comparisons. The final score for each panel can be obtained by averaging the sum of row and the sum of column (Table 3-10, second row). To compare the results, Table 3-9 can be divided into two separate tests along the diagonal. Revising the other part of diagonal as Table 3-2, the results of two tests are listed as test 1 and test 2.

Table 3-10 Average result of full comparison

Panel	A	B	C	D	E	F	G	H	I	J
Average	6.00	7.75	0.25	7.00	5.25	3.25	0.75	5.25	7.00	2.50
Test 1	4.5	7.5	0.0	7.5	6.0	3.5	1.0	5.5	7.0	2.5
Test 2	7.5	8.0	0.5	6.5	4.5	3.0	0.5	5.0	7.0	2.5

In Table 3-10, the score has been reduced to 0.25 for each observer. The risk of the misjudgment effect has been reduced. The correlation coefficient with the reference set of scores (Table 3-3) is 0.88, which is higher than test 1 (0.79) but lower than test 2 (0.91).

In addition, the inconsistent pair (A→B→A) and the circular triad A→B→C→A can be found in Table 3-9. The consistency of the observer can be pointed out.

3. 5. Conclusions

From the discussions above, the following conclusions can be drawn:

1). As visual assessment is a subjective procedure, the two methods presented can effectively provide objective results on the panels to be evaluated, not only the rank of these panels, but also the quantified value for each panel. The result can be used as reference to evaluate the instrumental results.

2). The reliability of these methods is based on a large number of observers. The number of observers must be large enough to ensure the accuracy of the results, which can obscure some inconsistent judgments.

3). The half score and full comparison could be more important when the number of judgments is small. It can reduce the risk of the misjudgment effect.

4). It is suggested that the few extremely inconsistent observers should be excluded, because they have difficulty in distinguishing between the items.

5). These methods can be also applied to other product quality inspection problems.

Chapter 4

Round Robin Test and Statistical Analysis

4.1. Introduction

After the literature survey, we know the situation in the area of paint appearance measurement. Currently the European car manufacturers use different parameters and instruments to measure the quality of paint appearance. To further investigate this situation, i.e. what parameters and instruments are being used in European car manufacturers, what is the relationship between these parameters and what is the correlation found between visual assessment and instrument and so on, a round robin test was launched among some major European car manufacturers.

This chapter presents the results of this round robin test. The relationships between the most-used parameters and the correlation between visual assessment and overall appearance are described. This chapter is an important part of the thesis since it provides a basis for the development of a measurement framework for paint appearance measurement.

4.2. Objective

The objective is to conduct a round robin test on paint appearance measurement amongst European car manufacturers, to investigate further the parameters and instruments being used by European car manufacturers

concerning paint appearance measurement and to identify the role of each parameter.

The objective will be accomplished by completing the following tasks:

- To confirm the Visual Assessment procedure
- To compare all the parameters available
- To reveal correlation between visual assessment and instrument results

4.3. Experiment Design

This round robin test involved six industrial companies (Volvo, Renault, IVECO, OCAS, PPG, British Steel) and Brunel University. 38 panels were selected and all the instruments available were used to perform the measurements on these panels. Table 4-1 is a list regarding the companies, instruments and parameters involved in this round robin test.

The panels were selected from our industrial partners with a range of steel texture, surface roughness, colour, and paint properties. Figure 4-1 presents the distribution of long wave (LW) and short wave (SW) results on these panels obtained with a 'Wavescan' instrument from BYK-Gardner. The long wave on these panels ranged from 0 to 45 and the short wave is from 0 to 70.

Table 4-2 shows the properties of these panels.

Table 4-1. Round Robin Test

Company	Visual Assessment	Instrument	Parameters
Brunel **BSSP** **PPG**	Non-professional	QMS	Gloss, DORI, Orange Peel, Overall
Volvo	Professional & Non-professional	Wavescan Panaspec Deltascop	LW & SW Gloss, Haze, DOI film thickness
Renault	Professional & Non-professional	Wave-scan Visiopaint HazeGloss MicroMetallic	LW & SW Tension & DOI Gloss 20^0 and Haze Thickness
OCAS	Professional & Non-professional	SUGA HunterLab Elcometer	NSIC & NSIC* Haze Thickness
IVECO	Professional & Non-professional	Glossmeter	Gloss 20^0

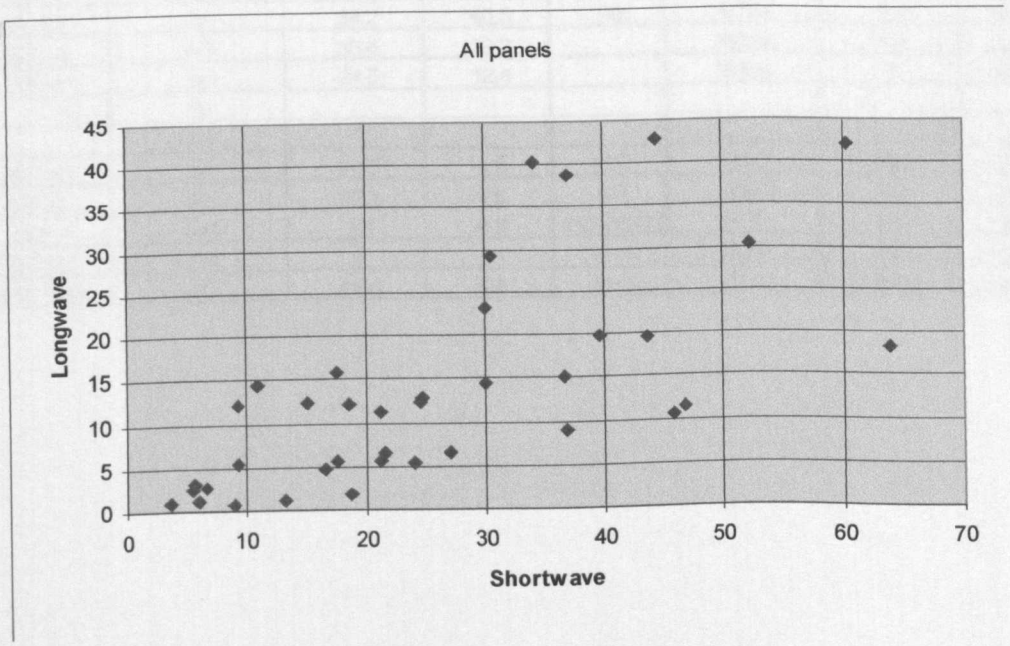

Figure 4-1 Longwave and Shortwave distribution of all panels

Table 4-2 Properties of Testing Panels

Former Code	Autosurf Code	Shortwave	Longwave	Substate	Colour	Clearcoat	Supplier
SIB 6	A	9.3	5.3	Sibetex	Black	2K	Volvo
SW1-3	B	37	38.7		White	No	Opel
SR2-2	C	36.9	8.9		Red	?	PSA
SB1-1	D	9	0.7	SB	Black	No	Volvo
MS2-3	E	18.8	1.9		Silver met.	?	VW
MB2-1	F	30	14.4		Black met.	?	MB
MGR2-2	G	21.6	6.5		Green met.	?	Renault
MGB2-1	H	13.2	1.1		Darkgreen Me	?	BMW
PANEL	I	60.4	42.1	SB	Blue	No	Volvo
SIB 7	J	10.9	14.4	Sibetex	Black	2K	Volvo
SR2-3	K	45.8	10.5		Red	?	PSA
SB1-3	L	52.3	30.3	SB	Black	No	Volvo
MB2-3	M	17.5	15.7		Black met.	?	MB
MGR2-4	N	63.9	18.3		Green met.	?	Renault
SIB 14	O	39.7	19.9	Sibetex	Black	2K	Volvo
SB2-3	P	44.4	42.8	SB	Black	1K	Volvo
MB2-5	Q	30	23.1		Black met.	?	MB
MGB2-3	R	21.3	11.2		Darkgreen Me	?	BMW
TRUNK	S	6.7	2.8		Green	No	Volvo
SIB 4	T	5.4	2.4	Sibetex	Black	2K	Volvo
ZN1	U	9.3	12.2	SB	Black	2K	Volvo
ZN3	V	5.7	3.2	SB	Black	2K	Volvo
ZN8	X	15.1	12.3	SB	Black	2K	Volvo
ZN10	Y	18.6	12.2	SB	Black	2K	Volvo
ZN22	Z	17.5	5.6	SB	Black	2K	Volvo
ZN11	AA	21.3	5.6	SB	Black	2K	Volvo
ZN 13	AB	46.7	11.5	SB	Black	2K	Volvo
ZN 14	AC	43.6	19.5	SB	Black	2K	Volvo
SR2-4	AD	36.6	15		Red	?	PSA
SB2-2	AE	24.7	12.8	SB	Black	1K	Volvo
PANEL	AF	34.2	40.3	SB	White	No	Volvo
SW1-2	AG	30.6	29.3		White	No	Opel
SW2-2	AH	24.5	12.4		White	?	Opel
	AI						
	AJ						
EDT GI	AK	24.1	5.5	EDT	RED	NO	OCAS
SB GI	AL	27.1	6.6	SB	RED	NO	OCAS
REF	AM	3.6	0.8	POLISHED	RED	NO	OCAS
EBT GI	AN	6	1.1	EBT	RED	NO	OCAS
EBT CRS	AO	16.6	4.8	EBT	RED	NO	OCAS

Test procedure

- For visual assessment

All the partners were required to be involved in visual assessment on the first twenty panels (A-T). The procedure and statistical methods have been described in Chapter 3. For industrial partners, there are two groups, professional and non-professional to conduct the test. For Brunel University, there is only a non-professional group. (Professional implies individuals who regularly assess the quality of paint finish in a production environment.)

- For instrumental parameters

The measurements were performed with all instruments available from our industrial partners on the 40 panels. There are five positions predefined on each panel (centre, upper, lower, left and right). Measurements were required to perform on these positions and the final result is the average of these five runs.

4.4. Results and Discussion

All the raw data referred to is in reference [Autosurf, 1998]. Here only the averaged results are listed. These results are categorised into three parts, visual assessment, surface topography properties, and spectral properties.

4.4.1. Visual assessment

All the visual assessment results are listed in Table 4-3. Each value has been normalised to a value (0-1), used with the statistical method introduced in Chapter 3.

The average standard deviation of panels A to T from professional groups (Volvo, Renault, Ocas and Iveco) is 0.03. The average standard deviation from non-professional groups (Volvo, Renault, Ocas, Iveco, and Brunel University) is 0.06. The average standard deviation for all is 0.045. It means the visual assessment results obtained with this method from different partners is very consistent. It proved again that the result obtained with this method is objective enough to be the reference to compare with instrumental results. Fig. 4-3 and 4-4 show the visual assessment results distributions in the professional group and the non-professional group.

Table 4-3 Visual Assessment Results

Panel	Volvo		Renault		Ocas		Iveco		Brunel
	Prof	Non-prof	Prof	Non-prof	Prof	Non-prof	Prof	Non-prof	Non-prof
A	0.64	0.60	0.70	0.52	0.72	0.71	0.71	0.72	0.58
B	0.19	0.08	0.13	0.10	0.09	0.15	0.30	0.22	0.26
C	0.61	0.53	0.56	0.64	0.56	0.56	0.57	0.62	0.53
D	0.99	0.90	0.95	0.96	0.98	0.88	0.96	0.94	0.76
E	0.91	0.84	0.91	0.98	0.90	0.95	0.91	0.92	0.82
F	0.47	0.46	0.47	0.42	0.41	0.41	0.42	0.40	0.5
G	0.66	0.72	0.66	0.65	0.62	0.61	0.58	0.62	0.68
H	0.90	0.89	0.86	0.86	0.84	0.84	0.85	0.93	0.79
I	0.11	0.15	0.05	0.23	0.14	0.15	0.19	0.17	0.21
J	0.33	0.29	0.32	0.26	0.28	0.29	0.42	0.25	0.4
K	0.62	0.53	0.59	0.71	0.65	0.70	0.55	0.63	0.64
L	0.14	0.23	0.15	0.19	0.20	0.23	0.16	0.18	0.32
M	0.40	0.44	0.44	0.39	0.38	0.40	0.26	0.46	0.49
N	0.26	0.38	0.23	0.38	0.25	0.24	0.19	0.21	0.37
O	0.55	0.59	0.61	0.68	0.67	0.70	0.58	0.58	0.49
P	0.02	0.06	0.03	0.03	0.02	0.02	0.10	0.05	0.08
Q	0.22	0.32	0.25	0.17	0.26	0.24	0.28	0.36	0.39
R	0.39	0.48	0.39	0.30	0.37	0.33	0.38	0.28	0.44
S	0.74	0.69	0.81	0.71	0.78	0.71	0.78	0.63	0.59
T	0.84	0.83	0.88	0.80	0.89	0.87	0.81	0.81	0.66

* Prof stands for professional group.
** Non-prof stands for non-professional group.

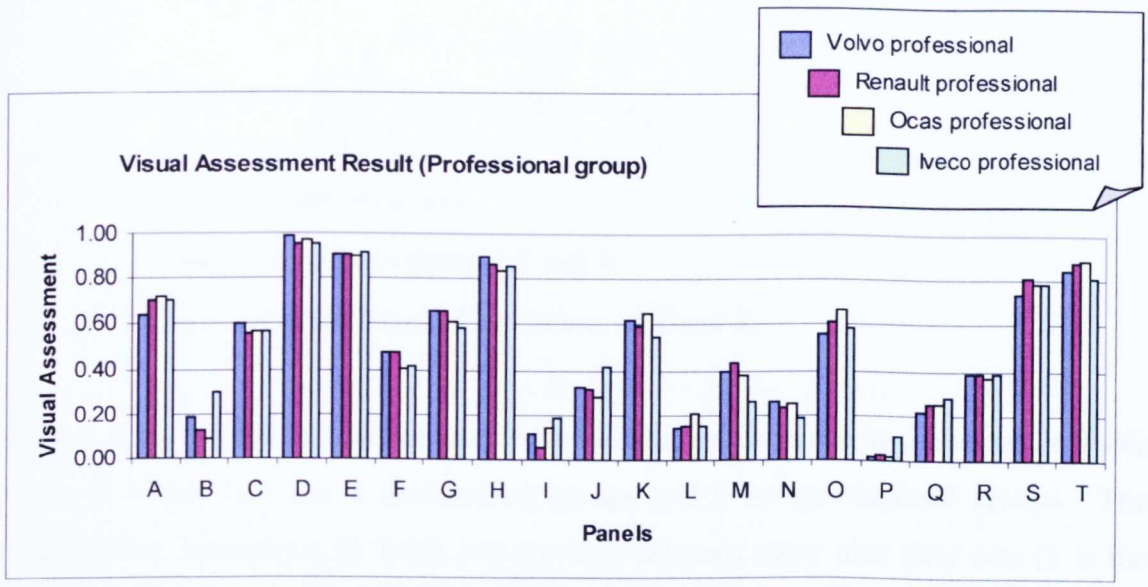

Figure 4-3 Visual assessment result from the professional group

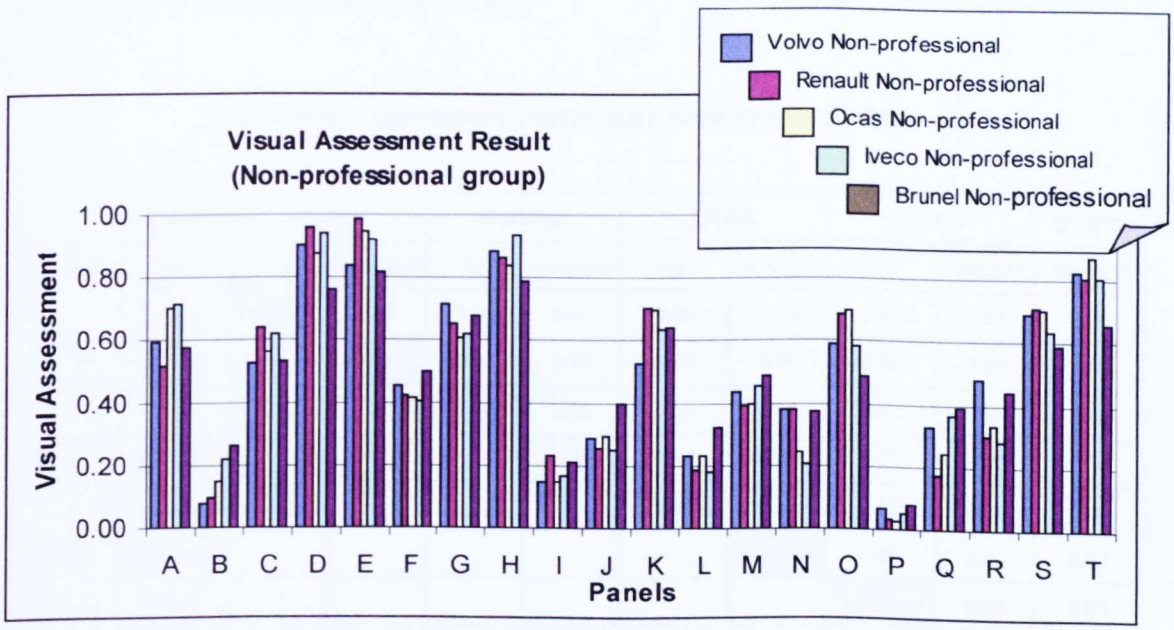

Figure 4-4 Visual assessment result from non-professional group

To check the correlation among these nine data sets (9 columns in Table 4-3), first of all, the correlation coefficient is used with the following definition:

$$\rho_{x,y} = \frac{Cov(X,Y)}{\sigma_x \sigma_y} \tag{4-1}$$

Where: $-1 \le \rho_{x,y} \le 1$

$$Cov(X,Y) = \frac{1}{n} \sum_{j=1}^{n} (x_j - \mu_x)(y_j - \mu_y)$$

X and Y are two data sets.

μ_x and μ_y are mean values of X and Y.

σ_x and σ_y are the standard deviations of X and Y.

The correlation coefficients between these visual assessment results are shown in Table 4-4, in which there are 4 professional groups and 5 non-professional groups. The correlation coefficients in Table 4-4 are high between these nine data sets (1 is the best) which means the procedure and statistical method used in visual assessment can provide us with very consistent results.

Table 4-4 Correlation coefficient between each data set

	Company	Volvo		Renault		Ocas		Iveco		Brunel
Company	Group	Prof	Non-prof	Prof	Non-prof	Prof	Non-prof	Prof	Non-prof	Non-prof
Volvo	Prof	1.00	0.97	0.99	0.97	0.98	0.98	0.97	0.97	0.96
	Non-prof		1.00	0.98	0.95	0.97	0.95	0.92	0.95	0.96
Renault	Prof			1.00	0.95	0.99	0.98	0.97	0.97	0.95
	Non-prof				1.00	0.97	0.97	0.92	0.95	0.93
Ocas	Prof					1.00	0.99	0.97	0.97	0.94
	Non-prof						1.00	0.96	0.97	0.94
Iveco	Prof							1.00	0.95	0.91
	Non-prof								1.00	0.95
Brunel	Non-prof									1.00

The visual assessment results can also be tested with the Spearman's Rank Correlation Coefficient in Equation (3-1) regarding its ranking consistency. The ranking result for each group on these twenty panels (A-T) is listed in Table 4-5 according to its score in Table 4-3. Spearman's correlation coefficients between each data set can be calculated

(Table 4-6). Comparing the results in Table 4-4 and Table 4-6, it can be seen that the correlation coefficients are both very high for the score method or the ranking method.

The visual assessment results show that the ranking of panels with the score method or the ranking method is very consistent. Thus, visual assessment results can be used as a reference for other instrumental measurement results.

Table 4-5 Visual assessment result by ranking

Panel	Volvo		Renault		Ocas		Iveco		Brunel
	Prof	Non-prof	Prof	Non-prof	Prof	Non-prof	Prof	Non-prof	Non-prof
A	7	7	6	10	6	5.5	6	5	8
B	17	19	18	19	19	18.5	14	16	18
C	9	9.5	10	9	10	10	9	8.5	9
D	1	1	1	2	1	2	1	1	3
E	2	3	2	1	2	1	2	3	1
F	11	12	11	11	11	11	11.5	12	10
G	6	5	7	8	9	9	7.5	8.5	4
H	3	2	4	3	4	4	3	2	2
I	19	18	19	16	18	18.5	17.5	19	19
J	14	16	14	15	14	14	11.5	15	14
K	8	9.5	9	5.5	8	7.5	10	6.5	6
L	18	17	17	17	17	17	19	18	17
M	12	13	12	12	12	12	16	11	11.5
N	15	14	16	13	16	15.5	17.5	17	16
O	10	8	8	7	7	7.5	7.5	10	11.5
P	20	20	20	20	20	20	20	20	20
Q	16	15	15	18	15	15.5	15	13	15
R	13	11	13	14	13	13	13	14	13
S	5	6	5	5.5	5	5.5	5	6.5	7
T	4	4	3	4	3	3	4	4	5

Table 4-6 Spearman's Ranking Correlation Coefficient

	Company	Volvo		Renault		Ocas		Iveco		Brunel
Company	Group	Prof	Non-prof	Prof	Non-prof	Prof	Non-prof	Prof	Non-prof	Non-prof
Volvo	Prof	1.00	0.98	0.99	0.97	0.96	0.98	0.96	0.97	0.98
	Non-prof		1.00	0.98	0.95	0.97	0.97	0.94	0.95	0.96
Renault	Prof			1.00	0.95	0.99	0.99	0.96	0.97	0.96
	Non-prof				1.00	0.96	0.97	0.96	0.92	0.94
Ocas	Prof					1.00	1.00	0.95	0.97	0.94
	Non-prof						1.00	0.95	0.97	0.95
Iveco	Prof							1.00	0.94	0.92
	Non-prof								1.00	0.96
Brunel	Non-prof									1.00

4.4.2. Surface topography parameters

Surface topography parameters are the measures of paint appearance properties due to the steel surface topography or interference between coating layers. Six parameters are selected as surface topography parameter in the round robin test, they are Long wave and Short wave (Wavescan, BYK), Tension (Visiopaint), NSIC* and NSIC (Suga), and Orange peel (QMS). The Long wave and Short wave (Wavescan) and Orange peel (QMS) have been introduced in Chapter 2. The Tension (Visiopaint) and NSIC* and NSIC (Suga) can be referred to the reference [Visiopaint 1995] [Suga 1985]. All these parameters are used to characterise the surface topography properties on paint appearance. Table 4-7 gives the average values of these parameters on panel A to T.

To compare the correlation between them, the correlation coefficients are listed in Table 4-8 to see its relationship among all these parameters.

Table 4-7 Surface topography parameters

Company	Volvo		Renault			Ocas		Brunel
Instrument	Wavescan		Wavescan		Visiopaint	Suga		QMS
Parameter	LW	SW	LW	SW	Tension	NSIC*	NSIC	Orange peel
A	4.00	10.64	4.40	10.00	18.86	60.66	65.64	70.20
B	38.26	37.78	41.10	42.00	11.69	13.14	19.44	32.20
C	8.76	36.94	8.30	35.40	17.15	47.82	55.54	57.00
D	0.72	9.14	1.00	8.90	21.06	82.26	86.56	82.40
E	2.04	18.88	2.00	18.20	18.78	57.72	74.06	75.90
F	13.20	31.26	13.40	30.20	15.13	50.72	58.66	46.50
G	6.72	22.34	7.00	22.60	18.12	63.70	66.84	61.70
H	1.90	13.66	1.40	13.70	20.55	85.36	88.04	79.90
I	39.24	62.50	40.30	62.80	10.88	10.80	19.92	26.30
J	14.76	10.88	15.70	12.50	14.92	40.42	44.04	40.20
K	12.44	46.24	10.90	47.30	16.43	39.50	48.36	52.10
L	33.56	59.24	31.30	55.70	11.29	19.58	26.80	33.20
M	16.52	17.60	15.50	16.80	13.98	26.56	35.96	41.70
N	19.74	65.38	18.80	65.60	11.60	8.04	17.84	35.10
O	16.74	42.46	17.60	41.00	16.02	44.52	57.50	56.40
P	43.84	42.94	44.80	44.80	10.99	6.36	19.22	20.10
Q	23.68	32.26	23.30	30.60	11.97	22.46	31.70	35.00
R	11.44	22.52	11.40	20.80	15.32	47.58	50.70	47.20
S	3.34	7.24	3.00	7.70	20.41	69.62	74.90	73.60
T	4.00	5.02	2.80	6.40	20.15	87.32	75.48	75.90

Table 4-8 Correlation coefficient between surface topography parameters

		Company	Volvo		Renault			Ocas		Brunel
		Instrument	Wavescan		Wavescan		Visiopaint	Suga		QMS
Company	Instrument	Parameter	LW	SW	LW	SW	Tension	NSIC*	NSIC	Orange peel
Volvo	Wavescan	LW	1.00	0.72	1.00	0.74	-0.92	-0.88	-0.90	-0.91
		SW		1.00	0.69	1.00	-0.78	-0.79	-0.76	-0.72
Renault	Wavescan	LW			1.00	0.72	-0.90	-0.87	-0.89	-0.90
		SW				1.00	-0.78	-0.80	-0.78	-0.73
	Visiopaint	Tension					1.00	0.97	0.98	0.98
Ocas	Suga	NSIC*						1.00	0.98	0.95
		NSIC							1.00	0.97
Brunel	QMS	Orange peel								1.00

In Table 4-8, the LW (long wave), Tension, NSIC*, NSIC, and Orange peel have a good correlation with each other (correlation coefficient between 0.88 – 0.92), which means that all these parameters correspond to the long wave phenomenon among the surface topography properties. They also have a good correlation with visual perception, which are shown in Fig. 4-5 to 4-8.

In the right corner of Fig. 4-5 to 4-8, an equation for the trendline is given which calculates the least square fit through points by using polynomial equation:

$$y = b + c_1 x + c_2 x^2 + c_3 x^3 + \ldots + c_6 x^6$$

Where b and $c_1 \ldots c_6$ are constants. Here the order of power is chosen to be two.

The coefficient of determination is also displayed in the right corner of figures as R^2, which is defined as [Montgomery 1991]:

$$R^2 = \frac{SS_R}{S_{yy}} = \frac{\sum_{j=1}^{n}(\hat{y}_j - \bar{y})^2}{\sum_{j=1}^{n}(y_j - \bar{y})^2} \qquad (4\text{-}3)$$

where n is the number of points.

R^2 is often used to judge the adequacy of a regression model. Clearly, $0<R^2\leq 1$. R^2 is referred as the proportion of variability in the data explained or accounted for by the regression model.

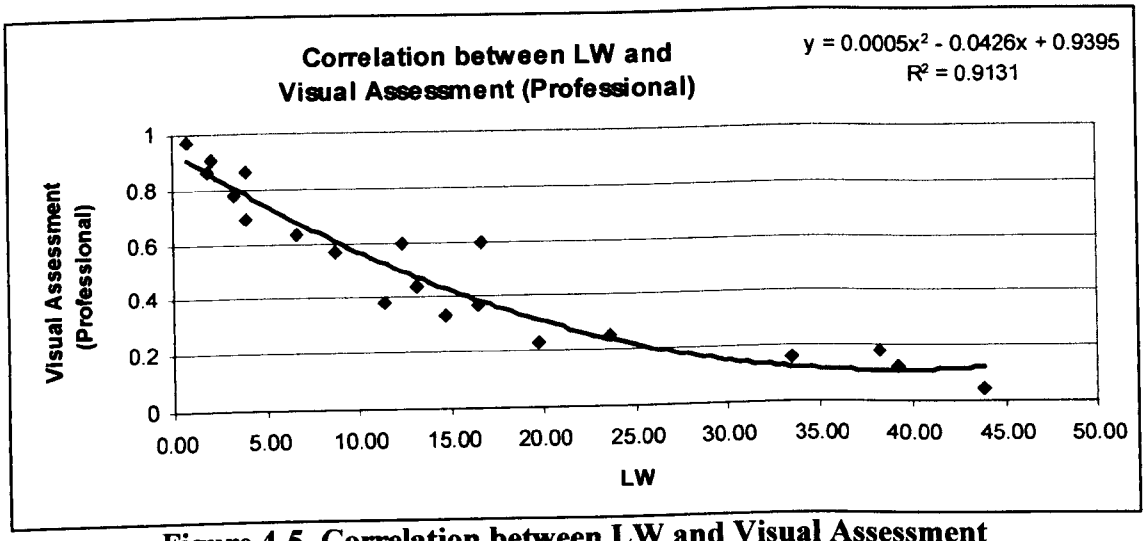

Figure 4-5 Correlation between LW and Visual Assessment

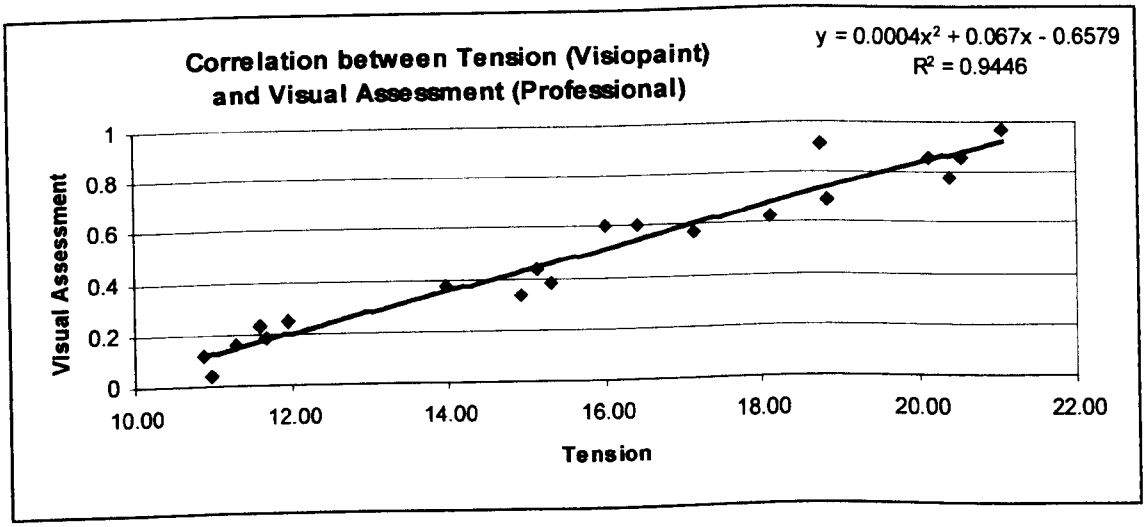

Figure 4-6 Correlation between Tension (Visiopaint) and Visual Assessment (Professional)

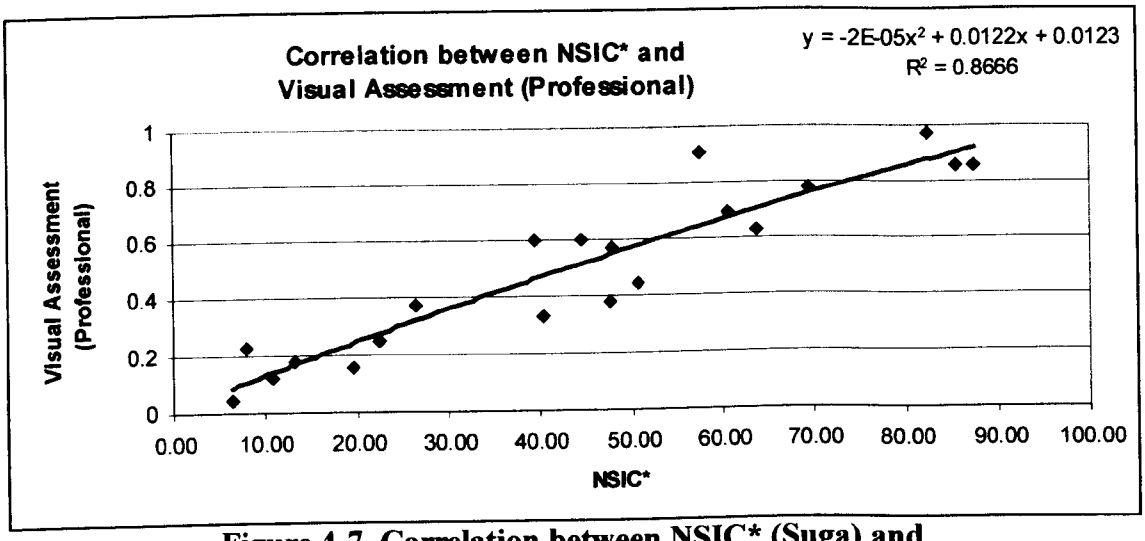

Figure 4-7 Correlation between NSIC* (Suga) and Visual Assessment (Professional)

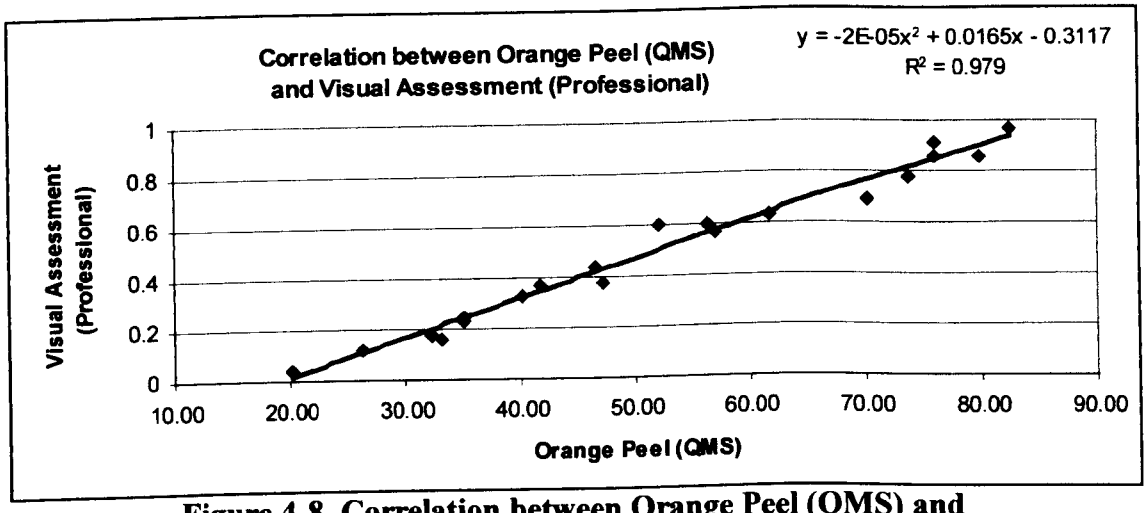

Figure 4-8 Correlation between Orange Peel (QMS) and Visual Assessment (Professional)

From the high R^2 value in Figure 4-4 to 4-8, it can be seen that these data can well explained by these regression curves. The correlation coefficients corresponding to Figure 4-4 to 4-8 are -0.91, 0.97, 0.93, and 0.99, which means that the parameters, LW, Tension, NTSC*, and Orange peel, have a good correlation with visual assessment (averaged professional). As these parameters present the long wave characteristics, the long wave is the dominant property which is driving surface appearance quality.

Comparing the difference between professional and non-professional visual assessment results regarding the correlation to the long wave parameter, it was found that the professional result has a higher correlation with long wave than the non-professional result (see Fig.4-5 and Fig. 4-9). It means the non-professional result distributes more widely than professional results, because the discrimination capability of professional groups is higher than that of non-professional groups.

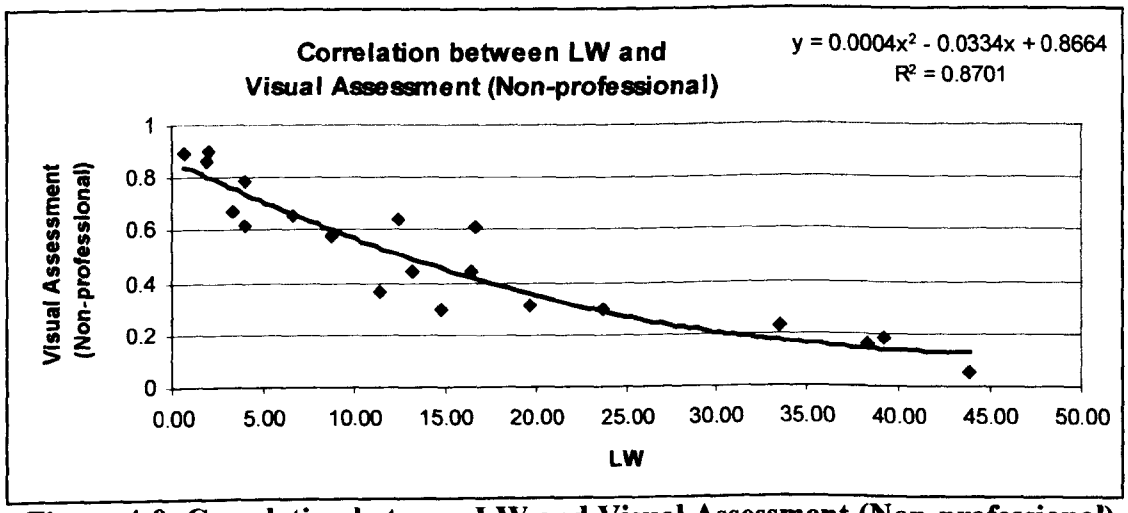

Figure 4-9 Correlation between LW and Visual Assessment (Non-professional)

On the other hand, as a topography parameter, the short wave (SW) did not reveal any significant correlation with visual assessment (Fig. 4-10). It also means that SW does not directly relate to the visual perception. Its correlation with visual perception should be further studied.

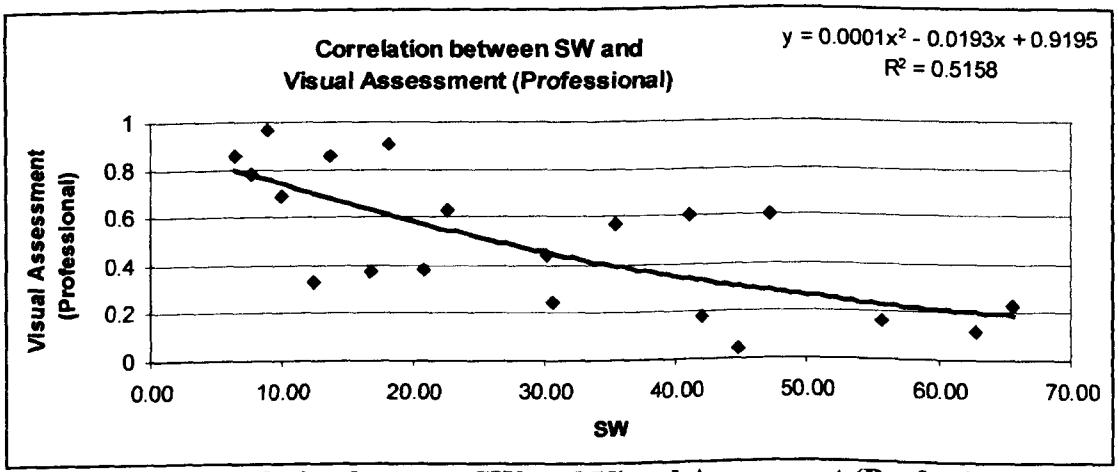

Figure 4-10 Correlation between SW and Visual Assessment (Professional)

4.4.3. Spectral Parameters

Spectral parameters are used to characterise the spectral properties of paint appearance. The most used parameters include Gloss, DOI, and Haze. As the different definitions and measurement methods exist in the instruments, these parameters could be measured with different instruments giving different results. To test the consistency of the instruments and their correlation with visual results, in this section measurements of these parameters derive from different instruments.

4.4.3.1. Gloss

Gloss is an important parameter in the evaluation of paint appearance. The measurements were performed with four different instruments, they are Panaspec®, MicroGloss®, Gloss 20® and QMS®, in which the Gloss 20® was used twice in different companies. The results are listed in Table 4-9.

Table 4-9 Gloss measurement with different instruments

Company	Volvo	Renault	OCAS	IVECO	Brunel
Instrument	Panaspec	MicroGloss	Gloss 20	Gloss 20	QMS
Parameter	Gloss	Gloss	Gloss	Gloss	Gloss
A	85.3	80.5	83.4	81.4	67.9
B	86.8	84.3	86.0	84.8	48.3
C	90.9	86.3	88.7	87.4	54.1
D	117.4	86.5	89.9	89.4	84.6
E	90.3	88.8	90.1	88.0	62.4
F	90.3	88.2	89.1	87.6	57.8
G	94.9	88.9	93.0	92.0	65.4
H	86.2	82.9	84.8	83.0	76.0
I	87.0	85.7	83.7	82.6	36.0
J	82.6	80.8	82.2	79.6	61.5
K	94.6	91.1	91.4	89.8	50.6
L	115.1	88.4	90.4	88.6	47.7
M	87.1	84.3	85.8	83.2	58.7
N	96.1	91.5	91.4	90.8	29.3
O	83.6	72.2	82.8	81.3	38.4

P	91.6	86.3	86.1	87.4	56.1
Q	87.2	83.6	84.4	86.4	53.7
R	86.6	83.3	83.9	85.0	59.3
S	91.3	86.8	86.4	82.6	69.8
T	85.0	81.1	82.9	79.8	73.8

To compare the consistency of gloss measurement with different instruments, the correlation coefficients between them are calculated in Table 4-10.

Table 4-10 Correlation coefficient of Gloss

Company	Volvo	Renault	OCAS	IVECO	Brunel
Volvo	1.00	0.51	0.66	0.64	0.14
Renault		1.00	0.82	0.78	0.07
OCAS			1.00	0.92	0.07
IVECO				1.00	0.15
Brunel					1.00

As Ocas and Iveco use the same instrument (Gloss 20°), they have the highest correlation coefficient (= 0.9223). Gloss with QMS has the weakest correlation with other instruments (Gloss 20°, Panaspec and MicroGloss). MicroGloss has a strong correlation with Gloss 20° (= 0.8232). Panaspec only has a part correlation with Gloss 20° and MicroGloss. As the gloss measurements with Panaspec (Volvo) and QMS (Brunel) use image processing techniques, they do not have a good correlation with general gloss meters (MicroGloss or Gloss 20). The MicroGloss and Gloss 20 use the definition contained in ISO 2813, so the results have a good correlation with each other.

All the gloss results have not been found to have a good correlation with visual assessment. Fig. 4-11 is the distribution of gloss values versus visual assessment. It does not mean gloss is not important. One reason is that the gloss values on these

panels are at a high level (measured value is more than 80). The correlation between gloss and visual perception needs to be further studied.

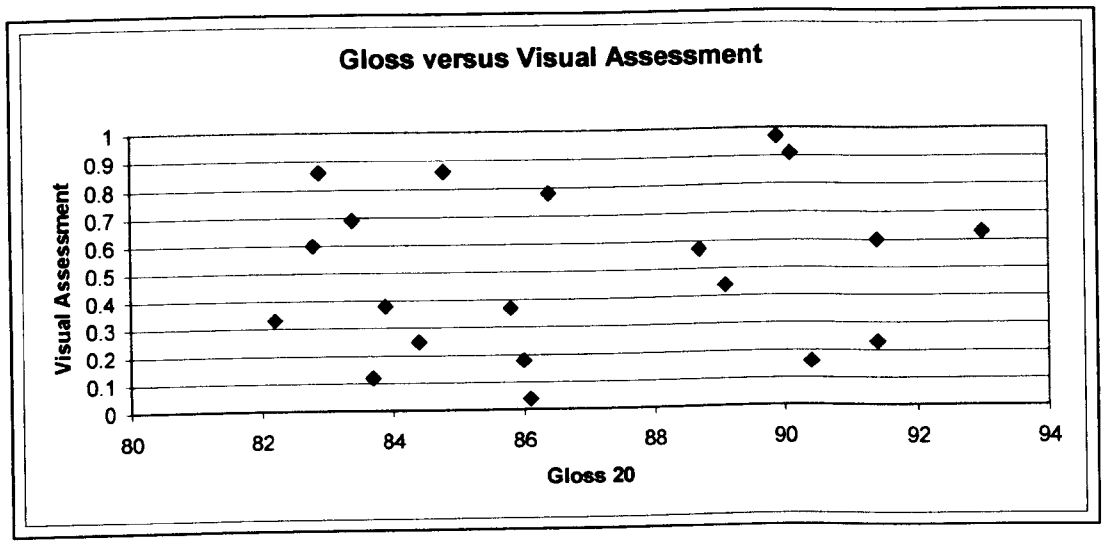

Figure 4-11 Gloss versus Visual Assessment

4.4.3. 2. DOI

Distinctness of image (DOI) is another often-used parameter to characterise the optical properties of paint appearance. Four instruments, Panaspec®, Visiopaint®, Dorigon II® and QMS®, were used to perform the measurements. The results are listed in Table 4-11.

Table 4-11 Distinctness of Image (DOI)

Company	Volvo	Renault	OCAS	Brunel
Instrument	Panaspec	Visiopaint	Dorigon II	QMS
Parameter	DOI	DOI	DOI	DOI
A	99.1	110.0	94.1	77.6
B	94.0	66.0	69.2	60.4
C	98.0	89.0	88.6	60.5
D	124.0	120.0	96.0	85.0
E	97.8	94.0	92.9	70.6
F	98.8	90.0	86.6	64.0
G	99.4	102.0	94.8	68.6
H	99.2	113.0	96.1	81.4
I	89.6	53.0	60.4	49.7
J	95.2	93.0	85.3	68.6
K	98.6	84.0	88.3	57.2
L	120.4	60.0	75.1	57.3
M	99.3	86.0	88.5	65.6
N	96.4	50.0	69.5	39.2
O	98.2	78.0	86.6	54.4
P	93.5	61.0	59.4	64.8
Q	98.6	71.0	82.1	63.2
R	99.0	95.0	88.2	67.8
S	99.0	116.0	93.5	77.8
T	99.3	115.0	96.9	82.0

The correlation coefficients are listed in Table 4-12, in which Panaspec (Volvo) has a very weak correlation with Visiopaint (Renault), Dorigon II (OCAS) and QMS (Brunel). But Visiopaint, Dorigon II and QMS have a good correlation with each other for DOI measurement.

Table 4-12 Correlation coefficient of DOI

Company	Volvo	Renault	OCAS	Brunel
Volvo	1.00	0.27	0.31	0.32
Renault		1.00	0.90	0.90
OCAS			1.00	0.70
Brunel				1.00

As these are different measurement methods, it is not certain which one is more reliable. So far no significant correlation has been found between DOI and visual assessment.

4.4.3. 3. Haze

Three instruments were used to measure Haze, which are Panaspec®, MicroGloss®, and HunterLab®. The results are listed in Table 4-13 with correlation coefficients in Table 4-14.

Table 4-13 Haze measurement result

Company	Volvo	Renault	Ocas
Instrument	Panaspec	MicroGloss	HunterLab
Parameter	Haze	Haze	Haze
A	0.15	13.52	0.48
B	2.06	53.78	1.42
C	0.38	30.42	0.14
D	0.5	69.94	0.3
E	4.04	130	1.64
F	0.32	23.96	0.22
G	0.48	37.5	0.28
H	0.2	20.34	0.24
I	1.36	53.9	0.6
J	0.06	15.1	0.06
K	0.46	21.94	0.28
L	0.6	33.52	0.02
M	0.4	22.66	0.22
N	0.28	21.96	0.14

O	0.3	115.76	0.28
P	0.16	25.76	20.98
Q	0.35	24.3	0.5
R	0.32	22.24	0.64
S	0.36	15.18	0.2
T	0.26	13.02	0.06

Table 4-14 Correlation Coefficient of Haze

		Company	Volvo	Renault	Ocas
		Instrument	Panaspec	MicroGloss	HunterLab
Company	Instrument	Parameter	Haze	Haze	Haze
Volvo	Panaspec	Haze	1.00	0.70	0.05
Renault	MicroGloss	Haze		1.00	0.04
Ocas	HunterLab	Haze			1.00

For haze measurement, the results are far away from consistent; this is mainly because the definition and measurement methods are different from each other. Also there is no correlation found with visual assessment. An international standard for haze measurement is highly desirable.

4.4.4. Overall Appearance

Overall appearance is an integrated parameter which combines individual parameters to a whole assessment of paint appearance. It should include all the aspects of appearance properties. Two empirical formulae described in Equations (2-4) and (2-5) regarding overall appearance are compared with visual assessment in this section.

4.4.4.1. Overall Appearance with QMS

QMS provides us an empirical overall appearance formula combining Gloss, DOI and Orange peel (see Equation 2-4). Assuming linear relationship between overall appearance and individual parameters, this formula just assigns an index to each parameter. To test the Equation 2-4, the correlation between Overall Appearance and visual assessment (professional and non-professional) is plotted in Fig. 4-15 and 4-16.

The Overall Appearance derived from Equation 2-4 still has a good correlation with visual assessment (correlation coefficient $\rho_1 = 0.94$ for professional, and $\rho_2 = 0.90$ for non-professional). But the correlation is much weaker than that in Fig. 4-8 ($\rho = 0.99$), which means the individual parameter, orange peel, has a stronger correlation with visual assessment than the combination of all the parameters (Equation 4-4). As the orange peel is more likely to have a linear relation with visual perception, the gloss and DOI are obviously not found to have a linear correlation with visual perception. It is concluded that it is not sufficient to treat the overall appearance as a simple combination of different indices.

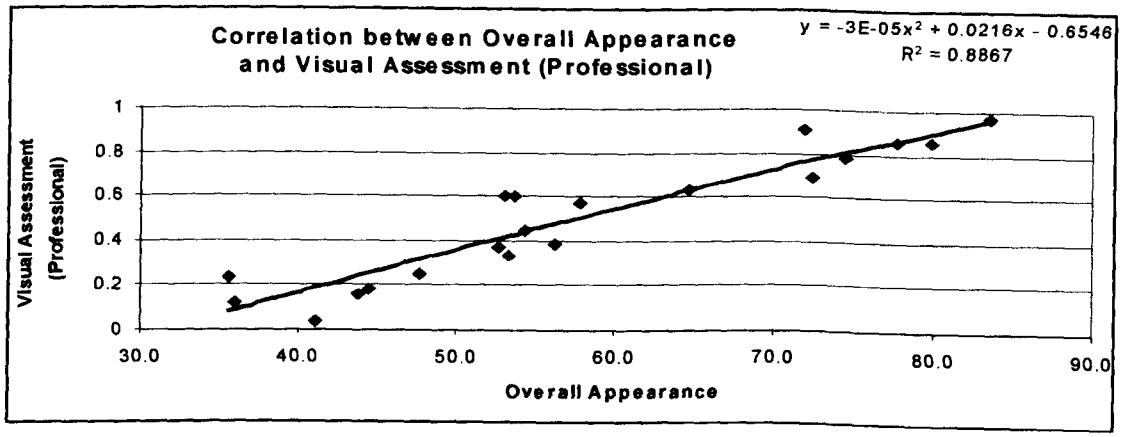

Fig. 4-15 Correlation between Overall appearance (QMS) and Visual Assessment (Professional)

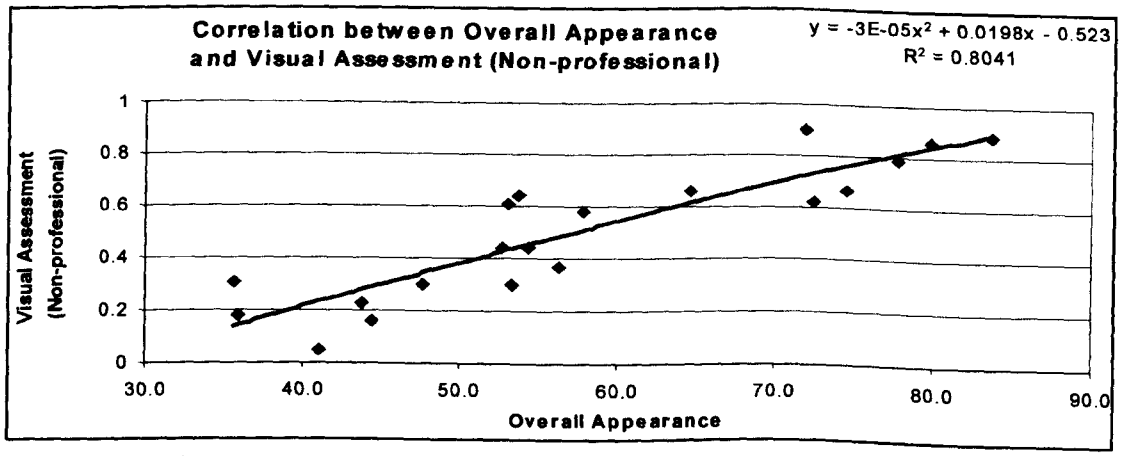

Fig. 4-16 Correlation between Overall appearance (QMS) and Visual Assessment (Non-professional)

4.4.4.2. Appearance Index from OCAS

Another experimental formula called the appearance index is from OCAS (Equation 2-5), which combines parameters of Gloss, DOI, NSIC*, and NSIC. It still works in the same way to assign indices to each individual parameter. The difference is that these parameters are measured with different instruments. Gloss is measured with Gloss 20®, DOI is from Dorigon II®, and the NSIC*, NSIC are from Suga®.

To verify AI's correlation with visual perception, the correlation of the AI with the visual assessment (professional and non-professional) are depicted in Fig. 4-17 and 4-18, in which the correlation coefficients are 0.95 and 0.93 respectively for professional group and non-professional group.

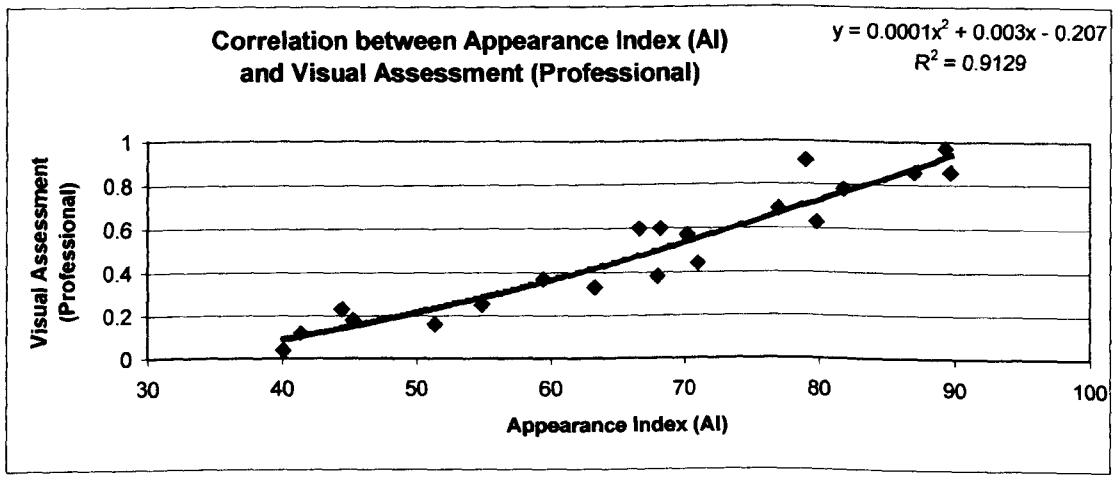

Fig. 4-17 Correlation between AI and Visual Assessment (Professional)

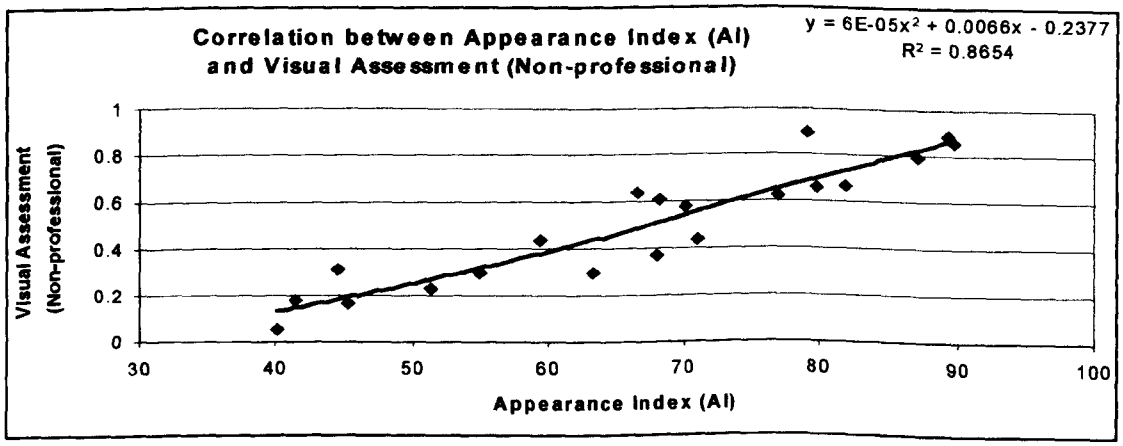

Fig. 4-18 Correlation between AI and Visual Assessment (Non-professional)

Compared with Fig. 4-7, the Appearance Index has a better correlation with visual perception than the individual parameter, NSIC* (ρ=0.93). But AI still considers all the individual parameters to have a linear correlation with visual perception.

4.5. Conclusion

From the results of this Round Robin Test, a clear understanding of the situation in the area of appearance measurement has emerged. The following conclusions can be drawn:

1. The current appearance measurement is far away from a standard. Due to the different understanding, definitions and measurement methods of parameters, there are many duplicated parameters. For example, the long wave property of a surface has been named tension, orange peel, NSIC*, LW, so on. On the other hand some parameters, like gloss, have the same name, but different results due to the different measurement methods. Desirably, these parameters need to be standardised in the automotive industry.
2. Orange peel has been verified to be a dominant factor in appearance measurement. But there are no standard definition and measuring method specified for it. The measurement framework for paint appearance measurement in the automotive industry has not yet been set up. Car manufacturers still use different ways to measure paint appearance, and have their own standards to control paint quality.
3. Overall appearance cannot reflect all the aspects of individual appearance properties. The index method is too simple to resolve the multiple-input, non-linear system problem. A new method needs to be developed to model the appearance measurement system.
4. To identify the causes of orange peel and metal texture, orange peel and metal texture should be evaluated separately.
5. Gloss and Haze have not been found to have a direct correlation with visual perception.

Chapter 5

Evaluation of the 'Orange Peel' Effect on Paint Appearance

5. 1. Introduction

According to the conclusion of the last chapter, the orange peel or long wave characteristic is a major parameter driving the quality of paint appearance in the automotive industry. Most instruments can only measure orange peel as a single parameter. In industry, the overall phenomenon of orange peel is often divided into two types according to the cause. In this chapter, the so-called 'orange peel' is split into two terms 'orange peel', which is usually the dominant one, and the 'metal texture effect'. The orange peel is considered as a large scale pattern (visible wavelength between 1mm-10mm) and is due to paint / coating properties (viscosity, paint flow, thickness of film, and whether the coating is waterborne or solvent based) and painting procedure (the distance of the paint gun/bell from the product, fluid flow, temperature and humidity conditions, baking position and conditions of application). The metal texture effect is considered to be the small scale patterns (visible wavelength between 0.1mm-1mm) which are completely caused by the surface topography of the substrate (roughness and waviness).

Both orange peel and metal texture are considered as surface topography properties. They have two aspects in common and another two points of difference.

Common:

1. Both of them are not simply physical profiles of the surface, but optical reflected phenomena on the painted surface that can be seen with the naked eye with the aid of a structured light source.
2. They have effects on the paint appearance.

Differences:

1. The cause is different. Orange peel is often believed to derive from paint/coating properties and painting procedure. The metal texture effect is completely caused by surface topography, especially texture.
2. The effect is different. The wavelength of orange peel is larger than that of the texture effect. The paint appearance is more likely to be sensitive to the orange peel effect. But at a reduced level of orange peel, the overall appearance could be mainly influenced by the metal texture effect.

The relationship between orange peel and metal texture is that the metal texture can affect the paint procedure adopted and cause orange peel, but it is not a critical factor for orange peel. The occurrence of a high level of orange peel is mainly due to improper control of the paint procedure or paint properties even if the metal texture is very smooth. When there is a large amount of orange peel, the metal texture effect is less prominent. When there is no orange peel, the metal texture effect becomes more obvious to paint appearance.

The reasons for separating the orange peel and metal texture effects areas follows:

a). Due to the different causes, the separation of the orange peel and metal texture effect can help us to determine clearly which is the major fact driving the paint appearance. Not only the values could be measured, but also the type of the parameters could be indicated. This makes it easier to find out how to improve paint quality.

b). In industry, paint surface is often assessed by the human eye to distinguish the orange peel and the metal texture effect. Orange peel is relatively easy to assess compared with the metal texture effect, which is time-consuming and not reliable. If the orange peel and metal texture effect could be measured separately and automatically with an instrument, it would be timesaving, more reliable and consistent.

c). The wavy pattern can be visually seen between 0.1mm and 10 mm. If they are evaluated together, the small wavy (texture effect) could not be well determined. Evaluating them separately can help us to see their effects more clearly.

The phenomenon of 'orange peel' and 'metal texture effect' are both considered as the structured properties of the paint surface. In this chapter, an image processing system is set up to measure the quality of paint appearance. The orange peel and metal texture effect are measured separately using the techniques of filter design and Fast Fourier Transforms (FFT). The preliminary results showed that this system could effectively evaluate both the orange peel and metal texture effects.

5.2. Painting film structure

To study the visual phenomena, it is necessary to understand the painted film structure. As mentioned previously, the paint film has four to five layers of coating. Before examining the paint film structure, the general painting procedure in the automotive industry will be described in Table 5-1 [Praschan 1995].

Table 5-1 Painting procedure of motor body

Stage	Procedure	Thickness (μm)	Ra (μm)
Stage 1	**Pre-treatment** (Cleaning with mild alkali) Rinse Conditioner (titanium) Full immersion (phosphate process with Zinc, Iron & Phosphate) Rinse Spray (Chrome passivation) Dry off (Oven)		0.8 – 1.3
Stage 2	**Electrocoat** Full immersion (electrostatic process, corrosion resistance) Visual inspection – rectification (disking etc.) Seam sealing (mastic material)	20-30	0.5
Stage 3	**Primer/surfacer** Spray – electrostatic 2 coats – wet on wet Anti-chip coating Dry off (Oven) Rectification (sanders etc.)	40-50	0.25
Stage 4	**Base coat** (Colour booth) Two base coats (wet on wet) Spray – electrostatic plus hand spraying Quick dry off (removing excess solvent)	30-50	0.1
Stage 5	**Clear coat** Two coats (wet on wet) Spray – electrostatic Oven (half hour, 130-140 ^{0}C) Rework (polishing)	50	0.05

*Ra is defined as the mean departure of the profile from the mean reference line (see chapter 6)

From the painting procedure above, we can see that the paint film structure on a car body is a multi-layer system (see Fig 5-1).

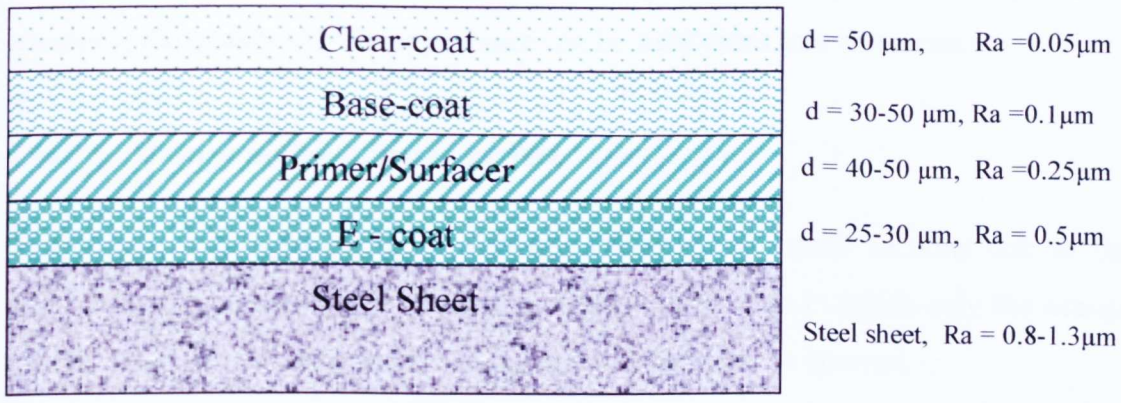

Figure 5-1 Paint film structure

Typically, there are four coating layers. As the top layer is a clear coat, most reflection happens at the second layer (see Fig. 5-2). As the thickness of each coating is small, the topography of the steel texture can be still seen under four coating layers. It is not simply the original steel texture, but a modification of it called the 'metal texture effect'. The interaction between each coating is the main reason for the orange peel phenomenon. Due to the paint flow ability, the high degree of roughness on each layer can cause large orange peel even if the steel surface is quite smooth. Normally the clear-coat is very smooth (Ra=0.05μm) so that measuring the profile would not reveal the visual effect.

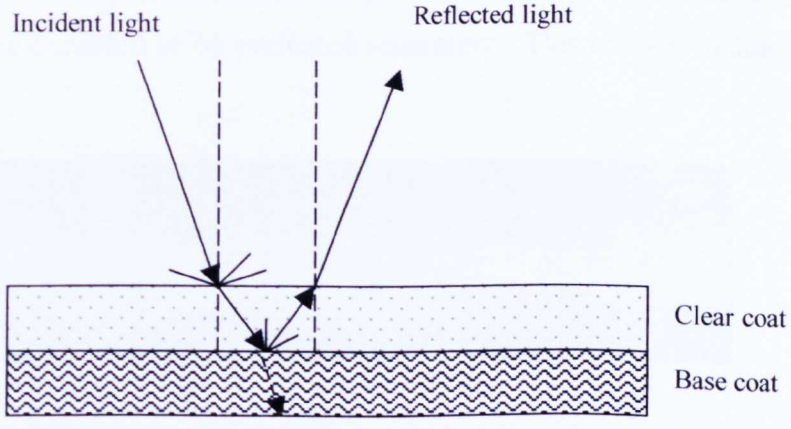

Figure 5-2 Light reflection on painting surface of car body

5.3. Orange Peel Classification

To separate the effect of metal texture from orange peel and improve the measurement accuracy, the quality of paint appearance can be subdivided into three cases

Case A. Orange peel dominated surface

In this case, the reflected image has been isolated into small sections due to the irregularity of the coatings (Fig. 5-3). It is an extreme case in which only the orange peel needs to be evaluated and the metal texture effect can be ignored.

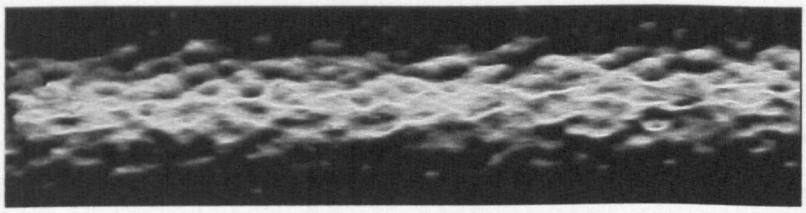

Figure 5-3 Reflected fluorescent tube on orange peel dominated paint surface.

Case B. Orange peel and metal texture co-occurrence surface

In this case, as orange peel is not at a high level, both orange peel and metal texture effects can be seen on the paint surface (Fig. 5-4). The effects from orange peel and metal texture are expected to be evaluated separately. This chapter mainly deals with this case.

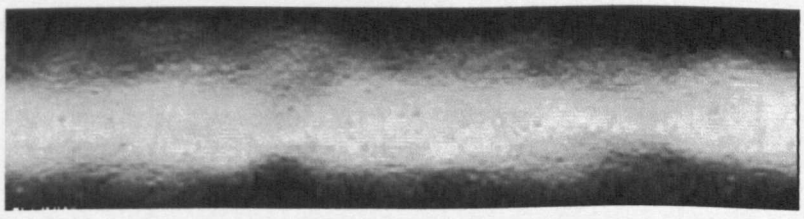

Figure 5-4 Reflected fluorescent tube on paint surface with both orange peel and metal texture.

Case C. Metal texture dominated surface

With improvements in painting procedure, the orange peel effect can be reduced. In this case the paint appearance is dominated by the metal texture effect (Fig. 5-5), only metal texture effect needs to be evaluated.

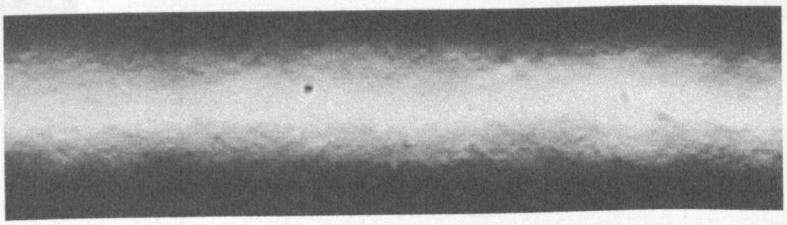

Figure 5-5 Reflected fluorescent tube on metal texture dominated paint surface

To accurately measure the orange peel and metal texture effect, case A needs to be separated from cases B and C first. Then the orange peel and metal texture effect can be separated and evaluated in cases B and C. For case A, only orange peel needs to be measured.

5.4. Image signal Processing

5.4.1. Image Acquisition

An image processing system is used to simulate visual perception. It includes an illumination system, a CCD camera, an image frame grabber and a signal processing system (PC). The image captured is a 768×576 array with 256 grey levels. The illumination system still uses a fluorescent tube source, which has been modified to provide several illuminated stripes.

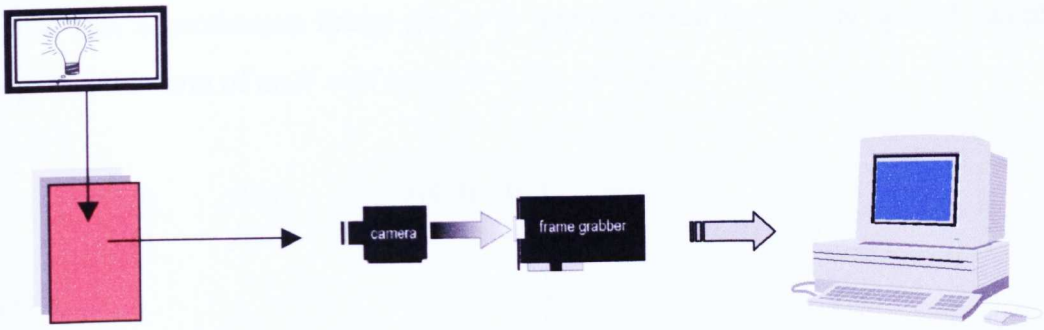

Figure 5-6 Image acquisition system

The image can be described as a two-dimensional light intensity function *f(x, y)*, where *x* and *y* denote spatial coordinates and the value of f at any point *(x, y)* is proportional to the brightness (or grey level) of the image at that point. Figure 5-7 illustrates the axis convention used in this system. A digital image is an image *f(x, y)* that has been discretized both in spatial coordinates and brightness. A digital image can be considered a matrix whose row and column indices identify a point in the image and the corresponding matrix element value identifies the grey level at that point. The elements of such a digital array are called image elements, or pixels [Gonzalez, 1992].

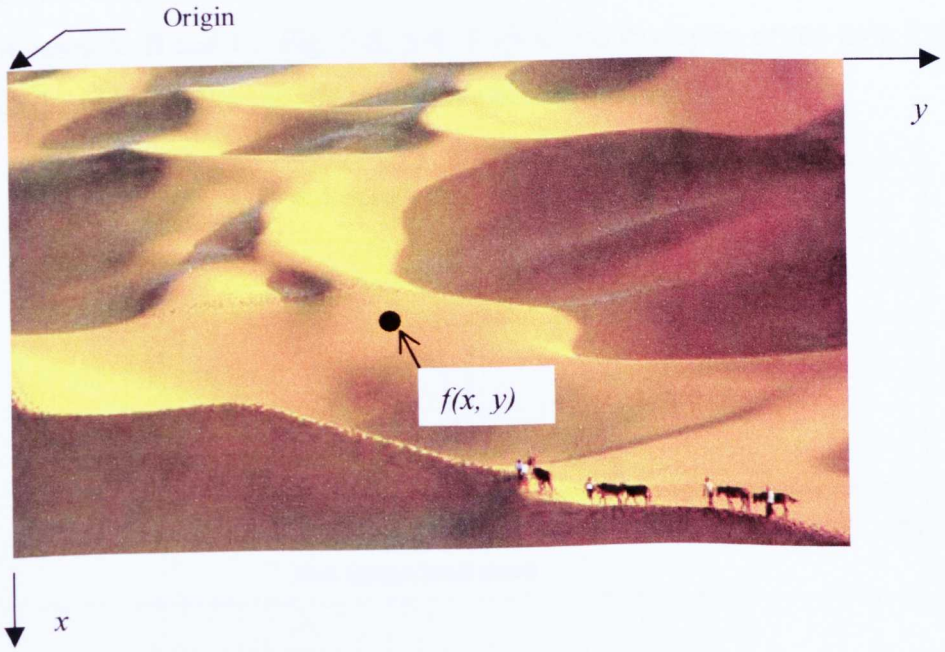

Figure 5-7 3-D image signal conventional coordinate

Suppose that a continuous image $f(x, y)$ is approximated by equally spaced samples arranged in the form of an $N \times M$ array, $0 < f(x, y) < 255$.

$$f(x,y) \approx \begin{vmatrix} f(0,0) & f(0,1) & \dots & f(0,M-1) \\ f(1,0) & f(1,1) & \dots & f(1,M-1) \\ \cdot & & & \\ \cdot & & & \\ \cdot & & & \\ f(N-1,0) & f(N-1,1) & \dots & f(N-1,M-1) \end{vmatrix}$$

5.4.2. Image Profile

To simplify the signal processing procedure and reduce the measurement time, the image profiles were extracted across the reflected fluorescent tube. As the image profile is a one-dimension spatial signal and has sufficient information to characterise the surface topography properties, it is convenient and efficient to use one-dimensional digital signal processing techniques to deal with it.

First of all, the image profile across the reflected fluorescent tube is extracted from the images of cases A, B and C. Fig. 5-8, 5-9, 5-10 shows examples of the light intensity profiles of the reflected fluorescent tube in the cases A, B, and C.

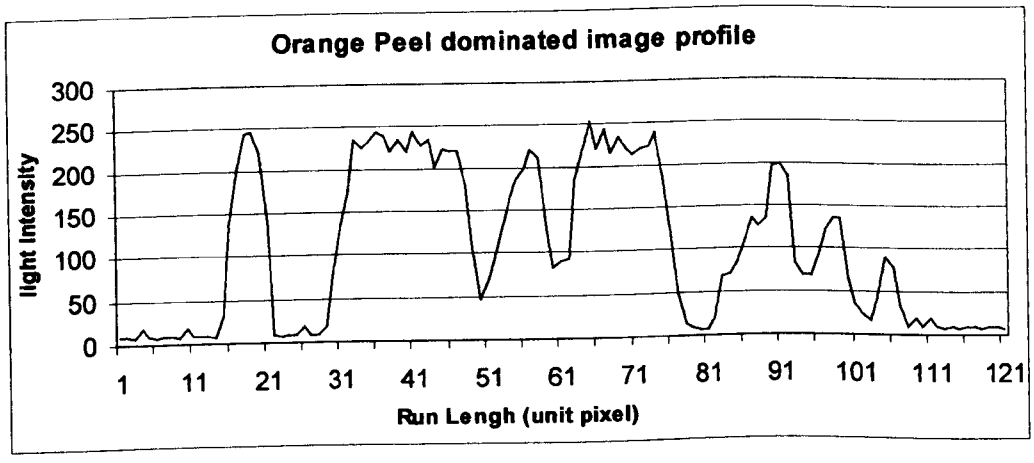

Figure 5-8 Orange peel dominated image profile (case A)

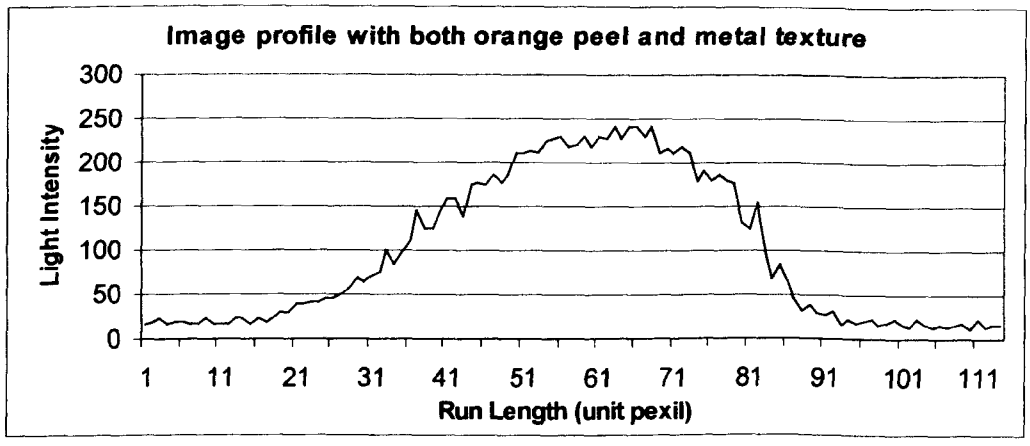

Figure 5-9 Image profile with both orange peel and metal (case B)

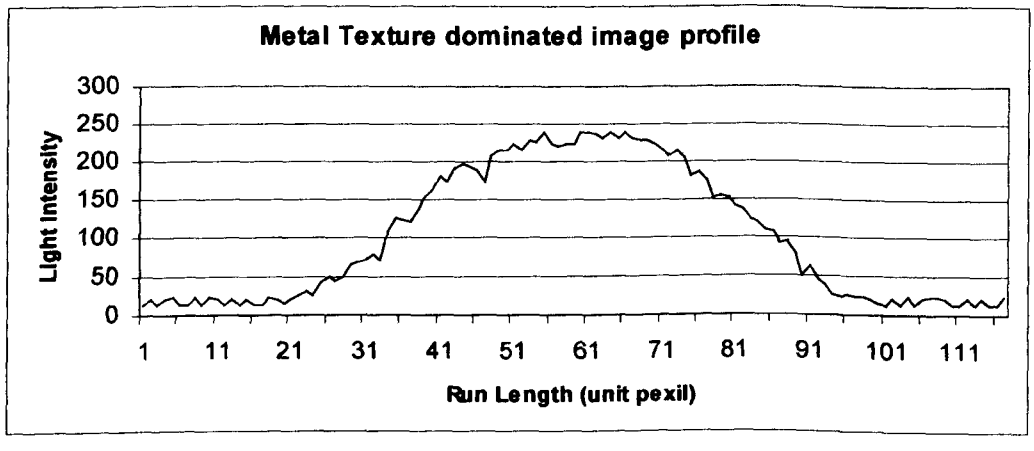

Figure 5-10 Metal texture dominated image profile (case C)

From Fig. 5-8, 5-9 and 5-10, it can be seen that case A can be easily recognised from case B and C from the image profile signal. For case A, the image has been broken into sections. The light intensity signal can be thought of as multi-frequency combined spatial signal, in which the light intensity represents the amplitude and the length between peaks of light intensity represents the wavelength. So the orange peel effect can be evaluated from the image profile signal. For cases B and C, as the changes of light intensity ride on the light bar, the texture effect can be evaluated with the designed filter. But the orange peel in case B cannot be assessed in this way. It can be evaluated in another way, called edge distortion detection.

5.4.3. Separation of Orange Peel Dominated Surface (case A)

To separate the orange peel dominated surface (case A) from the other two cases, B and C, the image profiles described above can be used for this purpose as an input signal. The signal processing techniques such as FFT and filters are used on this purpose.

5.4.3.1. Space-domain signal

The image profile signal can be treated as a discrete space-domain signal in which each pixel is a sampling point and the distance between two neighbouring pixels is the interval of the sampling signal (Fig. 5-11).

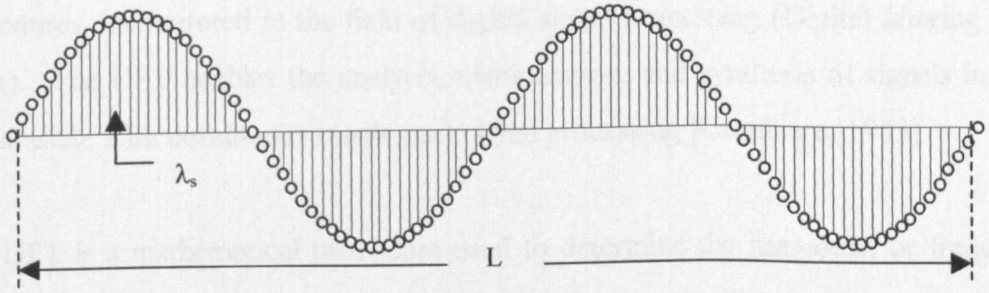

Figure 5-11 Discrete space-domain signal

As it is a spatial signal, the wavelength of the sampling signal can be obtained from:

$$\lambda_s = \frac{L}{N-1} \tag{5-1}$$

Where L is the length of the real object, N is the number of pixels over length L.

If the distance between object and camera is 0.5m, an object of length 116mm is presented by 576 pixels in the image. So the wavelength of the sampling signal is 0.2mm. Keeping the distance to 0.5m (because it is the normal distance between a panel and the human eye when viewing panels), then adjusting the magnification and focusing on the surface, the wavelength of the sampling signal can be set at 0.1mm.

As this is a spatial signal, the signal spreading speed has no meaning. The sampling frequency f_s can be calculated from the formula below.

$$f_s = \frac{1}{\lambda_s} \tag{5-2}$$

So if the wavelength of sampling signal, λ_s=0.1mm, the sampling frequency is 10,000 cycles/meter.

5.4.3.2. Discrete Fourier Transform (DFT)

The discrete Fourier transform (DFT) is one of the two most common, and powerful, procedures encountered in the field of digital signal processing (Digital filtering is the other). The DFT enables the analysis, manipulation, and synthesis of signals in ways not possible with continuous (analogue) signal processing [Crochiere, 1983].

The DFT is a mathematical procedure used to determine the harmonic, or frequency, content of a discrete signal sequence. DFT is defined as the discrete frequency-domain sequence *X(m)*,

$$X(m) = \sum_{n=0}^{N-1} x(n) e^{-j\frac{2\pi nm}{N}} \tag{5-3}$$

$$= \sum_{n=0}^{N-1} x(n)[\cos(2\pi nm / N) - j\sin(2\pi nm / N)]$$

where, *X(m)* is the m^{th} DFT output component.

m is the index of the DFT output in the frequency domain, *m=0, 1, 2, ..., N-1.*

x(n) is the sequence of input samples.

n is the time-domain index of the input samples, $n=0, 1, 2, ..., N-1$,

$j = \sqrt{-1}$.

N = the number of samples of the input sequence and the number of frequency points in the DFT output.

In this case, the number of input samples and the number of DFT outputs are the same $(=N)$. If the sampling frequency is f_s, then the analysis frequencies (the resolution of the frequency axis in DFT) are

$$f_{analysis}(m) = \frac{mf_s}{N} \tag{5-4}$$

The DFT is the most straightforward mathematical procedure for determining the frequency content of a time-domain sequence. But the calculation is very inefficient. For an N-point DFT, we have to perform N^2 complex multiplications. The FFT (Fast Fourier Transform) is a very efficient algorithm to implement the DFT. For an N-point DFT, the number of complex multiplications is approximately, $\frac{N}{2}\log_2 N$. The number of complex multiplications has been significantly reduced. The FFT is not an approximation to the DFT, it is exactly equal to the DFT.

The FFT can be directly evolved from the DFT [Lyons, 1997]. Here only the final result is presented.

$$X(m) = \sum_{n=0}^{(N/2)-1} x(2n)\, W_{N/2}^{nm} + W_N^m \sum_{n=0}^{(N/2)-1} x(2n+1)\, W_{N/2}^{nm} \tag{5-5}$$

$$X(m+N/2) = \sum_{n=0}^{(N/2)-1} x(2n)\, W_{N/2}^{nm} - W_N^m \sum_{n=0}^{(N/2)-1} x(2n+1)\, W_{N/2}^{nm} \tag{5-6}$$

where, $W_N^m = e^{-2\pi m / N}$

From the Equations 5-5 and 5-6, it is not necessary to perform any sine or cosine multiplication to get $X(m+N/2)$. We just change the sign of the factor W_N^m and use the results of the two summations from $X(m)$ to get $X(m+N/2)$. This is the basic principle of FFT. A N-point DFT ($N=2^k$, k=1, 2, ...) can be broken into a number of 2-point DFT, so the calculation time can be significantly reduced.

With the FFT method, the DFT can be effectively obtained. Then the frequency (wavelength) distribution of the image profile can be plotted. Here 512 points FFT was performed for each case. As the symmetric property of FFT, only half FFT result (256 points) is presented, which the frequency axis is normalised with the Nyquist frequency $\frac{f_s}{2}$. As the differences are mainly in the first 1000 cycles/meter, Figures 5-16 to 5-18 show the frequency distribution for only the first 52 points (0 to 1000 cycles/meter). Comparing the magnitude of DFT in each case the orange peel dominated case can be separated from cases B and C.

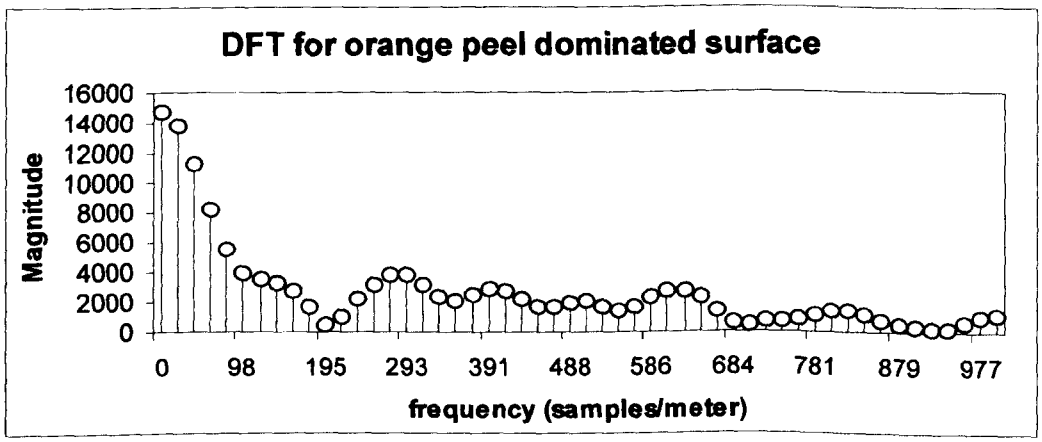

Figure 5-16 DFT of orange peel dominated surface (case A)

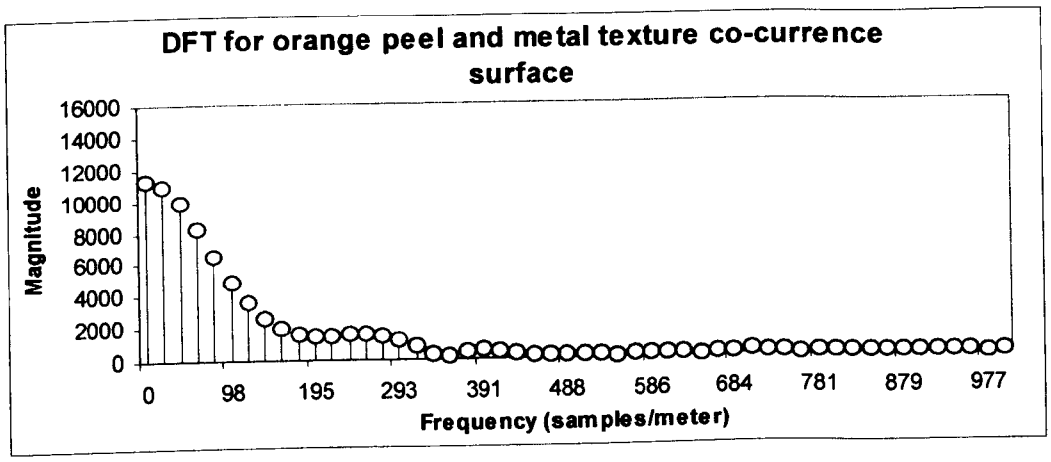

Figure 5-17 DFT of orange peel and metal texture co-occurrence surface (case B)

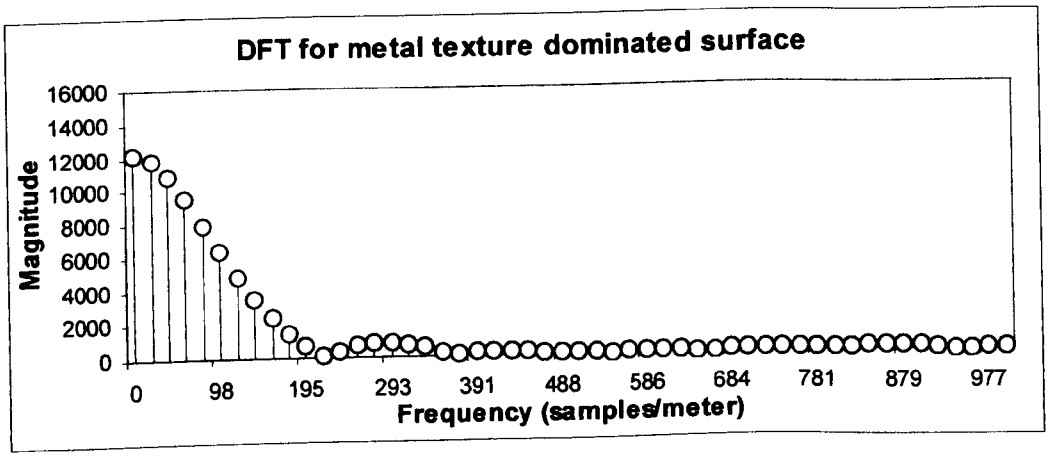

Figure 5-18 DFT of metal texture dominated surface (case C)

If the surface is dominated by orange peel, the magnitude of the frequency component between 200 to 1000 cycles/meter (wavelength between 5 mm to 1mm) is much higher than those in cases B and C. Table 5-1 shows the DFT average magnitude in case A, B and C.

Table 5-1. Average magnitude of DFT

Frequency (Cycles/meter)	100-200	200-1000
Wavelength (mm)	10-5	5-1
Case A	*2887*	*1516*
Case B	*3945*	*309*
Case C	*4349*	*279*

The DFT magnitude for which the frequency is distributed between 200-1000 cycles/meter in case A is nearly four times higher than in cases B & C. So case A can be easily separated from case B & C according to the magnitude of DFT in the frequency range 200 to 1000 cycles/meter. The DFT magnitude in the range 100 to 200 cycles/meter of cases B and C is larger than that in case A, because the image profiles in case B and C are based on a reflected fluorescent tube (Figure 5-4 and 5-5). A large frequency component (wavelength 5-10mm) exists for them.

5.4.3.3. Digital Filtering

In general, filtering is the processing of a signal resulting in some change in that signal's original content. The change is usually the reduction, or filtering out, of some unwanted input spectral components. Traditionally linear digital filters are of two types: finite impulse response (FIR) filters and infinite impulse response (IIR) filters.

Finite Impulse Response Filters

FIR digital filters use only current and past input samples, and none of the filter's previous output samples, to obtain a current output sample value. (That's why FIR filters are sometimes called nonrecursive filters.) Given a finite duration of nonzero input values, the effect is that a FIR filter will always have a finite duration of nonzero output values. If the FIR filter's input values suddenly becomes a sequence of all zeros, the filter's output will eventually be all zeros.

For a general M-tap FIR filter, the n^{th} output is

$$y(n) = \sum_{k=0}^{M-1} h(k)x(n-k) \tag{5-7}$$

This is the convolution equation as it applies to a digital FIR filter.

and analyse, and do not have linear phase responses. However, they are very efficient. IIR filters require far fewer multiplications per filter output to achieve a given frequency magnitude response. From a hardware standpoint, this means that IIR filters can be very fast, allowing the build up of real-time IIR filters that operate over much higher sample rates than FIR filters.

The IIR filter can be analysed with the z-transform. More details can be referenced in [Lyons, 1997]. The frequency response of an Mth-order IIR filter (exponential form) is shown in Equation (5-9) and the structure in Figure 5-20.

$$H_{IIR}(w) = H(z)\Big|_{z=e^{jw}} = \frac{\sum_{k=0}^{N} b(k)e^{-jkw}}{1 - \sum_{k=1}^{M} a(k)e^{-jkw}} \tag{5-9}$$

where, *a(k)* is the feedback coefficient.

b(k) is the feed forward coefficient.

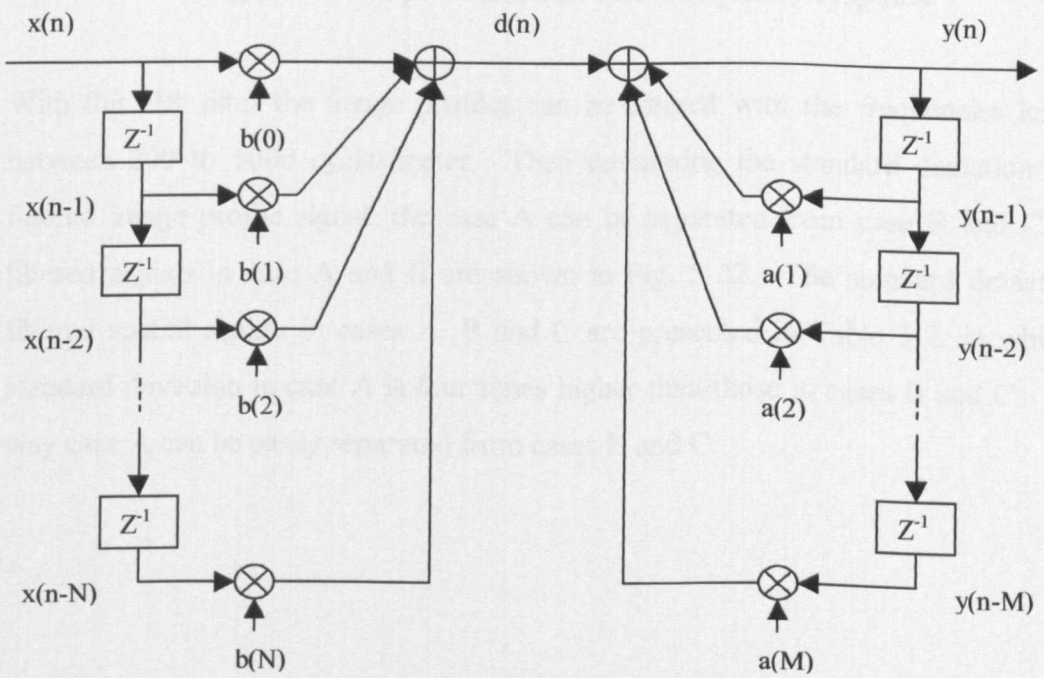

Figure 5-20 IIR filter structure

An important character of the z-plane is that the region of filter stability is mapped to the inside of the unit circle on the z-plane ($|z|<1$). If all poles are located inside the unit circle, the filter will be stable.

An eighth order IIR filter with a passband from 200 to 1000 cycles/meter was designed [Matlab, 1998] to filter the image profile signal in cases A, B and C. The frequency response for this filter is showed in Fig. 5-21.

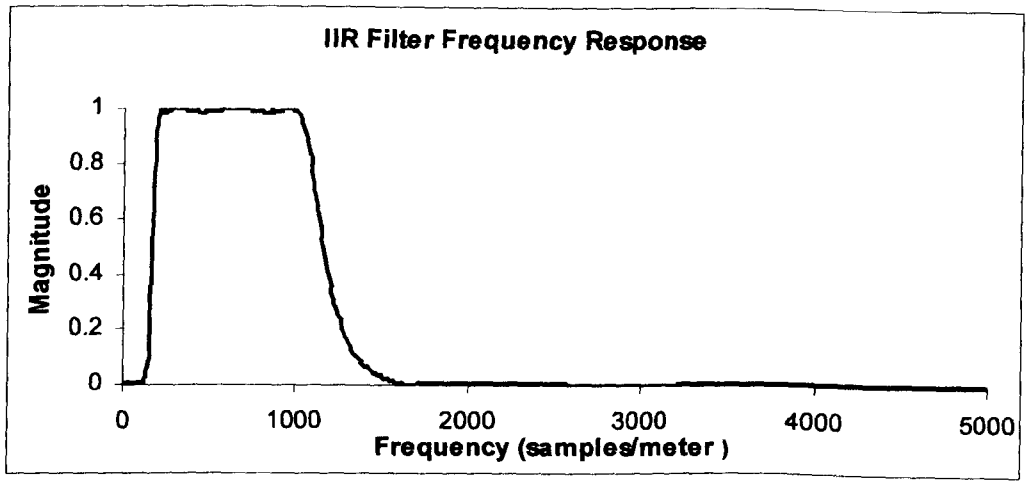

Figure 5-21 A passband IIR filter frequency response

With this IIR filter the image profiles can be filtered with the frequencies left only between 200 to 1000 cycles/meter. Then comparing the standard deviation of the filtered image profile signal, the case A can be separated from case B and C. The filtered signals in case A and B are shown in Fig. 5-22. The standard deviation of filtered spatial signals in cases A, B and C are presented in Table 5-2, in which the standard deviation in case A is four times higher than those in cases B and C. In this way case A can be easily separated from cases B and C.

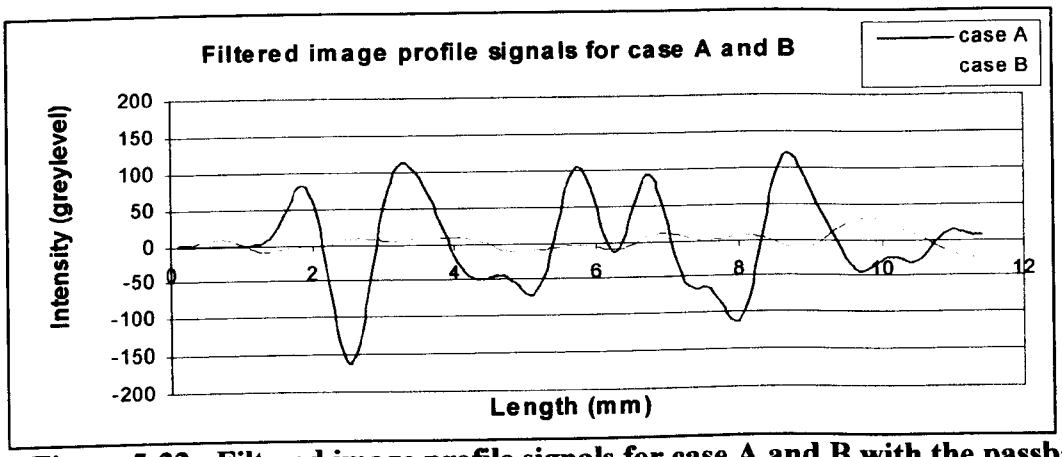

Figure 5-22. Filtered image profile signals for case A and B with the passband filter from 200 to 1000 cycles/meter.

Table 5-2. Average standard deviation of filtered spatial signal in case A, B & C

Frequency Range (cycles/meter)	200 - 1000
Wavelength (mm)	1 - 5
Case A	52.15
Case B	10.36
Case C	9.26

With DFT and filtering techniques the orange peel dominated surface (case A) can be effectively separated from the other two cases B and C. The evaluation of the orange peel effect in case A can be directly compared with the standard deviation of the filtered signal between 200 and 1000 cycles/meter. The evaluation for cases B and C will be presented in next section in which the orange peel and metal texture effect will be evaluated separately.

5.4.4. Evaluation of metal texture and orange peel

After the separation of case A from cases B and C, the concern is focused on how to evaluate the metal texture and orange peel effect in the situation of cases B and C. In

these two cases, the metal texture effect and orange peel effect are desired to be evaluated separately. Actually cases B and C can be evaluated together. The only difference between them is that the level of orange peel effect is much less in case C than in case B. In this section two methods are introduced to evaluate the metal texture effect and one method is presented for orange peel assessment.

5.4.4.1. Evaluation of Metal Texture

IIR filter

An IIR filter was designed with a high pass from 1000 cycles/meter (1mm and below) [Matlab, 1998]. The frequency response of this filter is displayed in Fig. 5-23.

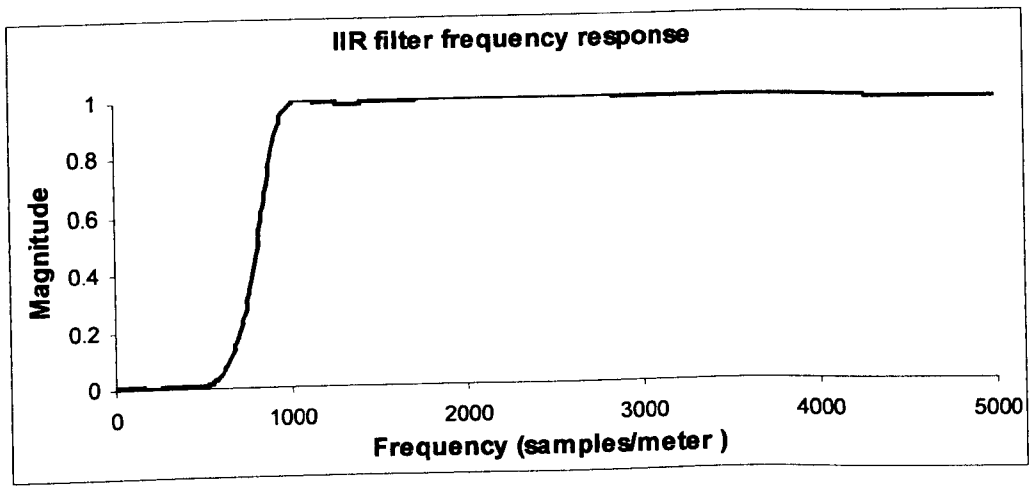

Figure 5-23. Frequency response for a high pass IIR filter

With this filter the light bar can be filtered out from the image profile. A filtered image profile in case C is illustrated in Fig. 5-24 in which the wavelengths between 0.2mm and 1mm are left. The metal texture can then be evaluated by comparing the standard deviation of the filtered signal.

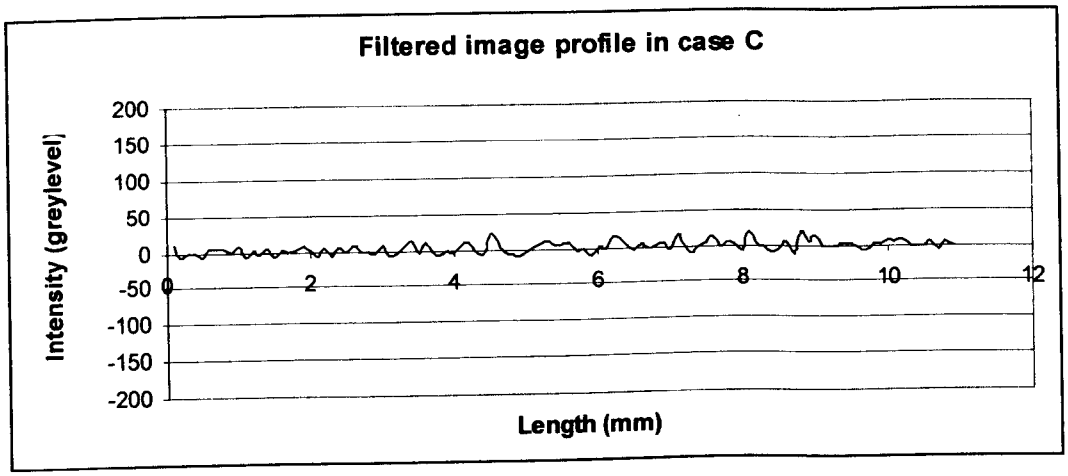

Figure 5-24. Filtered image profile in case C

$$Metal\,Texture\,Effect = Std[P_f(x)]$$

$$= \sqrt{\frac{n\sum P_f{}^2(x) - \left(\sum P_f(x)\right)^2}{n(n-1)}} \qquad (5\text{-}10)$$

where, $P_f(x)$ is filtered image profile signal

$Std\,[\,]$ is the operation of standard deviation

n is the number of samples in $P_f(x)$

In this case (Fig. 5-26), the standard deviation is 6.28. The value of the metal texture effect is 6.28.

Intensity Difference

As the human eye is sensitive to the difference of light intensity between neighbouring regions, we can directly compare the intensity difference between these regions by comparing the output from neighbouring pixels, then calculate the standard deviation of the intensity difference. As the metal texture effect can be viewed with the aid of fluorescent light, to evaluate the metal texture effect, we need to remove the effect of the light. As the intensity of the light bar is not fixed (Fig. 5-10), the intensity

difference can be calculated by comparing the difference of light intensity between each pixel and its average neighbours on the image profile.

$$D_I(x) = abs[I(x) - \frac{1}{2m+1}\sum_{i=x-m}^{x+m} I(i)] \qquad (5\text{-}11)$$

Where, $D_I(x)$ is the light intensity difference in pixel x.

$I(x)$ is the intensity in pixel x.

m is the number of pixels away from x.

$\frac{1}{2m+1}\sum_{i=x-m}^{x+m} I(i)$ is the average light intensity in pixel x with its 2m+1 neighbouring pixels.

The difference between original and average profiles can well reflect the metal texture effect to the human eye. The metal texture effect can then be calculated with the standard deviation of the intensity difference signal.

$$Metal\,Texture\,Effect = Std[D_I(x)]$$

$$= \sqrt{\frac{n\sum D_I{}^2(x) - \left(\sum D_I(x)\right)^2}{n(n-1)}} \qquad (5\text{-}12)$$

where, $D_I(x)$ is light intensity difference signal

$Std\,[\ ]$ is the operation of standard deviation

n is the number of samples in $D_I(x)$ signal

Fig. 5-25 shows the original image profile and the average profile in case C. Fig. 5-26 is the light intensity difference in case C, in which the level is similar to Fig. 5-24. The standard deviation of the intensity difference in Fig. 5-26 is 4.04.

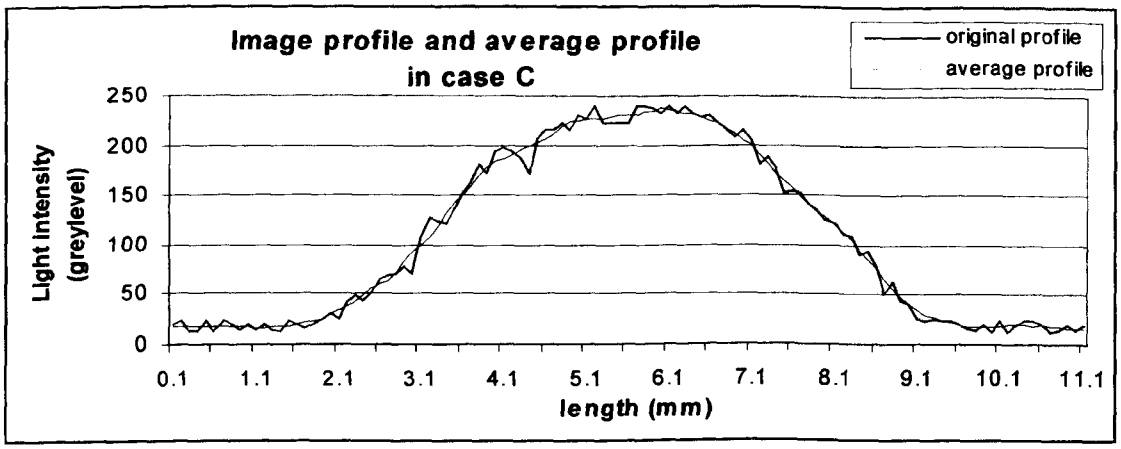

Figure 5-25 Image profile and its average profile in case C

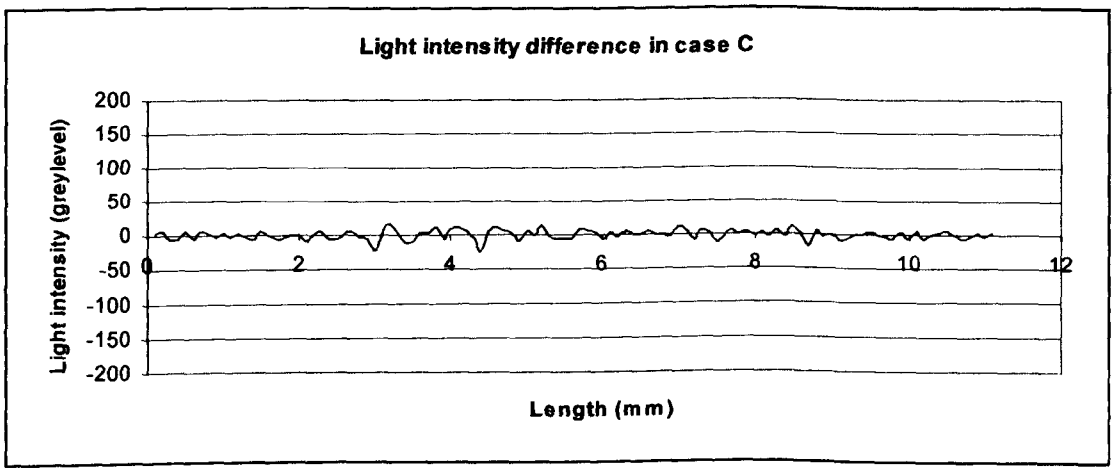

Figure 5-26 Light intensity difference in case C

With these two methods, high-pass filtering and intensity difference, the metal texture effect can be effectively extracted and evaluated, which has a good correlation to human visual assessment. The test result will be presented in section 5.5.

5.4.4.2. Evaluation of Orange Peel

The evaluation of orange peel can be divided into two different situations. Case A is an extreme case, in which the orange peel effect is high enough to break the image into sections. In this case the orange peel is evaluated with the standard deviation of the

image profile. In cases B and C, the orange peel effect is in the middle level or low level. The effect can be only observed on the edge distortion of the reflected image. Here we present one evaluation method for each situation.

Case A

After the separation of case A from cases B and C, the orange peel can be evaluated with the filtered image profiles. The filter's frequency response is depicted in Fig. 5-21, in which the pass band is from 200 to 1000 Cycles/meter (wavelength 1mm to 5mm). The orange peel effect is the standard deviation of the filtered image profiles.

$$OP = Std[P_f(x)] = \sqrt{\frac{n\sum P_f{}^2(x) - \left(\sum P_f(x)\right)^2}{n(n-1)}} \qquad (5\text{-}13)$$

where, $P_f(x)$ is light intensity difference signal

$Std\ [\ ]$ is the operation of standard deviation

n is the number of samples in $P_f(x)$ signal

The orange peel evaluated with Equation 5-13 in Figure 5-8 (case A) is 61.67.

Cases B & C

In case B and C, the orange peel effect is different from case A, because the "depth" of light intensity difference is not sufficient to separate the image into small sections like case A. The effect is on the distortion of the edges of the reflected image (Figure 5-4). In this case, we do not directly measure the magnitude of the light intensity, we measure the variability of the image edges at a variety of grey levels. So the features along the edges of the light tube can be extracted to measure the edge distortion.

The edge distortion can be measured with the standard deviation at different grey levels. The standard deviations at different grey levels can be averaged as a measure of orange peel for cases B and C.

Orange Peel Effect:

$$OP = \frac{1}{n}\sum_{I=I_1}^{I_2} Std[E(I)] \tag{5-14}$$

Where, OP is the orange peel effect.

$E(I)$ is the detected edges at grey level I.

$Std[\ ]$ is the operator for standard deviation.

I represents the light intensity (grey level).

I_1 is the start intensity (grey level).

I_2 is the end intensity (grey level).

n is the total number of the edges at grey level from I_1 to I_2.

Figure 5-27 has a dual edge at the intensity grey levels of 100 extracted from Fig. 5-5 (case C). A programme has been developed to calculate the orange peel effect by averaging the standard deviation of the edges detected at different grey levels.

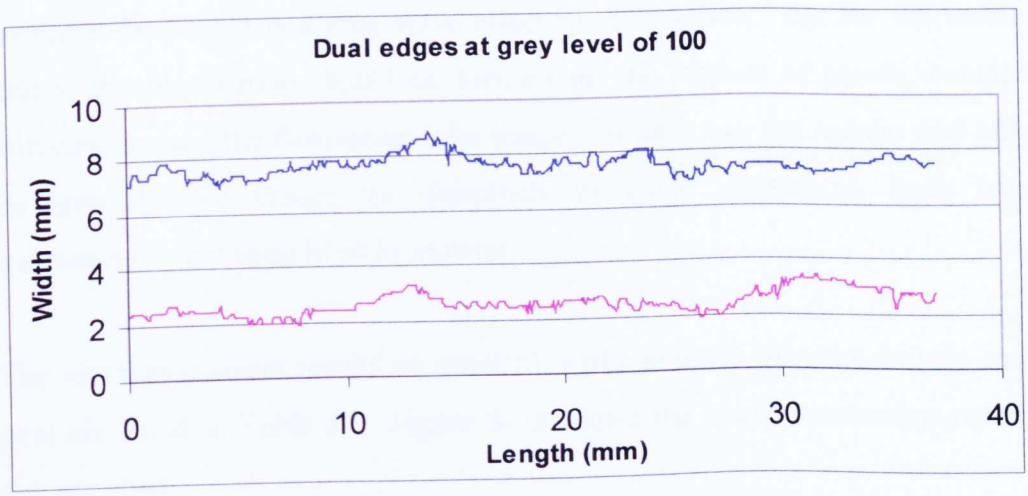

Figure 5-27 Dual edge of fluorescent tube at grey level of 100

As the variation of the edges is mainly focused on both sides of the reflected fluorescent tube, the grey levels are selected between 50 to 150. The value of OP in Fig. 5-5 (case C) is calculated to be 4.14.

5.4.5. Experimental Results

Eleven panels (p1-p11) were selected from car manufacturers to test the correlation between metal texture, orange peel and visual assessment. All these panels meet the requirement for cases B and C. First of all, these panels were visually assessed by the experts in terms of the metal texture effect and the orange peel effect respectively. The visual assessment method and statistical procedure was described in Chapter 3. All the visual assessment results were normalised to the range 0 to 1 (1 is the best panel). Then these panels were tested with the experiment methods described above.

5.4.5.1. Visual assessment result

To test the experiment results on the evaluation of metal texture and orange peel, the visual assessment on these panels is also required to be conducted in terms of metal texture and orange peel respectively. For orange peel it is easy to observe and evaluate, because it is a long wave effect on the surface. But for the metal texture effect, the observation should be focused on the surface of panels, comparing the waviness around the fluorescent tube image. In this case, the orange peel effect must be ignored. To ensure the objectivity of visual assessment, these two visual assessments were completed by experts.

The visual assessment results on panel p1 – p11 in terms of metal texture and orange peel are listed in Table 5-3. Figure 5-28 shows the visual assessment results in the column chart.

Table 5-3 Visual assessment result

Visual assessment result		
Panel	Metal Texture	Orange Peel
p1	1.000	0.225
p2	0.775	0.900
p3	0.750	0.800
p4	0.675	0.050
p5	0.650	0.875
p6	0.550	0.300
p7	0.475	0.250
p8	0.325	0.750
p9	0.150	0.225
p10	0.150	0.575
p11	0.000	0.575

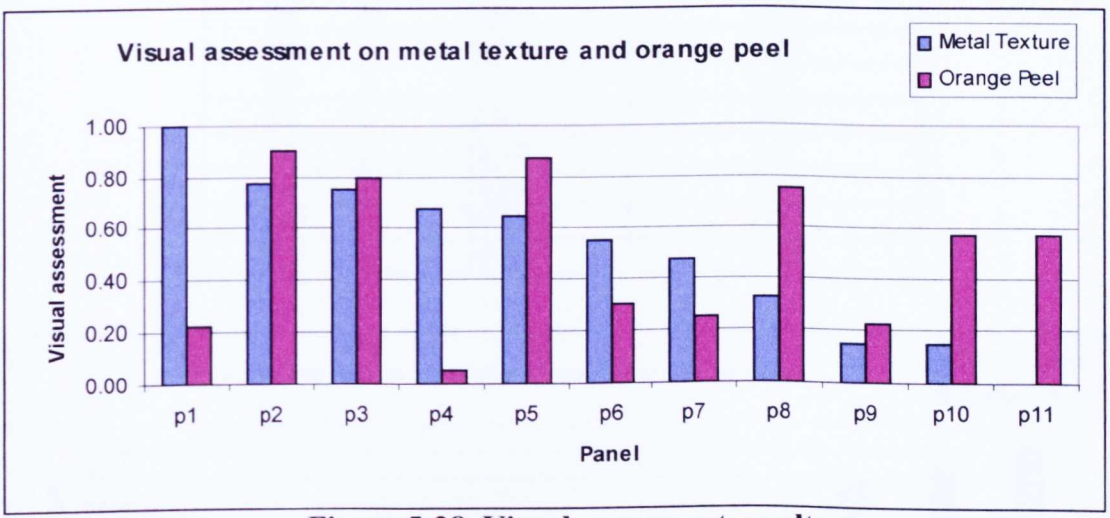

Figure 5-28 Visual assessment results

For visual assessment (1 is best, 0 is worst), the metal texture effect and orange peel are two different types of surface characteristics. There is no direct relationship between them. For example, panel p1 has a low metal texture effect but has a large orange peel effect. Panel p11 has low orange peel effect but a high metal texture effect.

5.4.5.2. Experiment Result

The experiment results obtained with the methods described in section §5.4.4. Metal texture is measured with Equation 5-10; orange peel is evaluated with Equation 5-14. The experimental results are listed in Table 5-4 and depicted in Figure 5-29.

Table 5-4 Experiment result on metal texture and orange peel

Experiment result		
Panel	Metal Texture	Orange Peel
p1	5.79	3.32
p2	7.58	1.26
p3	8.26	1.67
p4	9.07	5.83
p5	9.37	1.82
p6	9.57	2.91
p7	9.93	3.3
p8	12.16	1.97
p9	16.02	2.87
p10	16.88	2.07
p11	18.49	2.28

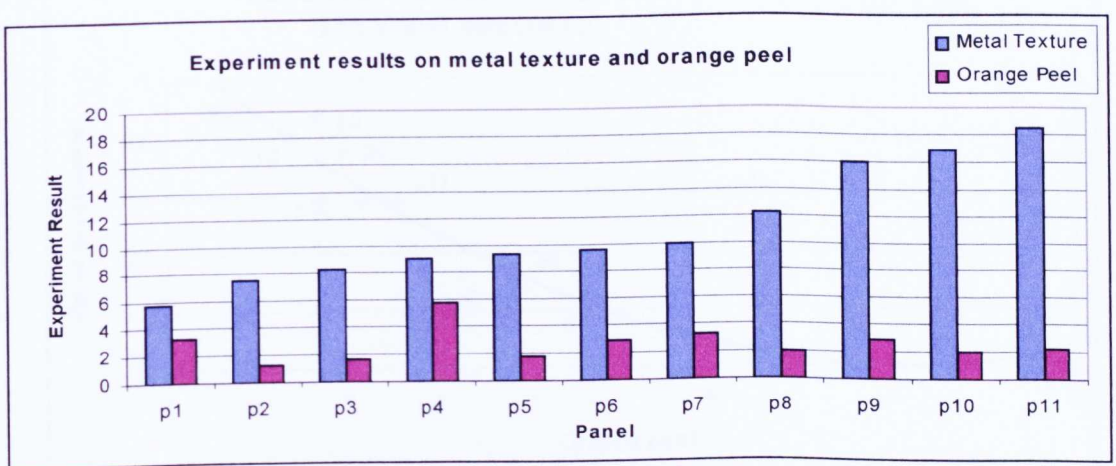

Figure 5-29 Experiment results on metal texture and orange peel

5.4.5.3. Correlation

To test if the experiment results of metal texture and orange peel correspond to human perception, the visual assessment results are employed as a reference to check the

correlation between visual assessment, metal texture, and orange peel, The correlation coefficients are $\rho_1 = 0.98$ in Fig. 5-30 and $\rho_2 = 0.87$ in Fig. 5-31.

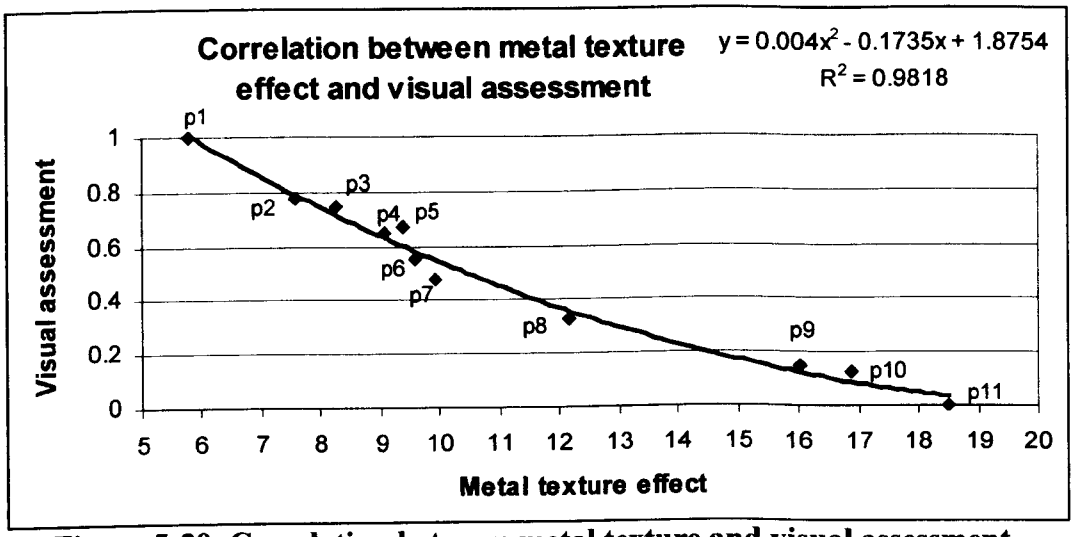

Figure 5-30 Correlation between metal texture and visual assessment

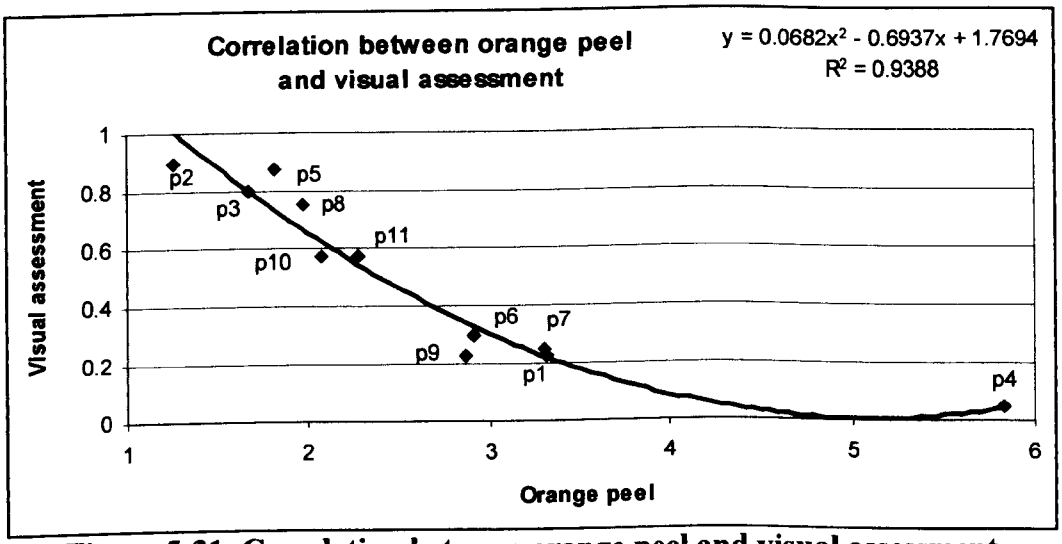

Figure 5-31 Correlation between orange peel and visual assessment

It can be seen that the metal texture effect evaluated with the filtering method (Equation 5-10) has a very strong correlation with the experts' perception ($\rho_1 = 0.98$). It demonstrates that this method can effectively measure the metal texture effect on the paint surface as perceived by the human eye. For the orange peel evaluation, as in case B and C, the orange peel effect stays at a low level (standard deviation is from 1 to 6 in

Figure 5-31), it is not easy to distinguish them with these samples. But they still have a good correlation with visual assessment.

From the experimental results and correlation between them it can be seen that with the method of filtering and standard deviation calculations, the metal texture and orange peel can be separated and evaluated corresponding to human perception.

From the description above, the separation and evaluation of the metal texture effect and orange peel can be summarised in the flowchart (Figure 5-32):

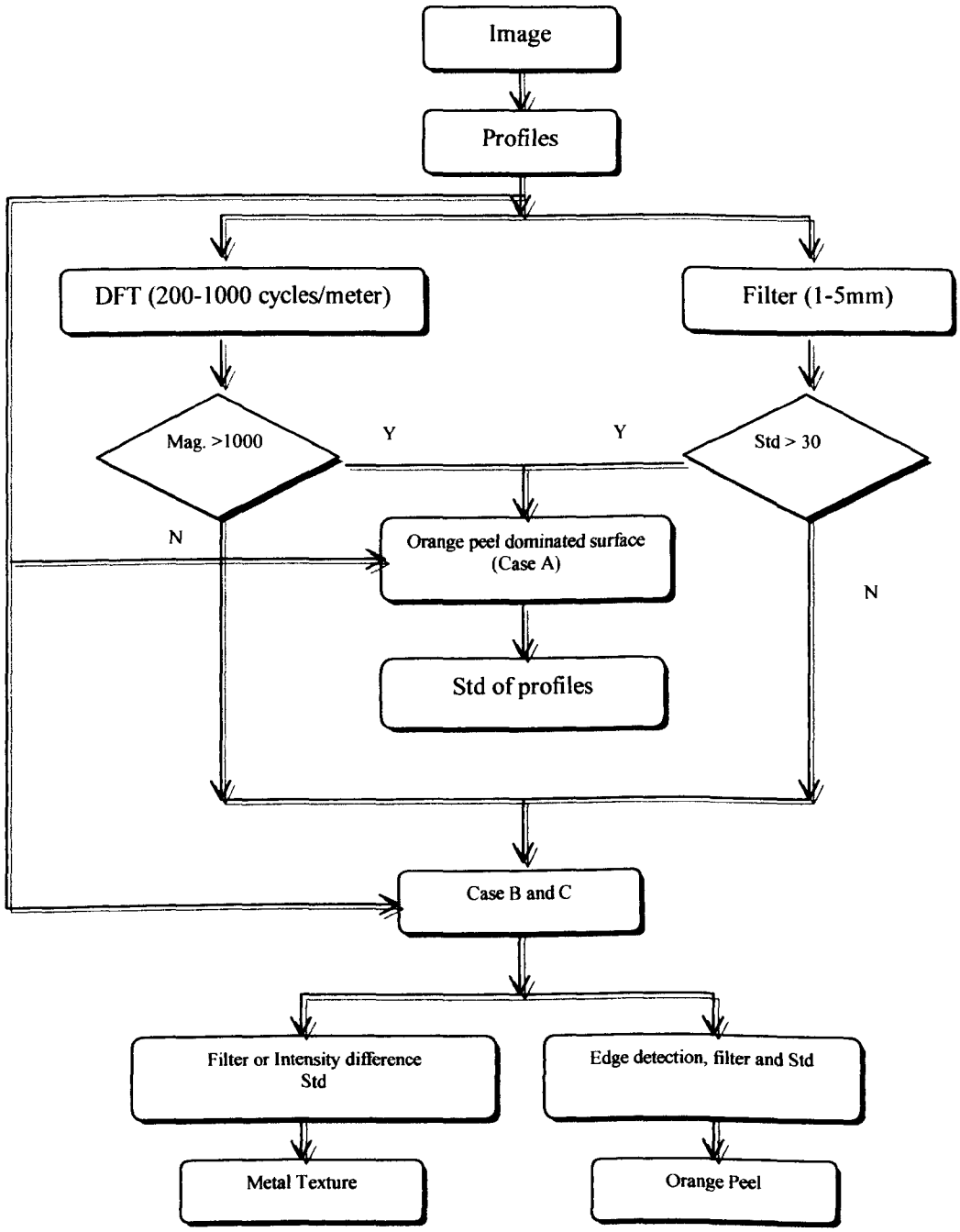

* Std - standard deviation operation.

** Mag. – Magnitude.

Figure 5-32 Flowchart for evaluation of orange peel and metal texture

5.5. Conclusion

The painted surface can be effectively evaluated in terms of the metal texture effect and orange peel effect as perceived by human eyes. By separating the two different effects, we can clearly determinate causes that drive the painted surface appearance. The method provides an objective way to compare the paint quality and indicates which parameter is more effective.

The main conclusions can be summarised as following:

1. The separation of orange peel and metal texture effect is necessary and possible. With the measurement method described in this chapter the orange peel and metal texture effect can be effectively separated and evaluated.

2. The measurement methods, filtering and DFT, are proved to be a very effective way to separate and evaluate the orange peel and texture effect. As only a few profiles are extracted from the surface image, the calculation can be completed in a few seconds. The texture must distribute evenly to ensure the reliability of test results.

3. To further analyse the texture effect, more computable parameters need to be developed to characterise the texture features in all aspects.

Chapter 6
Evaluation of the Metal Texture Effect on Paint Appearance

6.1. Introduction

From previous chapters, it has been established that orange peel is a major factor which drives the overall appearance of painted autobody. Using FFT and filtering techniques, the orange peel and metal texture can be effectively separated and evaluated. Effective evaluation of the metal texture effect on the paint appearance is becoming more important as reductions in the orange peel effect are achieved. In the last chapter, only the standard deviation of the image profile to represent the texture effect was used. To study the metal texture effects in more depth, traditional texture feature extraction methods [Rosenfeld, 1984] from 3-D image have been investigated.

In this chapter, a set of computable textural parameters based on grey-tone spatial-dependence matrices, which directly correspond to visual perception, have been employed. The preliminary experimental results showed that this method could effectively evaluate the metal texture effect as perceived by the human eye.

6.2. Surface Texture

Before discussing the metal texture effect on paint appearance, surface texture itself will be reviewed

6.2.1. The nature of surface texture

Surface textures are mainly produced by machining processes. It is preferable in practice to separate roughness, waviness and form error according to their causes, since this tends to correspond to factors affecting performance. Based on this criterion, the following can be defined. [Dagnall 1980]:

Roughness: the irregularities which are inherent in the production process, left by the actual machining agent (e.g. cutting tool, grit, spark).

Waviness: that component of the texture upon which roughness is superimposed. It may result from such factors as machine or work deflections, vibrations, chatter, various causes of strain in the material, and extraneous influences.

Form error: the departure from the intended shape of the surface, caused generally by flexure of the machine or workpiece, or by errors in the slideway.

Surface characteristics could be very complex since roughness, waviness and form error could exist in combination (see Fig. 6-1). For surfaces with a short wavelength structure ($\lambda < 0.8$ mm) the effect is commonly defined as 'roughness'. If the wavelength is $0.8 < \lambda < 8$ mm, the effect is called 'waviness'. If the wavelength is larger than 8 mm, the effect is defined as 'form error'.

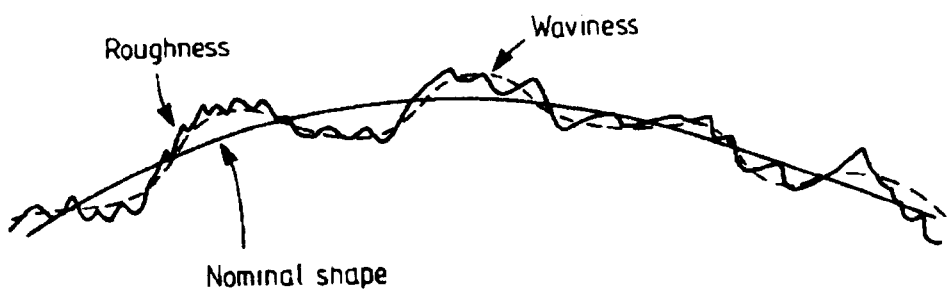

Figure 6-1 Surface structure

6.2.2. Surface parameters

The complex nature of the texture is the main reason why so many parameters have been proposed to quantify the various surface characteristics. In the automotive industry, the characteristics of steel sheet are often described using Ra and Pc. Ra is defined as the mean departure of the profile from the mean reference line. This is shown in Fig. 6-2.

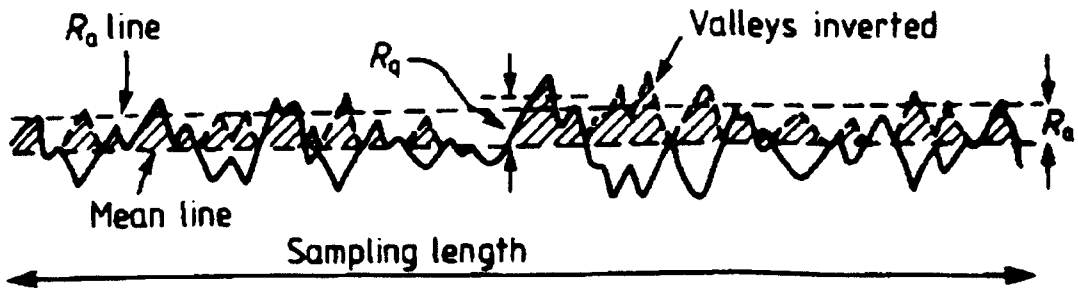

Figure 6-2 Parameter Ra

If $z = f(x)$ is the profile measured from the reference mean line and L is the length of the profile being assessed. So,

$$R_a = \frac{1}{L}\int_0^L |z| dx$$

Pc is the number of peaks in the surface profile which cross selected thresholds around the mean reference line.

For example, in the European car industry, the steel sheet specifications are Ra < 1.5 μm and Pc > 50 pks/cm with the wavelength less than 2.5 mm.

6.2.3. Steel Texture Type

The typical steel textures used in automotive industry are named according to the rolling texturing techniques employed in their manufacture [Scheers 1996]. They are Shot Blast Texture (SBT), Electrical Discharge Texture (EDT), Electrical Beam Texture (EBT), and Laser Texture (LT). These four types of texture can be ranked based on the degree of randomness (or determinism) of the surface profiles. SBT and EDT are strongly random, LT is more deterministic and EBT is fully deterministic which is built up by a repeating pattern. Fig. 6-3 and Fig. 6-4 show the patterns of EDT and EBT.

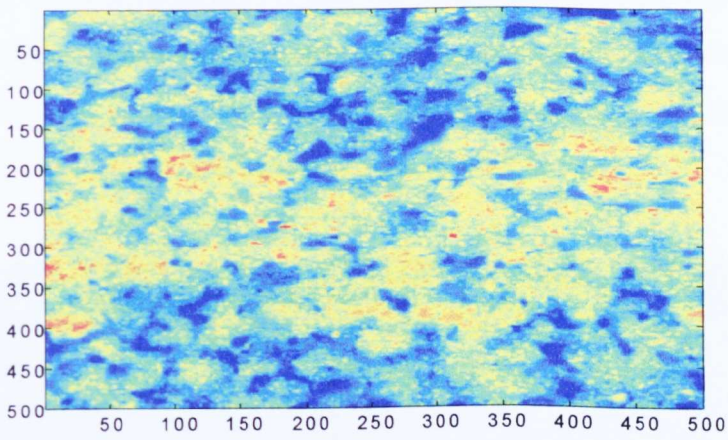

Figure 6-3 Pattern of EDT

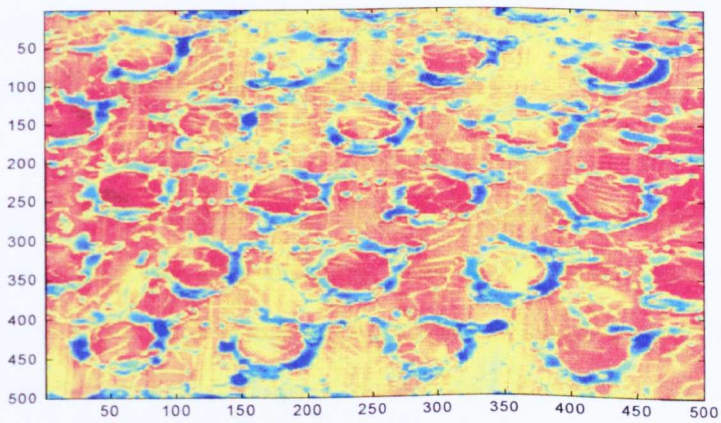

Figure 6-4 Pattern of EBT

Normally steel sheet with low average roughness Ra and high peak count Pc can result in a good paint appearance. The effect from steel roughness can be still seen on the paint surface with the aid of a structured light source. Although the texture is under several layers of coatings, its effect on surface appearance cannot be ignored.

6.2.4. Metal texture effect

As described in previous chapters, the metal texture effect can still be seen after painting. For example, Fig. 6-5 shows a painted panel, the metal texture can be easily seen with a fluorescent tube reflected on it. The roughness Ra of the steel sheet in this case is 2.85 μm, the film thickness is 96.7 μm. the roughness Ra of the topcoat is 0.13 μm. The painted surface (clear-coat) is very smooth, but the metal texture effect on paint appearance is obvious, and the visual texture seems even worse than the real texture on bare steel sheet due to the light scatter and reflection.

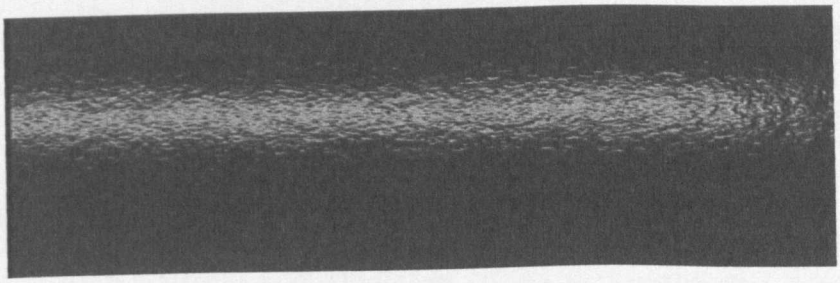

Figure 6-5 Effect of metal texture on a painted panel for steel roughness Ra=2.85μm, topcoat Ra=0.13μm (both with cut-off 2.5mm), the film thickness is 96.7μm.

The desired situation is that the steel sheet should be perfectly smooth. The metal texture cannot then be seen at all after painting. This causes other problems, such as poor forming behaviour and a high sensitivity to surface damage during handling. A certain roughness is needed to optimise appearance. For the painting procedure itself, a certain roughness is also necessary to retain the paint especially when the painting is performed on vertical panels.

Knowing the nature of the metal texture effect, the next important step is to evaluate objectively its effect as perceived.

6.3. Texture Evaluation

The ideal paint appearance is that there is no texture seen after painting. If the texture can still be seen under several layers of coatings, the texture can be described in terms of some textural features which correspond to human visual perception. The more the textural features can be seen, the worse the paint appearance. Various kinds of textural features for image classification have been proposed which can also be used for visual texture assessment.

In a search for meaningful features for describing texture, it is natural to look for the types of features which human beings use in interpreting pictorial information. It is necessary to identify textural features which approximate to visual perception and proceed to a set of computational parameters.

6.3.1. Basic Textural Properties

A strict definition for visual texture is difficult. However from an analytical point of view, we may regard texture as what constitutes a macroscopic region, within which are repetitive patterns consisting of elements or primitives arranged according to a "placement rule". Hence it can be written as [Tamura 1978][Reed 1993]:

$$f = R(e)$$

Where R denotes a placement rule (or relation) and e denotes an element. We can obtain texture f if R is a function which satisfies the notions mentioned above, and we can express "microtexture" if e is recursively replaced by f.

Texture is often considered on two levels, statistical and structural. On the statistical level, texture is observed from a macroscopic view as a functional combination of R and e. Thus the difference between textured regions is measured by using the statistics of local properties. On the other hand, the structure level requires more information about each R and e. Considering a computational analysis of a given texture pattern, it is fairly difficult to parse its structure generally because the factors R and e generally have a considerable variation, it seems impossible to approximate them separately. In this case, we are obliged to take a statistical approach where a set of statistics is extracted from local measurements.

Reference [Tamura 1978] gives us the following six specific features which correspond to visual texture.

1) Coarseness – Coarse versus Fine

The coarseness is the most fundamental textural feature. In a narrow sense, the texture means the coarseness. When patterns differ only in scale, the magnified one is coarser. For patterns with different structures, the bigger its element and/or the less its element are repeated, the coarser it is.

2) Contrast – High Contrast versus Low Contrast

In the narrow sense, contrast corresponds to picture quality. We assume the following four factors for contrast:

i) Dynamic range of grey levels

ii) Polarisation of the distribution of black and white or the grey level histogram or ratio of black and white areas.

iii) Sharpness of edges

iv) Period of repeating patterns

3) Directionality – Directional versus Non-directional

This is a global property over the given region. Directionality involves both element shape and placement rule.

4) Line-likeness – Line-like versus Blob-like

This concept is concerned only with the shape of a texture element.

5) Regularity – Regular versus Irregular

This is a property for variations of a placement rule.

6) Roughness – Rough versus Smooth

Bearing these properties in mind, we put the emphasis on the parameter 'contrast' to evaluate the metal texture effect for human visual perception. Some basic approaches to texture analysis have been well summarised in reference [Davies 1997]. Among them, the grey-level co-occurrence matrices had the best innate discriminative ability. The contrast is directly derived from it.

6.3.2. Grey-Tone Spatial-Dependence Matrices [Haralick, 1973]

It is also frequently called grey-level co-occurrence matrices, which is based on studies of the statistics of pixel intensity distributions. During the 1970s it became to a large degree the "standard" approach to texture analysis [Davies, 1997].

Suppose an image to be analysed is rectangular and has N_x resolution cells in the horizontal direction and N_y resolution cells in the vertical direction. The grey tone appearing in each resolution cell is quantified to N_g levels.

Let, $L_x = \{1, 2, \ldots, N_x\}$ to be the horizontal spatial domain.

$Ly = \{1, 2, \ldots, N_y\}$ to be the vertical spatial domain.

$G = \{1, 2, \ldots, N_g\}$ to be the set of grey tones

We consider a resolution cell to have eight nearest-neighbour resolution cells, i.e. four directions, horizontal (0^0), vertical (90^0), right-diagonal (45^0), and left-diagonal (135^0). See Fig. 6-6.

The grey-tone spatial-dependence matrices are a function of the angular relationship of grey level between the neighbouring resolution cells as well as a function of the distance between them. They are defined as

$$P(i, j, d, 0^0) = \#\{((k, l), (m, n)) \in (L_y \times L_x) \times (L_y \times L_x) \,/_{k-m=0,\ |l-n|=d}$$
$$I(k, l) = i,\ I(m, n) = j\}$$

$$P(i, j, d, 45^0) = \#\{((k, l), (m, n)) \in (L_y \times L_x) \times (L_y \times L_x) \,/_{(k-m=d,\ l-n=-d) \text{ or } (k-m=-d,\ l-n=d)}$$
$$I(k, l) = i,\ I(m, n) = j\}$$

$$P(i, j, d, 90^0) = \#\{((k, l), (m, n)) \in (L_y \times L_x) \times (L_y \times L_x) \,/_{|k-m|=d,\ l-n=0,}$$
$$I(k, l) = i,\ I(m, n) = j\}$$

$$P(i, j, d, 135^0) = \#\{((k, l), (m, n)) \in (L_y \times L_x) \times (L_y \times L_x) \,/_{(k-m=d,\ l-n=d) \text{ or } (k-m=-d,\ l-n=-d)}$$
$$I(k, l) = i,\ I(m, n) = j\}$$

Where # denotes the number of elements in the set. The (k, l) and (m, n) are a pair of cells with the distance of d and grey tone of i and j.

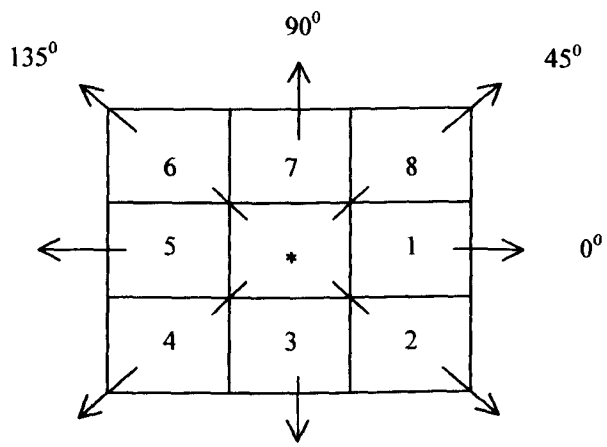

Figure 6-6 Angular relationship between the neighbouring resolution cells

An example is given in Fig. 6-7. (a) is a 4 × 4 image with four grey tones, ranging from 0 to 3. (b) is the general form of any grey-tone spatial-dependence matrix. (c) - (f) are the grey-tone spatial-dependence matrices in four direction with distance 1.

0	0	1	1
0	0	1	1
0	2	2	2
2	2	3	3

(a)

Grey Tone	0	1	2	3
0	#(0, 0)	#(0, 1)	#(0, 2)	#(0, 3)
1	#(1, 0)	#(1, 1)	#(1, 2)	#(1, 3)
2	#(2, 0)	#(2, 1)	#(2, 2)	#(2, 3)
3	#(3, 0)	#(3, 1)	#(3, 2)	#(3, 3)

(b)

0^0

$$P_H = \begin{pmatrix} 4 & 2 & 1 & 0 \\ 2 & 4 & 0 & 0 \\ 1 & 0 & 6 & 2 \\ 0 & 0 & 1 & 2 \end{pmatrix}$$

(c)

90^0

$$P_V = \begin{pmatrix} 4 & 2 & 1 & 0 \\ 2 & 4 & 0 & 0 \\ 1 & 0 & 6 & 2 \\ 0 & 0 & 1 & 2 \end{pmatrix}$$

(d)

135^0

$$P_{LD} = \begin{pmatrix} 4 & 2 & 1 & 0 \\ 2 & 4 & 0 & 0 \\ 1 & 0 & 6 & 2 \\ 0 & 0 & 1 & 2 \end{pmatrix}$$

(e)

45^0

$$P_{RD} = \begin{pmatrix} 4 & 2 & 1 & 0 \\ 2 & 4 & 0 & 0 \\ 1 & 0 & 6 & 2 \\ 0 & 0 & 1 & 2 \end{pmatrix}$$

(f)

Figure 6-7 An example for grey-tone spatial-dependence matrix

6.3.3. Textural feature - Contrast

Based on this matrix, a set of computable parameters is defined to characterise textural features [Haralick, 1973][Venkat 1996] (see Annex). Some of them relate to specific textural characteristics of the image such as homogeneity, contrast, and the presence of organised structure within the image. Others characterise the complexity and nature of grey-tone transitions which occur in the image. Among these features, f_1 *(angular second-moment,* ASM), is a measure of homogeneity of the image; *f2 (contrast)* is a difference moment of the *P* matrix and is a measure of the contrast or the amount of local variations present in an image. *f2* has been found to be more significant

corresponding to the visual perception, since the difference of grey-tone is squared. The more the difference of grey–level between two cells, the more contribution it makes to contrast.

Angular Second Moment (ASM):

$$f_1 = \sum_{i=1}^{N_g} \sum_{j=1}^{N_g} \{p(i,j)\}^2 \tag{6-1}$$

Contrast:

$$f_2 = \sum_{n=0}^{N_g - 1} n^2 \left\{ \sum_{\substack{i=1 \, j=1 \\ |i-j|=n}}^{N_g \quad N_g} p(i,j) \right\} \tag{6-2}$$

where: $p(i,j) = \dfrac{P(i,j)}{R}$ is the *(i, j)*th entry in a normalised grey-tone spatial-dependence matrix *P*. *R* is a normalising constant, which is the number of all the cell pairs.

N_g is the number distinct grey levels in the quantified image.

Here an example is given to illustrate how to use contrast to evaluate the texture effect. Fig. 6-8 (a) and (b) are two steel panels with different intensities of visual texture, which can be easily viewed around the reflected fluorescent tube. Fig. 6-9 (a) and (b) give the 3-D profiles of these two panels. It can be seen that the visual texture is superimposed on the reflected fluorescent light image. It is desirable to get rid of the light bar's effect. As the formula "contrast" only compares the difference of grey-level with its neighbours, the effect of fluorescent light can be reduced to a low level by comparing the cell neighbours in a horizontal direction (Y axis). Fig. 6-10 gives the comparison results of these two textures including angular second-moment features and contrast in four predefined directions.

(a) (b)

Figure 6-8 Visual texture around a reflected fluorescent tube

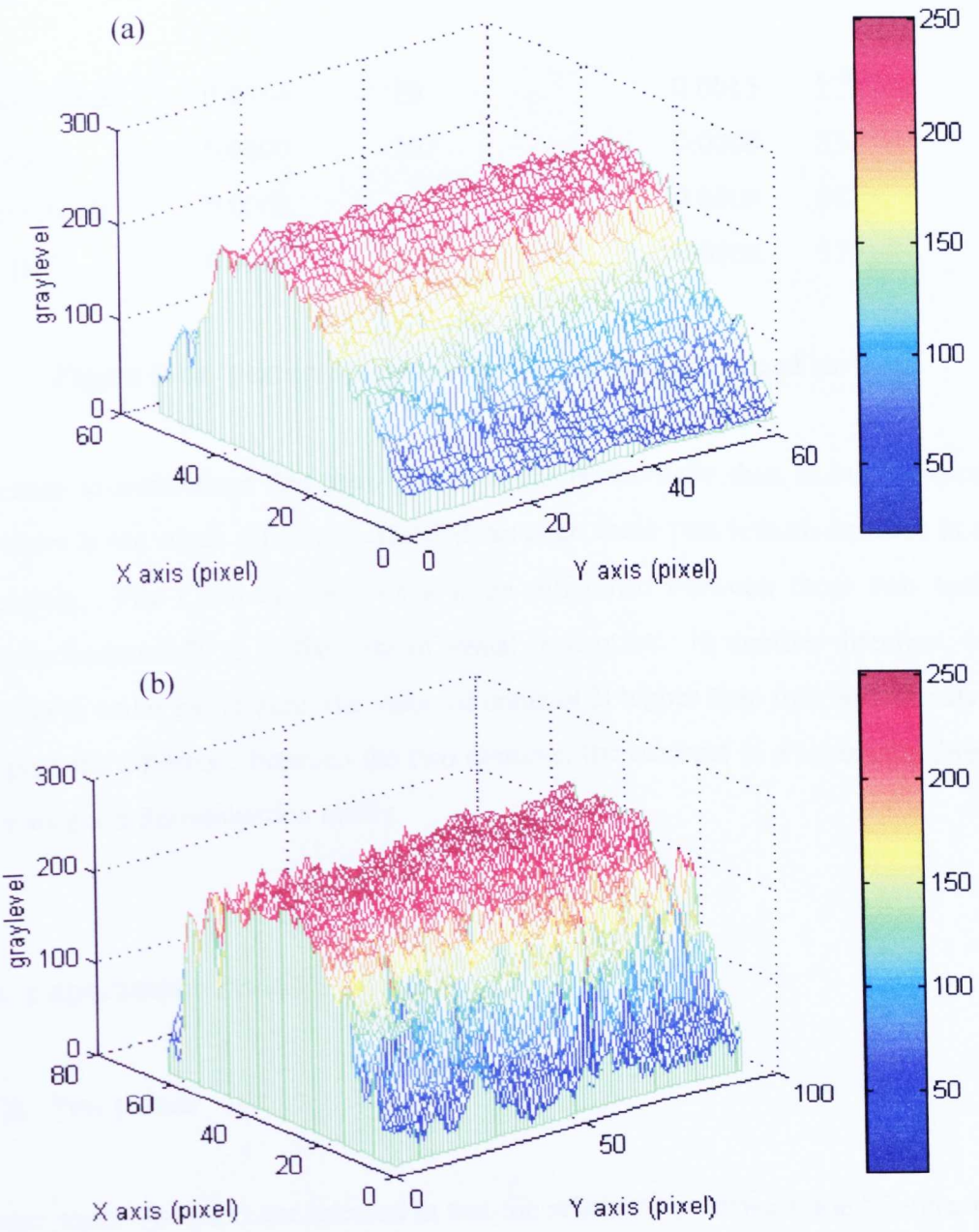

Figure 6-9 Visual texture 3-D Profiles

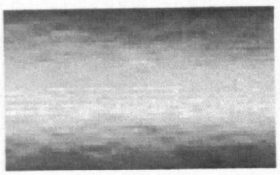

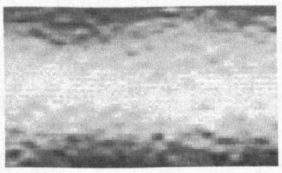

Angle	ASM	Contrast	ASM	Contrast
0^0 (horizontal)	0.0014	79	0.0015	179
45^0 (right)	0.0009	267	0.0008	531
90^0 (vertical)	0.0008	268	0.0008	581
135^0 (left)	0.0008	271	0.0008	579

Figure 6-10 Textural features for two different textured surfaces

It is easy to understand that the ASM is larger horizontally than in other directions. But there is not much difference of ASM between these two texture surfaces in other directions. The Contrast gives us a large difference between these two textured surfaces horizontally as in the case of visual perception. In another direction, as the light bar is under the texture, the value of contrast is higher than that horizontally. To compare the difference between the two textures, the contrast in a horizontal direction presents good discrimination ability.

6.4. Experiment result

6.4.1. Test panels

Eleven panels (p1-p11) are selected to test the relationship between the "Contrast" and the human visual perception of the metal texture effect. The images of these 11 panels are shown in Fig. 6-11, in which the size for each image is 80×100 (pixel×pixel) and the grey level is from 0 to 255. The distance between adjacent pixels represents

0.1mm in real distance which corresponds to the human eye resolution. As the texture can be only seen around the reflected light bar, an attempt is made to test if the 'Contrast' can give us the same result as human perception. In Fig. 6-11, the texture level extends over a wide range. At the same time, some panels have orange peel as well.

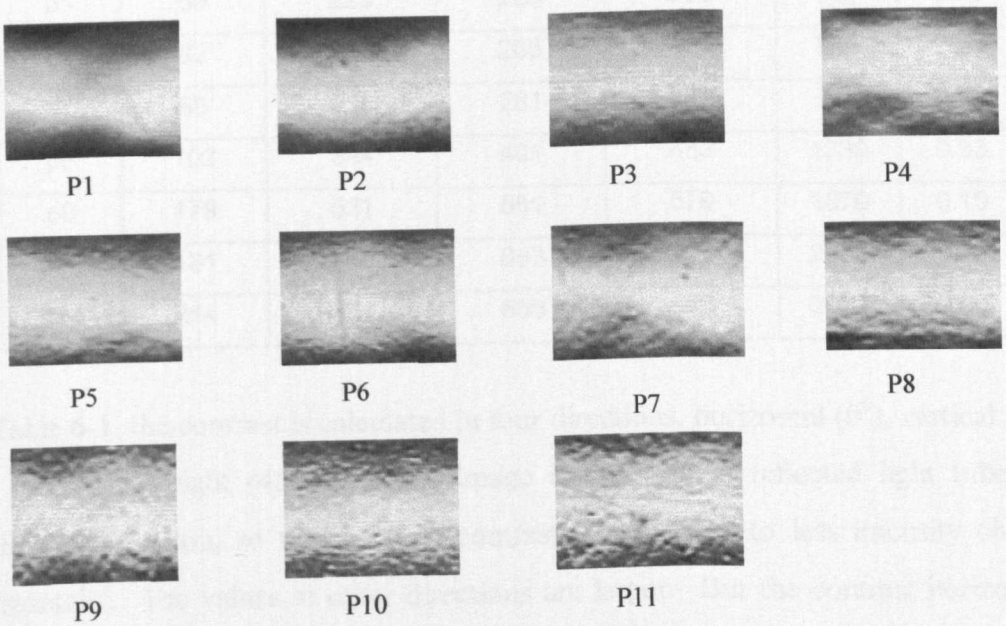

Figure 6-11 Test panels with visual texture

6.4.2. Correlation between contrast and visual assessment

A program has been developed to calculate the 'Contrast' of these images in four directions using equation (6-2), the test results are shown in Table 6-1.

Table 6–1 Contrast in four directions and visual assessment

Panel	Contrast_h	Contrast_v	Contrast_ld	Contrast_rd	Sum	Visual
p1	66	177	170	184	599	1.00
p2	64	218	226	216	724	0.78
p3	79	267	268	271	885	0.75
p4	72	254	267	262	855	0.65
p5	69	223	233	232	757	0.68
p6	82	257	265	277	881	0.55
p7	86	256	281	282	905	0.48
p8	102	394	401	433	1330	0.33
p9	179	531	581	579	1870	0.15
p10	181	656	693	727	2257	0.13
p11	214	567	658	643	2082	0.00

In Table 6-1, the contrast is calculated in four directions, horizontal (0^0), vertical (90^0), left (135^0) and right (45^0). As the image is based on a reflected light tube in a horizontal direction, so the value of contrast is small due to less intensity changes horizontally. The values in other directions are larger. But the contrast horizontally can reflect the texture level as it is. The visual assessment result on these panels is also presented in the last column. The procedure of visual assessment and statistical methods was described in Chapter 3. The only difference is that the panels are assessed only in terms of metal texture effect [ASTM, D4449]. Our emphasis is mainly on the correlation between contrast (horizontal) and visual assessment. Fig. 6-12 shows a good correlation (ρ = -0.91) between Contrast (horizontal, distance = 1) and the visual assessment in terms of the metal texture effect. It shows that the contrast (horizontal) can be used as an effective measure to evaluate the metal texture effect on a painted surface.

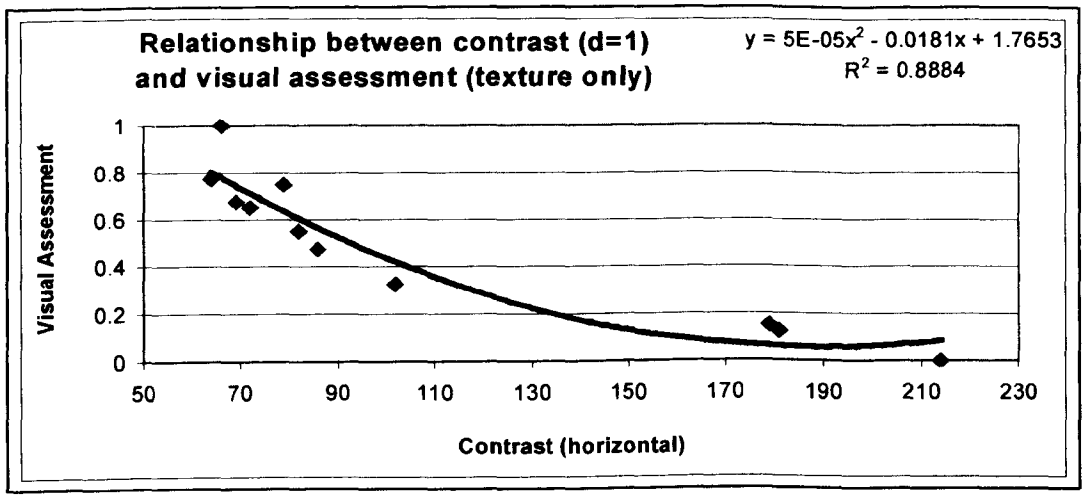

Figure 6-12 Relationship between contrast (horizontal) and visual assessment

6.4.3. Contrast Distance

In Figure 6-13, if the grey-level of the pixel ' * ' is only compared with its adjacent neighbours (pixel 1-8) in the four predefined directions, that means that the contrast distance is one (d=1). Actually the grey-level of any pixel can be compared with other pixels at distance (d>1) in the four predefined directions within an image. For example, if the contrast distance is two, then the pixel * compares grey-level with the pixels from 9 to 16.

As the size of texture is different, changing the contrast distance can allow us to find more suitable distances between two pixels for which the contrast can have a stronger correlation with visual assessment. i.e. the contrast at this distance can really reflect the texture effect in the same way as human visual perception.

As the visual assessment has a good correlation with contrast horizontally, here only the contrast result in horizontal directions is given with different contrast distances (Table 6-2).

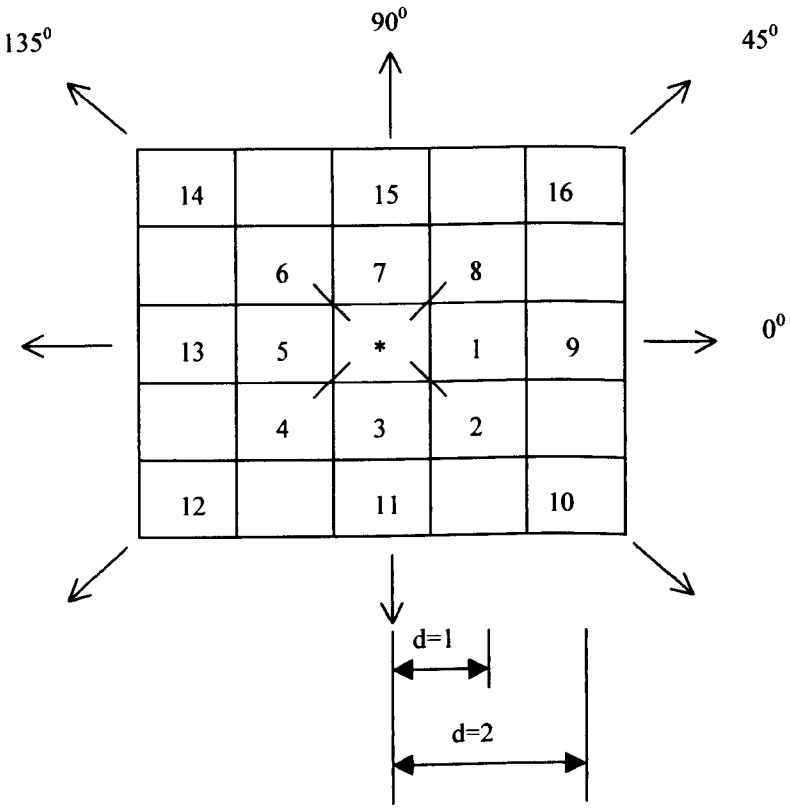

Figure 6-13 Contrast distance

Table 6-2 Contrast (horizontal) at different distance

Panel	d=1	d=2	d=3	d=4
p1	66	79	109	133
p2	64	94	133	157
p3	79	118	168	191
p4	72	141	225	295
p5	69	127	194	240
p6	82	162	241	283
p7	86	176	282	360
p8	102	216	346	434
p9	179	412	659	801
p10	181	457	708	833
p11	214	549	888	1094

Fig. 6-14 displays the changes of Contrast at different distances. The contrast value increases as the distance becomes larger. Especially for the panels with a high texture level, the contrast value increases dramatically. This means that for the high texture level panels, the large distance should be chosen.

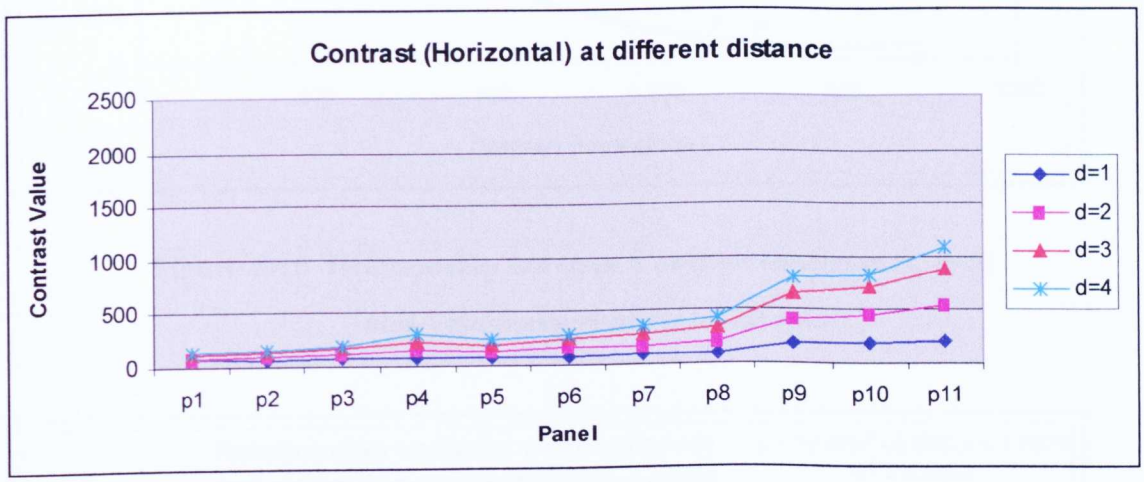

Figure 6-14 Contrast (horizontal) at different distances

The correlation between contrast (horizontal) and visual assessment (texture only) at different distance are presented in Fig. 6-15 to 6-17.

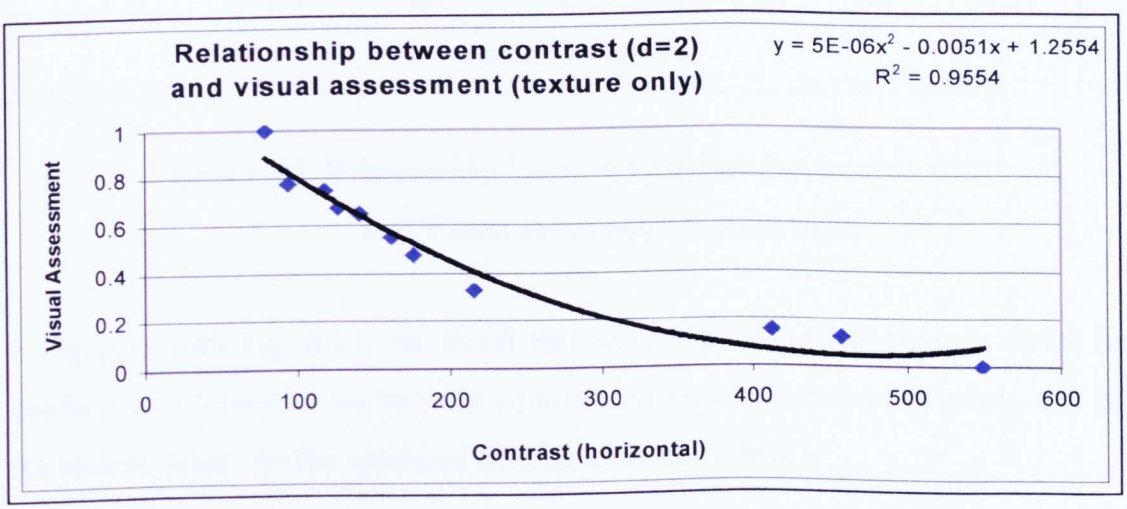

Figure 6-15 Relationship between Contrast (horizontal, d=2) and Visual assessment (texture only)

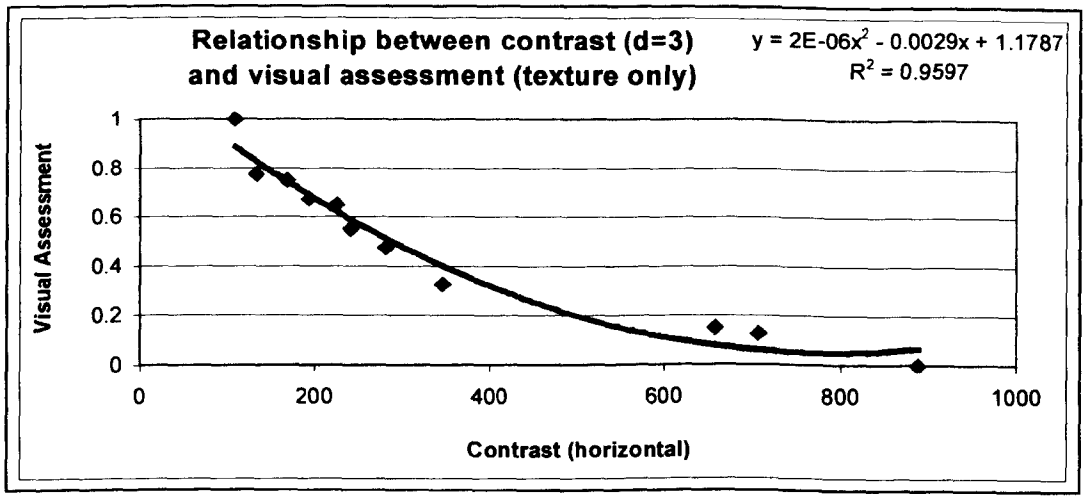

Figure 6-16 Relationship between Contrast (horizontal, d=3) and Visual assessment (texture only)

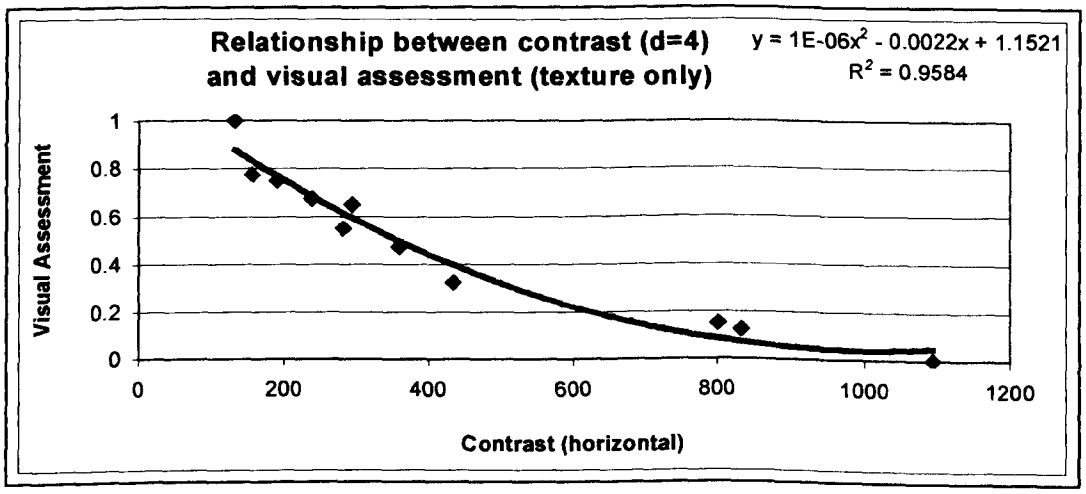

Figure 6-17 Relationship between Contrast (horizontal, d=4) and Visual assessment (texture only)

Comparing with Fig. 6-12, we found that when the contrast distance is three, the coefficient of determination between contrast and visual assessment (texture only) has the highest value. So the optimised contrast distance is three.

6.4.4. Grey-level difference

In Equation (6-2), the contrast is calculated by comparing all the differences of the pixel's grey-level (from 0 to N_g -1) with its neighbouring pixels, then magnifying twice of the grey-level difference. The more the difference of grey-level between two pixels, the more impression of texture people can perceive. So the grey-level difference is another important factor to contribute to 'Contrast'. As human visual perception can not discriminate the small change of grey-level, the contrast value mainly depends on the large difference of grey-level. So the small differences of grey-levels do not need to be calculated, only those which the difference of grey-level is above a threshold need to be calculated. Table 6-3 gives the Contrast value based on a variety of grey-level differences. If $\Delta I > 0$, it is the original formula which is used and all the grey-level differences would be calculated. If $\Delta I > 5$, only the grey-level differences above 5 would be calculated.

Table 6-3 Contrast (d=3) based on variety of grey-level difference

Panel	I > 0	I > 5	I > 10	I > 15
p1	109	106	92	63
p2	133	130	116	90
p3	168	166	152	125
p4	225	223	208	181
p5	194	192	177	155
p6	241	239	226	193
p7	282	279	267	242
p8	346	344	332	309
p9	659	657	648	625
p10	708	706	697	674
p11	888	886	876	855

The data in Table 6-3 is drawn in Fig. 6-18, in which the contrast value only slightly decreases with the increase of the threshold of grey-level difference. It means that the small difference of grey-level does not affect the Contrast result, which can result in the improvement of the calculation speed and the reduction of the effect of image signal noise.

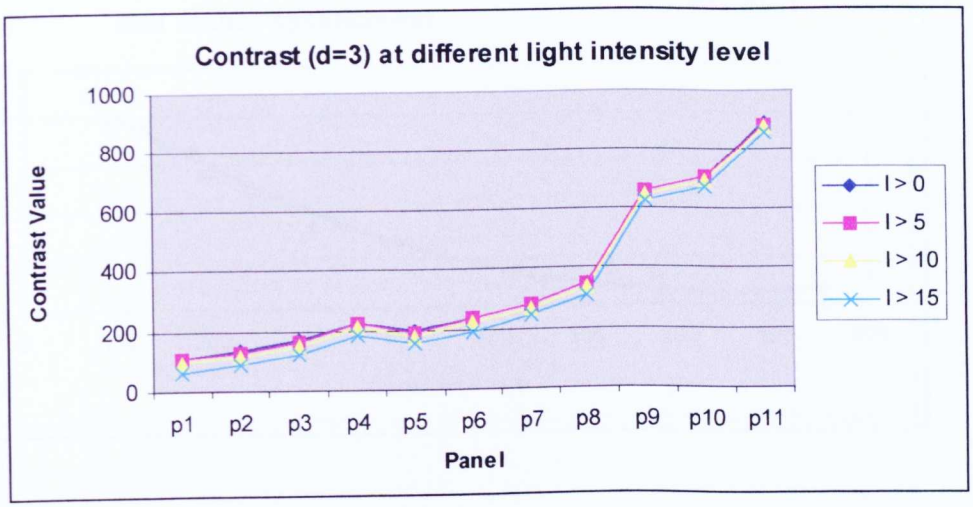

Figure 6-18 Contrast (d=3) based on a variety of grey-level differences

The correlation between Contrast (d=3) at grey-level difference above 10 and 15 are depicted in Fig. 6-19 and 6-20. The correlation coefficient is slightly improved. So the contrast with the distance being 3 and grey-level difference above 15 gives us the best correlation with visual assessment.

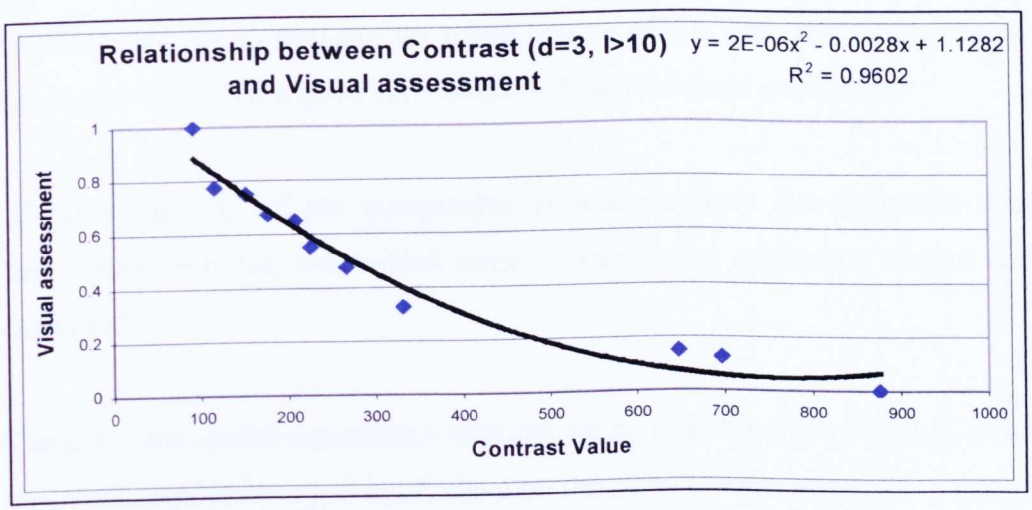

Figure 6-19 Relationship between Contrast (d=3, ΔI>10) and visual assessment

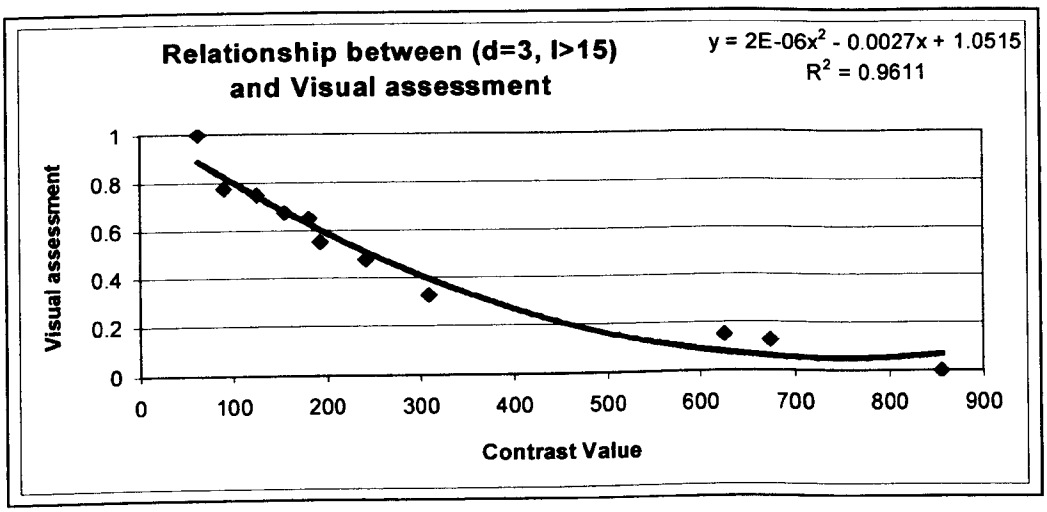

Figure 6-20 Relationship between Contrast (d=3, ΔI>15) and visual assessment

6.5. Conclusions

Based on the above description, the following conclusions can be drawn:

1. 'Contrast' derived from grey-tone spatial-dependence matrices can be used as an effective measure to evaluate the metal texture effect. The preliminary test result has shown that it has a good correlation with human visual perception.

2. 'Contrast' is one of the computable parameters from the grey-tone spatial-dependence matrices, with which more characteristics of surface texture can be compared.

3. The grey-tone spatial-dependence matrices are suitable for cases B and C, in which the orange peel has not too much effect on the metal texture result.

4. The disadvantage for this method is that it takes a long processing time for large-size images.

Chapter 7

Modeling of Overall Appearance Using Artificial Neural Network

7.1. Introduction

In this study, human perception of paint appearance quality is normally represented by a single index (0 to 1, 1 being the best) combining as many relevant properties of paint appearance as possible. As mentioned in Chapter 4, the existing methods for obtaining overall appearance consists of empirical formulae which assign indexes to the measurable parameters. In these circumstances, the correlation between overall appearance and individual parameters is assumed to be linear. In practice the correlation between overall appearance and individual parameters is far from linear. A solution to the multi-dimensional, non-linear regression problem is needed.

In this chapter, a novel technique, artificial neural networks (ANNs), will be introduced to model overall appearance. The reasons for choosing neural networks are as follows:

- **Power.** Neural networks are very sophisticated non-linear modelling techniques, capable of modelling extremely complex functions. Neural networks also address the dimensionality problem that bedevils attempts to model non-linear functions with large numbers of variables.

- **Ease of use.** Neural networks learn by example. The neural network user gathers representative data, and then invokes training algorithms to automatically learn the

structure of the data. The user does need to have some heuristic knowledge of how to select and prepare data, how to select an appropriate neural network and how to interpret the results. The level of user knowledge needed to successfully apply neural networks is much less than would be the case using (for example) more traditional statistical methods.

The significance for using ANNs is to establish the relationship between overall appearance and individual parameters easily and economically. The overall appearance will be calculated as the output of the neural network model with the measurable parameters as the input of model.

7.2. Artificial Neural Networks

7.2.1. The Definition of Neural Networks

Neural networks grew out of research in artificial intelligence, specifically, attempts to mimic the fault-tolerance and capacity to learn of biological neural systems by modelling the low-level structure of the brain. Placing the emphasis on the parallel computation ability, Haykin [Haykin, 1994] defines a *neural network* as:

A massively parallel distributed processor that has a natural propensity for storing experiential knowledge and making it available for use. It resembles the brain in two respects:

(1) Knowledge is acquired by the network through a learning process.

(2) Interneuron connection strengths known as synaptic weights are used to store the knowledge.

The study of neural network has a history of about five decades but has found solid application only in the past fifteen years, and it is still developing rapidly. More details

about neural network theory can be referenced to [Haykin, 1994] and [Demuth, 1998]. A brief summary about the conception of neural network is presented below.

7.2.2. Model of a Neuron

A neuron is the basic information-processing unit in the operation of a neural network. The model of a neuron is shown in Fig. 7-1, which includes an externally applied threshold for lowering the net input of the activation function. In mathematical terms, we describe a neuron k by writing the following pair of equations:

$$u_k = \sum_{j=1}^{p} w_{kj} x_j \tag{7-1}$$

and

$$y_k = \varphi(u_k - \theta_k) \tag{7-2}$$

Where x_1, x_2, ..., x_p are input signals; w_{k1}, w_{k2}, ..., w_{kp} are the synaptic weights of neuron k, u_k is the linear combiner output; θ_k is the threshold; $\varphi(\bullet)$ is the activation function; and y_k is the output signal of the neuron.

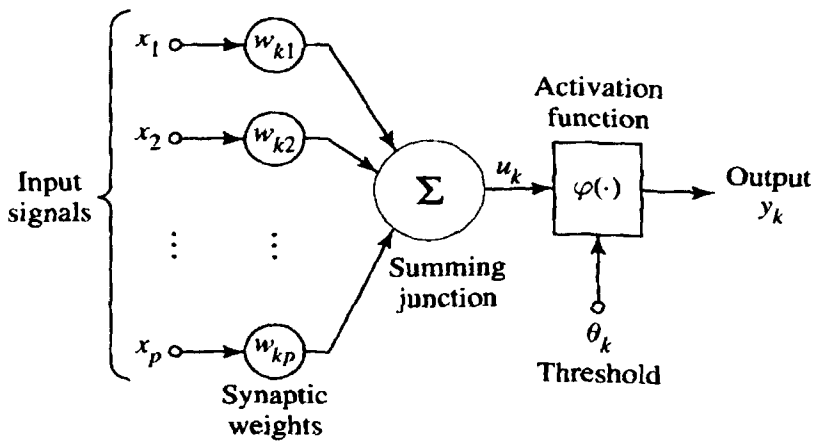

Figure 7-1 Model of a Neuron

7.2.3. Architecture and Algorithm

Based on the individual neuron, typically, the neural network consists of a set of sensory units that constitute the input layer, one or more hidden layers of computation

nodes, and an out put layer of computation nodes. The input signal propagates through the network in a forward direction, on a layer-by-layer basis. These neural networks are commonly referred to as multilayer perceptrons (MLPs). The architecture of MLPs with two hidden layers is shown in Fig. 7-2.

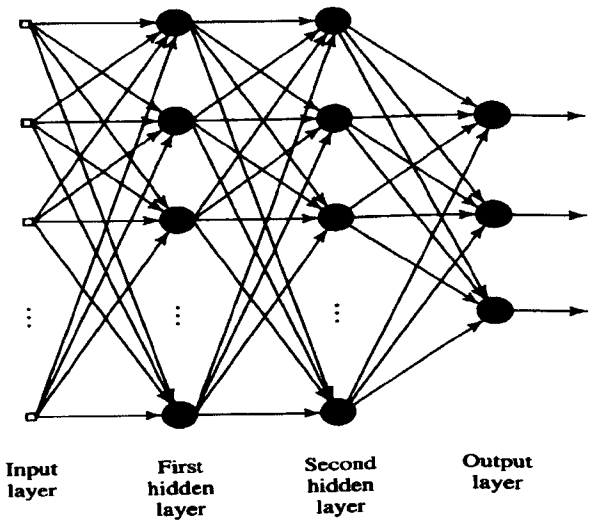

Figure 7-2 Architecture of MLPs with two hidden layers

Multilayer perceptrons have been applied successfully to solve some difficult and diverse problems by training them in a supervised manner with a highly popular algorithm known as the error back-propagation algorithm. There are two passes in the error back-propagation process (see Figure 7-3), a forward pass, in which the signal propagates through the network, layer by layer, the synaptic weights are then fixed; a backward pass, in which the synaptic weights of the network are all adjusted in accordance with the error-correction rule.

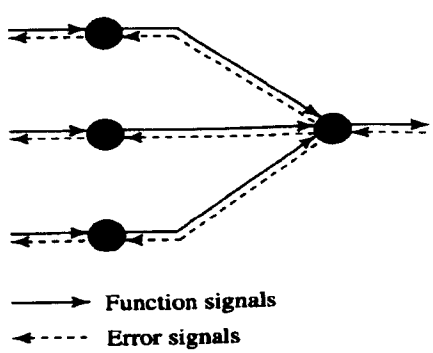

Figure 7-3 Forward propagation of function signals and back-propagation of error signals.

7.2.4. Benefits and Limitation

A neural network derives its computing power through, first its massively parallel distributed structure and, second, its ability to learn and therefore generalise; generalisation refers to the neural network producing reasonable outputs for inputs not encountered during training (learning). The most important benefits from ANN are:

1. Nonlinearity. As a neuron is basically a nonlinear device, a neural network, made up of an interconnection of neurons is nonlinear.
2. Input-Output Mapping. With supervised learning, the synaptic weights could be modified by applying a set of training samples until the difference between the desired response and the actual response reaches a minimum. An input-output mapping for the problem is established.
3. Adaptivity. Neural networks have a built-in capability to adapt their synaptic weights to changes in the surrounding environment. It is an open system and can be easily retrained to adapt to the changes.
4. Fault Tolerance.

Although neural network is a very powerful tool to deal with complex problems, they are not a cure-all. Neural networks are fully based on the training samples. If the training samples are insufficient or do not cover all the typical conditions of the problem, this can cause large errors with testing samples. If the training samples are too much, this can also cause overfitting problem. The most important limitation is that the exact nature of the relationship between inputs and outputs is not known.

7.3. Modelling of Overall Appearance

In this section, we will use neural network to model overall appearance. The objective is to set up the relationship between the overall appearance and the individual parameters. With the neural network model, the overall appearance could be predicted

as an output of the neural network with the individual parameters as inputs. This problem normally is categorised as regression. Here six typical steps are summarised for modelling overall appearance, which can be also applied to other neural network applications.

7.3.1. Definition of the problem

For prediction problems, there are two main categories: classification and regression. We need to make these questions clear: what relationship are we trying to establish? If there is a relationship existing between them (not just noise)? Why do we need a neural network?

In the modelling of overall appearance, we are trying to establish the relationship between overall appearance and the measurable parameters. We know all the parameters (orange peel, metal texture, gloss, DOI, etc.) have a certain relationship with overall appearance, especially the parameter, orange peel, which has the highest correlation with overall appearance (see Chapter 4).

7.3.2. Architecture

As introduced in last section, the most popular architecture of neural networks is the multilayer perceptrons. As neural networks are fully based on the training samples, before the training, the architecture of the neural networks cannot be decided. Typically, an initial configuration is selected with an input layer, one hidden layer and an output layer. For the input layer, the key issue is how to choose variables. Initially it is guided by intuition. Expertise in the problem domain will provide some ideas of which input variables are likely to be influential. During the training processing, variables can be selected and deselected. For the hidden layer, the number of neurons is initially set to half the sum of the input and output number. Iteratively, a number of experiments with each configuration are conducted and the best network retained in

terms of the verification error. A number of experiments are required with each configuration to avoid being misled if training locates a local minimum.

For each experiment, if under-learning occurs (the network does not achieve an acceptable performance level), adding more neurons to the hidden layer(s) can be tried. If this does not work, an extra hidden layer may be added. If over-learning occurs (the verification error starts to rise) removing neurons in the hidden layer, or possibly hidden layers may be tried.

For the overall appearance model, the input variables are initially selected as orange peel, metal texture, gloss, haze, and contrast. The output is the overall appearance index. One hidden layer is chosen with three neurons (Figure 7-4).

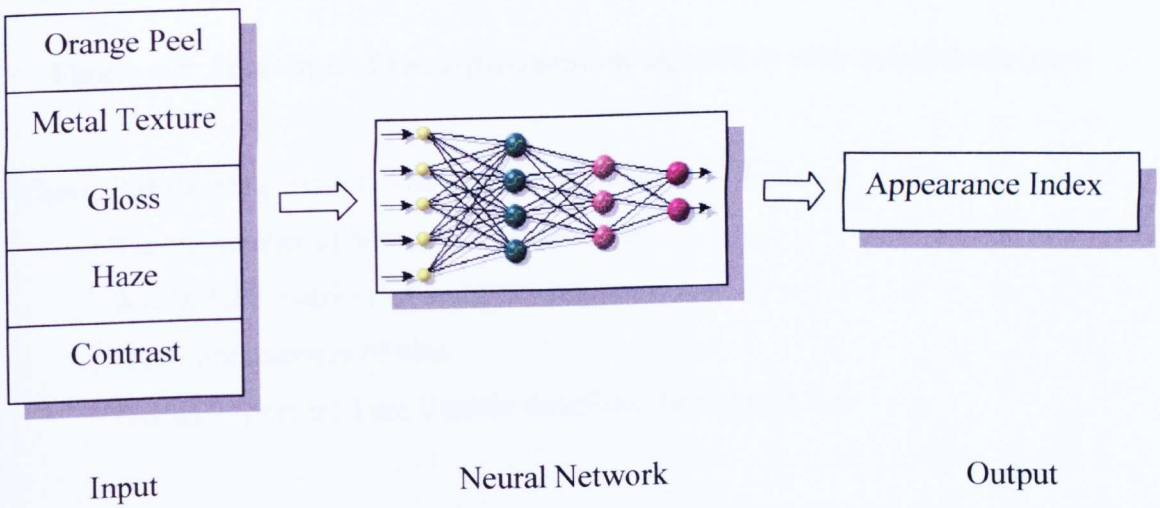

Figure 7-4 Overall Appearance Model using a Neural Network

7.3.3. Algorithm

Back-propagation is the most popular algorithm. Among those algorithms the Levenberg-Marquardt algorithm is reputed to be the fastest [Hagan 1994][Demuth, 1998]. The main drawback of the Levenberg-Marquardt algorithm is that it requires

large amount of computer memory. An abbreviated notation of the neural network with R inputs and one output is presented in Fig. 7-5.

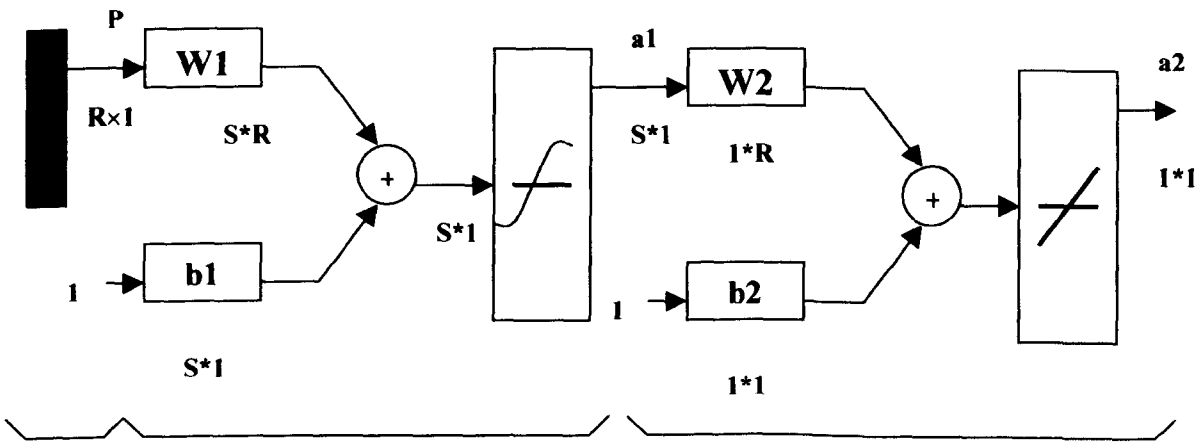

Figure 7-5 Structure of back-propagation algorithm with one-hidden layer

Where, P is the input vector. The number of variables is R.

S is the number of neurons in hidden layer.

W1, W2 are matrices of synaptic weights.

b1, b2 are matrices of bias.

Tansig( ), purelin( ) are transfer functions. See Figure 7-6.

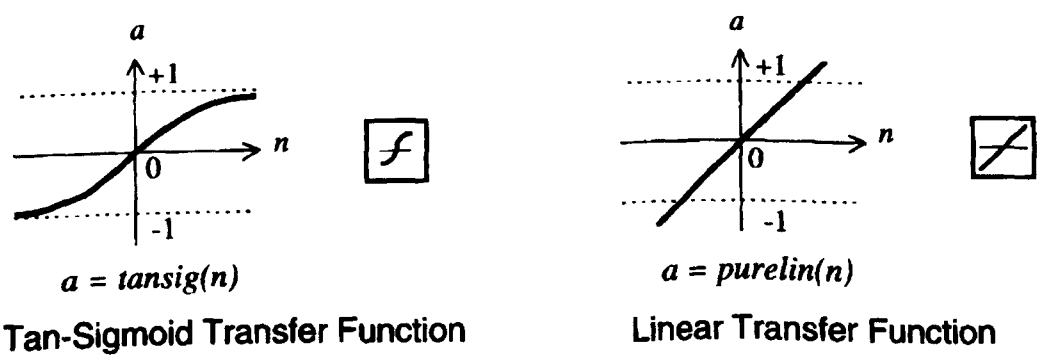

Figure 7-6 Transfer Functions

7.3.4. Data Preparation

Once the architecture and algorithm of the neural networks are determined, data for training purposes is gathered. The training data set includes a number of cases, each containing values for a range of input and output variables. The numeric values have to be scaled into a range which is appropriate for the network. Typically, raw variable values are scaled linearly into range of –1 to 1. The data preparation also includes some pre-processing to find out if the data comes from same population, or if the data has been contaminated by noise, or if there is missing data in each case.

For the overall appearance model, the input data for training and testing can be directly derived from the image-processing based measurement system, which is called 'Smart Appearance' (details see Chapter 9). The orange peel and metal texture can be evaluated using the methods presented in Chapter 4 and 5, the gloss haze can be measured using the similar principle of the QMS equipment (see Chapter 2). Measurements on a set of panels are taken, followed by conducting visual assessments on the same set of panels using the method introduced in Chapter 3. The measurement results are used as the data for the input to the model and the visual assessment result can be used as the target for neural network learning. 23 panels are selected to train and test the neural network model. All the data are listed in Table 7-1.

In Table 7-1, the input data, orange peel (OP), metal texture (MT), Gloss, Haze and Contrast have been normalised to the range of 0 to 100. The visual assessment is still in the range 0 to 1. The output of the neural network is called the appearance index (AI). The performance of the network can be assessed by comparing the difference between the network output (AI) and the target (visual assessment).

Table 7-1 Data for ANN Application

Panel	OP	MT	Gloss	Haze	Contrast	Visual Assessment
am	10.31	27.21	80.00	55.00	31.00	0.99
ba	16.50	35.40	82.10	55.56	81.41	0.88
bb	16.80	41.34	81.13	56.71	76.16	0.81
v	29.55	27.17	81.38	51.58	69.95	0.75
be	18.83	38.96	86.14	55.69	76.50	0.73
421	25.58	41.96	83.05	56.07	47.15	0.55
bc	31.13	42.99	88.65	66.60	68.66	0.45
aa	33.08	41.42	82.86	48.22	72.78	0.43
ab	24.00	61.04	83.28	55.69	78.26	0.37
k	24.75	58.97	82.09	58.14	42.83	0.25
bm	22.65	78.81	83.18	62.64	89.73	0.27
bi	16.73	40.16	82.96	47.20	65.71	0.74
bj	16.03	57.83	84.00	63.00	77.00	0.56
bn	28.05	55.02	85.00	65.00	77.00	0.37
417	24.17	66.45	84.00	58.00	48.00	0.18
al	26.03	40.34	83.00	50.00	24.00	0.42
an	12.53	35.00	80.00	62.00	36.00	0.91
ao	26.82	36.55	84.00	62.00	31.00	0.61
ak	25.97	37.26	84.00	53.00	25.00	0.48
y	43.53	35.80	78.00	50.00	65.00	0.38
h	17.85	29.65	82.00	58.00	56.00	0.96

To train and test the neural network model, the data samples are randomly arranged. Then two thirds of them are selected for training and the rest of them (one third) are used to test the model. The format of input vector and output vector and the data selected for training after random arrangement are listed in Table 7-2 and Table 7-3.

Table 7-2 Input Vectors of Training Data Set

Panel	bj	al	y	417	ba	aa	bn
OP	16.03	26.03	43.53	24.17	16.5	33.08	28.05
MT	57.83	40.34	35.8	66.45	35.4	41.42	55.02
Gloss	84	83	78	84	82.1	82.86	85
Haze	63	50	50	58	55.56	48.22	65
Contrast	77	24	65	48	81.41	72.78	77

Panel	am	421	v	bi	bm	be	k
OP	10.31	25.58	29.55	16.73	22.65	18.83	24.75
MT	27.21	41.96	27.17	40.16	78.81	38.96	58.97
Gloss	80	83.05	81.38	82.96	83.18	86.14	82.09
Haze	55	56.07	51.58	47.2	62.64	55.69	58.14
Contrast	31	47.15	69.95	65.71	89.73	76.5	42.83

Table 7-3 Output Vectors of Training Data Set

Panel	bj	al	y	417	ba	aa	bn
Visual	0.56	0.42	0.38	0.18	0.88	0.43	0.37
Panel	am	421	v	bi	bm	be	k
Visual	0.99	0.55	0.75	0.74	0.27	0.73	0.25

Table 7-4 Input Vectors of Testing Data Set

Panel	ao	ak	bb	h	ab	bc	an
OP	26.82	25.97	16.8	17.85	24	31.13	12.53
MT	36.55	37.26	41.34	29.65	61.04	42.99	35
Gloss	84	84	81.13	82	83.28	88.65	80
Haze	62	53	56.71	58	55.69	66.6	62
Contrast	31	25	76.16	56	78.26	68.66	36

Table 7-5 Output Vectors of Testing Data Set

Panel	ao	ak	bb	h	ab	bc	an
Visual	0.61	0.48	0.81	0.96	0.37	0.45	0.91

7.3.5. Supervised Training and Testing

Once the number of layers and number of neurons in each layer have been selected, the network's weights and thresholds (bias) must be set so as to minimise the prediction error made by the network. This is the role of the training algorithms. The historical cases (data) which have been gathered are used to automatically adjust the weights and thresholds in order to minimise this error. This process is equivalent to fitting the model represented by the network to the training data available. The error of a particular configuration of the network can be determined by running all the training cases through the network, comparing the actual output generated with desired or target outputs.

To avoid the error caused by network initiation. For the same network architecture the training and testing are performed three times. Each time there is an initial set of weights and biases for the neural network. After the training with the presented data set, a final network structure including weights and bias can be decided. Then the validation with the training data set and testing with testing data set can be conducted. The network with best testing result should be chosen as a final network structure.

A programme has been developed with MATLAB to perform the neural network training and testing

Architecture summary:
Input parameters: 5
Output parameters: 1
Neural network layers: 2
Neuron number in hidden layer: 16

Algorithm: Levenberg-Marquardt

First run:

With the training data set (Table 7-2 and 7-3), first training takes only 6 epochs to finish the training procedure. The training error goal is 0.0001. Fig. 7-7 shows the error track of this training procedure.

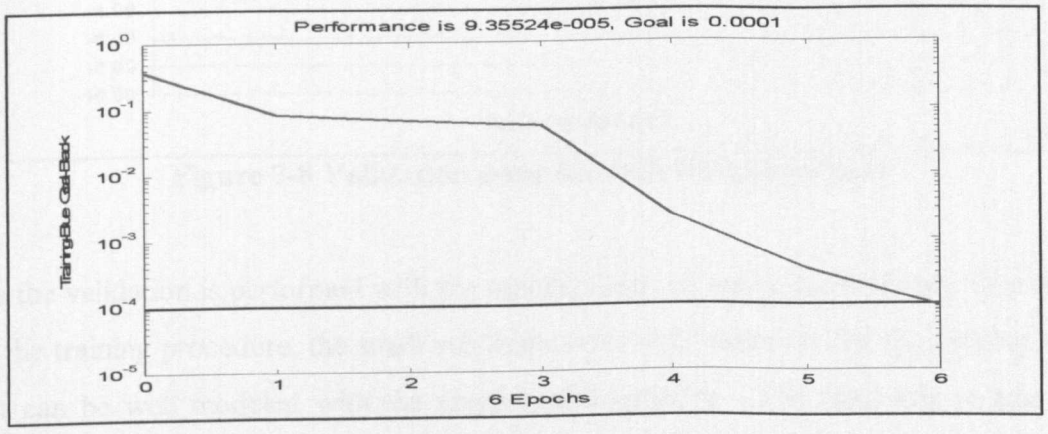

Figure 7-7 Training procedure of first run

After training, the weights and biases can be decided. From Table 7-6, it can be seen that although the network was trained by the target as the output, there is still a difference between them. The absolute mean error is 2.03% and the absolute standard deviation is 2.08. Fig. 7-8 depicts the error for each training sample.

Table 7-6 Validation result of first run

Panel	Prediction	Target	Error(%)
bj	0.57	0.56	0.91
al	0.42	0.42	1.17
y	0.39	0.38	3.71
417	0.18	0.18	0.11
ba	0.89	0.88	0.57
aa	0.44	0.43	1.51
bn	0.38	0.37	3.54
am	0.99	0.99	0.31
421	0.56	0.55	0.96
v	0.75	0.75	0.32
bi	0.75	0.74	1.32
bm	0.29	0.27	7.04
be	0.74	0.73	1.64
k	0.26	0.25	5.36

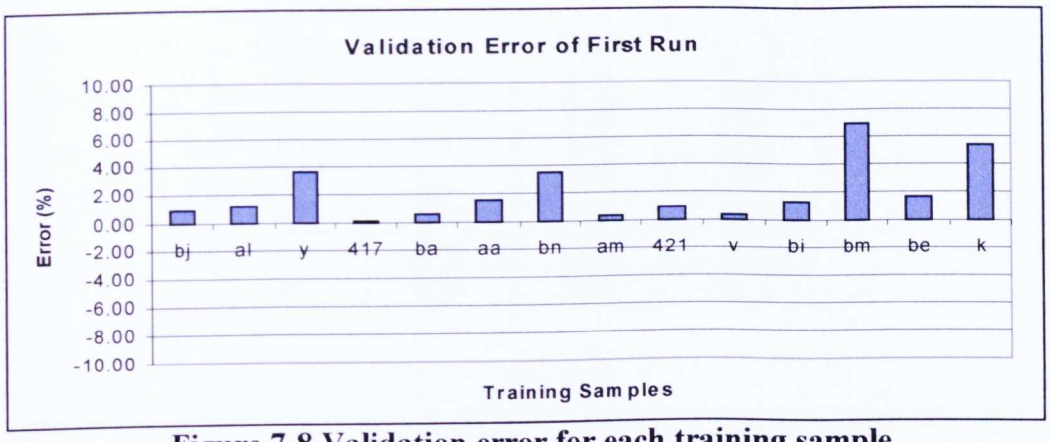

Figure 7-8 Validation error for each training sample

As the validation is performed with the training data set, which were already presented in the training procedure, the small validation error only indicates that the training data set can be well modeled with the given neural network. The best way to test the generalisation ability of neural network model is to test the network with the data set which the network never met before. That is why the whole data set is randomly arranged and one third of them are reserved.

The reserved test data set (Table 7-4 and 7-5) are used to test the trained network. The neural network outputs can also be compared with the target outputs of the test data samples. The result is presented in Table 7-7 and Fig. 7-9, the test error (%) is displayed in Fig. 7-10 (the mean absolute error is 4.36%; the standard deviation of test error is 4.88). The test errors are obviously larger than validation errors, because the test data set is never met by the network before. But from Fig. 7-9, the output of the neural network predicts the visual assessment (target) very well. We can also calculate the correlation between these two data sets, which is 0.99. This means that the overall appearance can be well modelled using a neural network with the presented data set including the training and testing data set.

Table 7-7 Test Result of First Run

Panel	predict	target	error(%)
ao	0.52	0.61	-14.34
ak	0.48	0.48	0.25
bb	0.81	0.81	-0.33
h	0.91	0.96	-5.23
ab	0.35	0.37	-5.59
bc	0.44	0.45	-1.76
an	0.88	0.91	-3.07

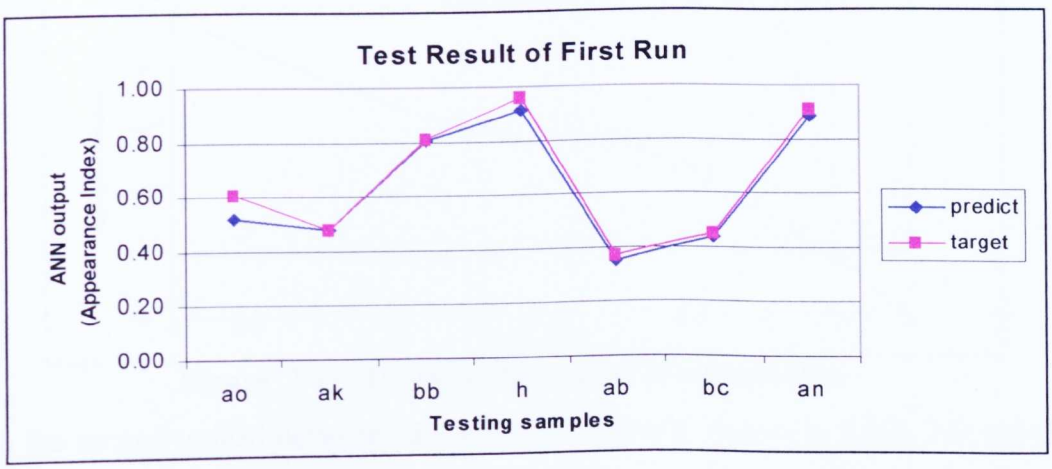

Figure 7-9 Test Result of First Run

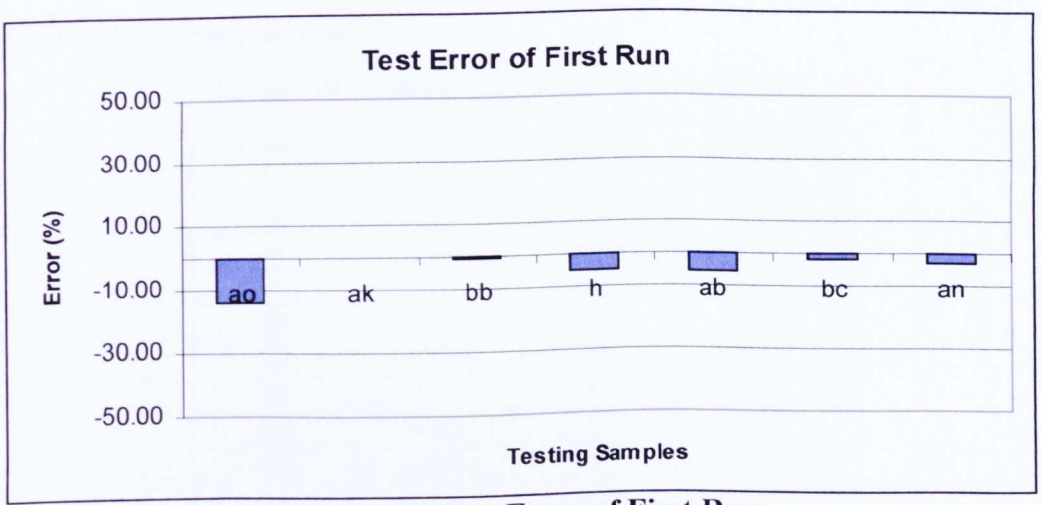

Figure 7-10 Test Error of First Run

Second Run:

The experiment was repeated three times with the same data set and structure to avoid the training being trapped by a local minimum error. Each time the system will assign an initial set of weights and biases to the neural network. As the initiation of the network is different, it can lead to a different network setting (weights and bias). Fig. 7-11 is the error track of the second run, in which the training goal (0.0001) can be achieved with only 5 epochs.

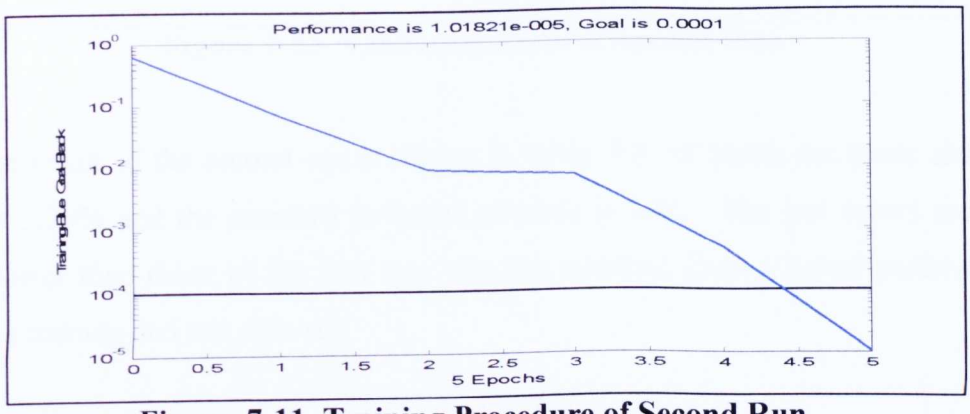

Figure 7-11 Training Procedure of Second Run

With the second trained network, the validation result is shown in Table 7-8 and the validation error is drawn in Fig. 7-12, in which the mean absolute error is 0.54% and the standard deviation of the error is 0.69. The validation error of the second run is much lower than first run. That means the network setting of the second run is more suitable for the training data set.

Table 7-8 Validation Result of Second Run

Panel	predict	target	error(%)
bj	0.56	0.56	-0.38
al	0.42	0.42	-0.76
y	0.38	0.38	-1.18
417	0.18	0.18	-0.22
ba	0.88	0.88	0.02
aa	0.43	0.43	0.07
bn	0.37	0.37	0.30
am	0.99	0.99	-0.29
421	0.55	0.55	-0.18
v	0.74	0.75	-0.83
bi	0.74	0.74	0.22
bm	0.26	0.27	-2.67
be	0.73	0.73	0.25
k	0.25	0.25	0.28

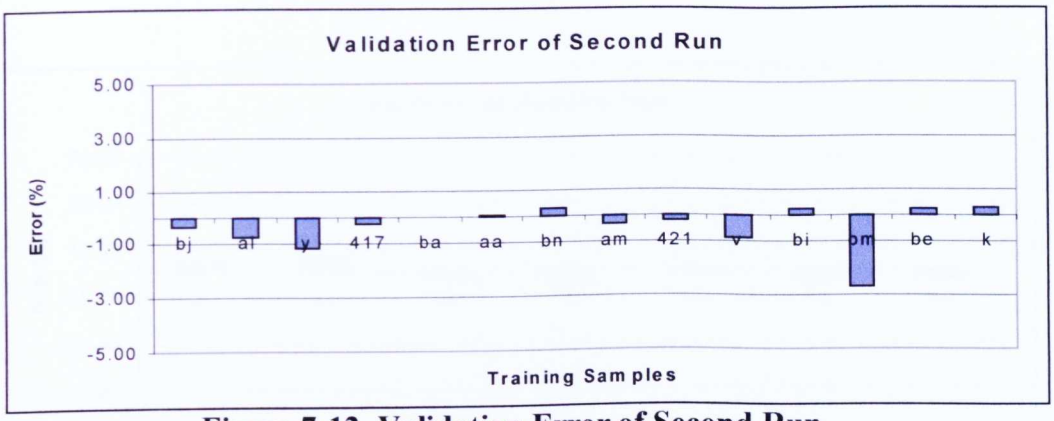

Figure 7-12 Validation Error of Second Run

The test result of the second run is shown in Table 7-9, in which the mean absolute error is 3.29% and the standard deviation of error is 1.86. The test errors are also much lower than those of the first run. So this network gives a better performance with the training and test data set.

Table 7-9 Test Result of Second Run

Panel	predict	target	error(%)
ao	0.64	0.61	5.15
ak	0.51	0.48	6.48
bb	0.79	0.81	-2.85
h	0.92	0.96	-4.45
ab	0.37	0.37	-0.59
bc	0.43	0.45	-4.27
an	0.88	0.91	-3.63

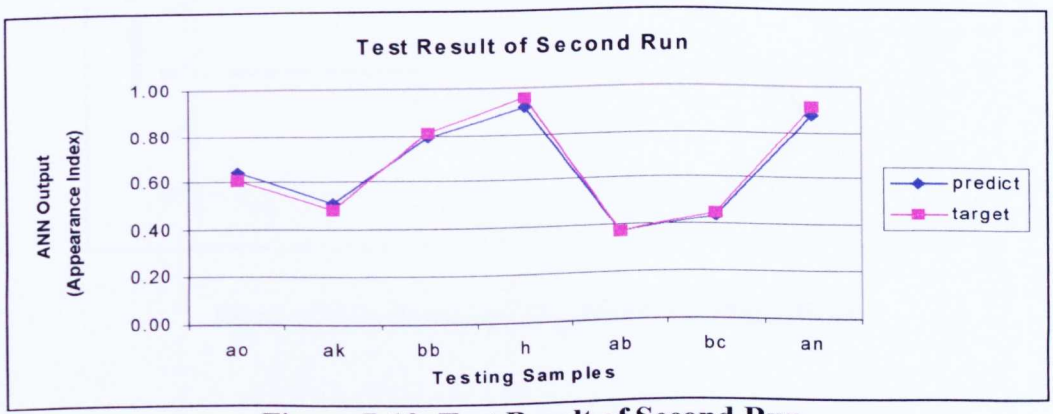

Figure 7-13 Test Result of Second Run

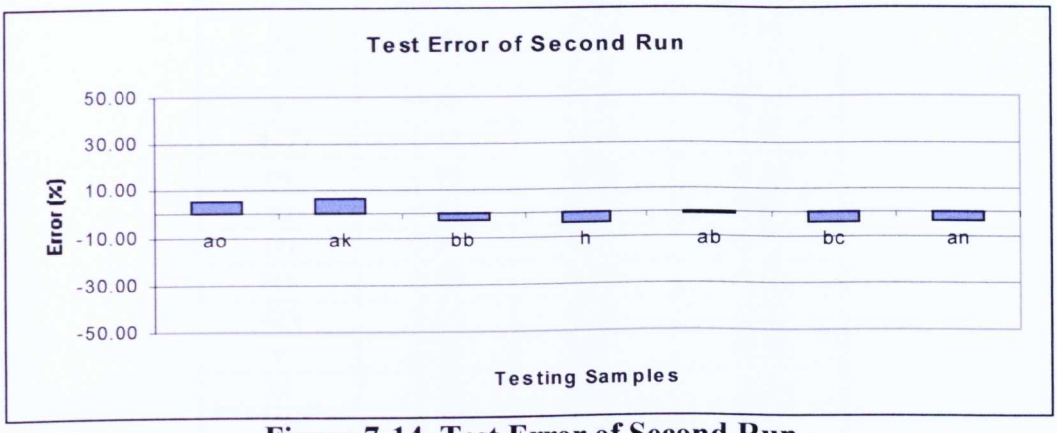

Figure 7-14 Test Error of Second Run

Third Run:

In third run, the network takes 5 epochs to finish the training procedure (Fig. 7-15). The validation result is shown in Table 7-10, in which the mean absolute error is 0.29 and the standard deviation of the error is 0.16

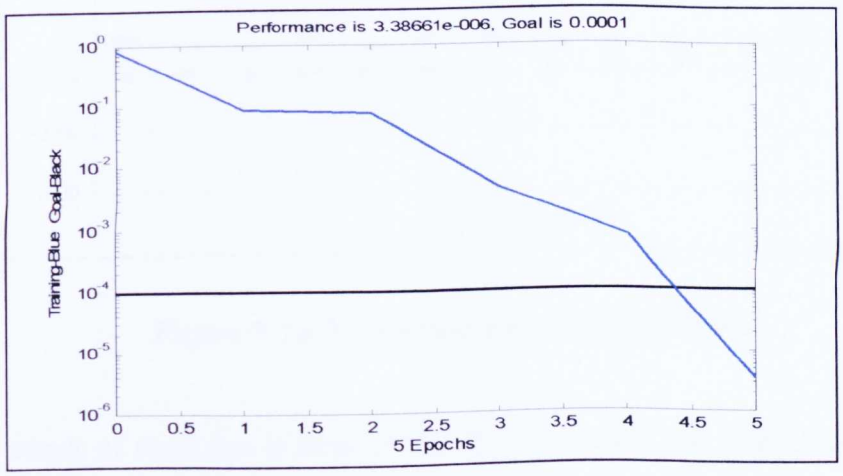

Figure 7-15 Training Procedure of Third Run

Table 7-10 Validation Result of Third Run

Panel	predict	target	error(%)
bj	0.56	0.56	0.29
al	0.42	0.42	-0.14
y	0.38	0.38	-0.11
417	0.18	0.18	0.56
ba	0.88	0.88	-0.23
aa	0.43	0.43	0.26
bn	0.37	0.37	0.46
am	0.99	0.99	-0.33
421	0.55	0.55	-0.33
v	0.75	0.75	-0.52
bi	0.74	0.74	-0.03
bm	0.27	0.27	0.52
be	0.73	0.73	-0.25
k	0.25	0.25	0.16

The validation error is drawn in Fig. 7-16. Comparing with previous two runs, the third run has the lowest mean validation error and standard deviation.

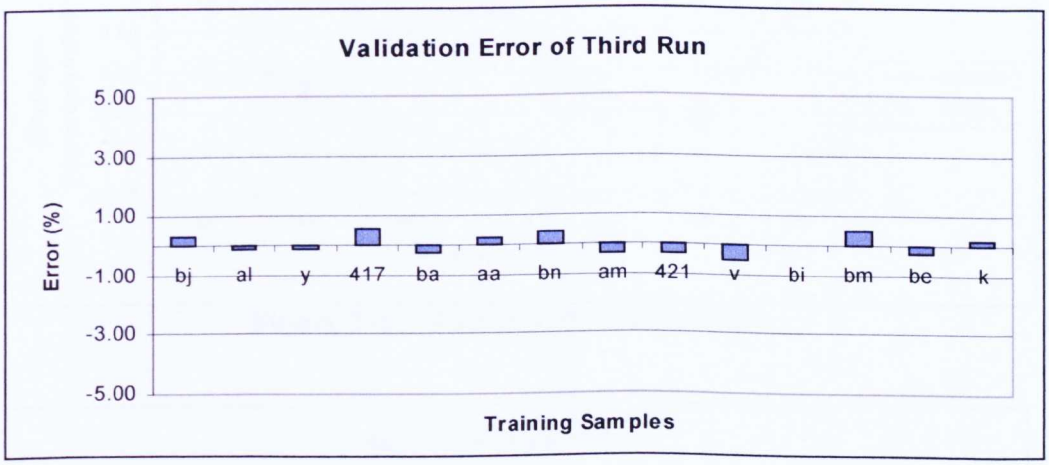

Figure 7-16 Validation Error of Third Run

The test result of third run is listed in Table 7-11, where the mean absolute error is 12.76 and standard deviation of error is 12.55.

Table 7-11 Test Result of Third Run

Panel	predict	target	error(%)
ao	0.67	0.61	10.08
ak	0.55	0.48	13.90
bb	0.80	0.81	-1.06
h	0.89	0.96	-6.89
ab	0.47	0.37	27.41
bc	0.33	0.45	-26.49
an	0.94	0.91	3.54

Fig. 7-17 and 7-18 present the test result and test error of the third run. The error between neural network output (appearance index) and target (visual assessment) is higher than the previous two runs. It can be seen that even if the network has a small validation error with the training data, the test error could still be large. The network must be adapted to both data sets.

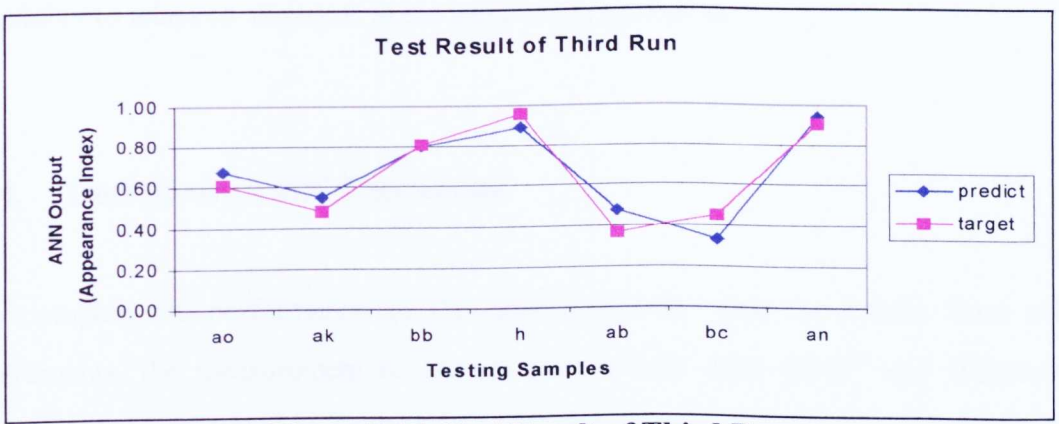

Figure 7-17 Test Result of Third Run

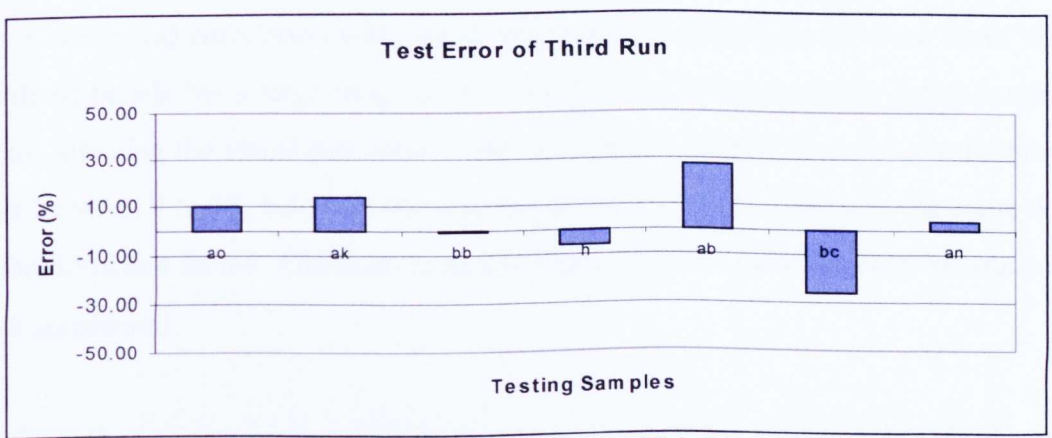

Figure 7-18 Test Error of Third Run

The results from the three runs show that the network setting from the second run has the best results. As the validation data set is the training data set which has been already presented in the training procedure, the validation error is normally small. As the test data is the new data to the neural network, the test result can demonstrate more generalisation ability of the neural networks. Generally, the network with the best results to both validation and testing should be chosen as the final network setting. In the above case, the network of the second run should be the best one.

7.3.6. Retraining

The neural network is an open system that enables the user to retrain the network when the environment has been changed. This characteristic gives the network more flexibility to adapt to changes in the system it is applied to.

7.4. Comparison and Discussion

To compare the performance of the neural network with the results from other instruments, the measurement results on these panels from QMS® and Wavescan® equipment are presented in Table 7-12. The distribution of long wave and short wave from Wavescan is shown in Figure 7-19. In Chapter 4, we know that the long wave has a very good correlation with visual assessment, it is because the long wave effect on those panels has a large range (0-45). In this case, the long wave is the dominant factor affecting the visual perception. But in Figure 7-19, the long wave is distributed only between 0 to 13, but short wave is ranged from 0-50. In this case, the short wave is the dominant factor. The discrimination ability of short wave for each instrument is now considered.

The correlation between long wave, short wave and visual assessment is displayed in Figure 7-20 and 7-21. The correlation between long wave and visual assessment (0.66) is weaker than that (0.91) in Figure 4-5. But the short wave has a stronger

correlation with visual assessment (0.72) than that (0.51) in Figure 4-10. It can be explained that in this case of long wave being similar but short wave being different, the discrimination ability of short wave is not good enough to correlate with human visual perception. Therefore, the overall appearance cannot rely on a single parameter, either long wave or short wave.

As the Wavescan® equipment does not provide a formula to present the correlation with visual assessment, we compare the output of the neural network model and the result from QMS® equipment.

Table 7-12 Measurement Results from QMS and Wavescan

	QMS				Wavescan		Visual Assessment
Panel	Gloss	DOI	Orange Peel	Overall	LW	SW	
bj	72.23	66.07	71.23	70.93	3.70	23.80	0.56
al	55.20	61.80	56.60	58.20	7.00	27.00	0.42
y	58.80	67.70	43.30	54.30	12.22	18.52	0.38
417	62.60	71.50	74.60	71.40	6.20	32.60	0.18
ba	74.90	72.63	77.37	75.43	5.00	16.40	0.88
aa	65.70	73.80	69.80	70.60	3.72	20.98	0.43
bn	41.40	82.68	58.69	51.72	8.30	24.40	0.37
am	74.00	78.40	76.70	76.90	0.80	3.50	0.99
421	51.70	61.50	67.40	63.00	7.60	26.30	0.55
v	76.80	84.10	76.20	78.90	2.62	6.06	0.75
bi	73.77	67.33	74.30	72.87	5.90	16.30	0.74
bm	58.91	83.80	58.82	69.69	8.20	40.20	0.27
be	72.03	70.80	75.07	72.90	3.70	19.70	0.73
k	50.60	57.20	52.10	53.70	10.32	46.16	0.25
ao	71.00	74.90	64.30	69.00	5.10	16.70	0.61
ak	53.40	60.30	57.20	57.70	5.50	24.00	0.48
bb	75.73	75.00	80.00	77.13	3.90	12.10	0.81
h	76.00	81.40	79.90	79.90	1.32	13.76	0.96
ab	45.50	57.30	59.90	56.80	10.44	46.40	0.37
bc	69.17	63.90	70.00	68.67	10.10	18.80	0.45
an	80.30	84.00	79.20	81.10	1.10	6.00	0.91

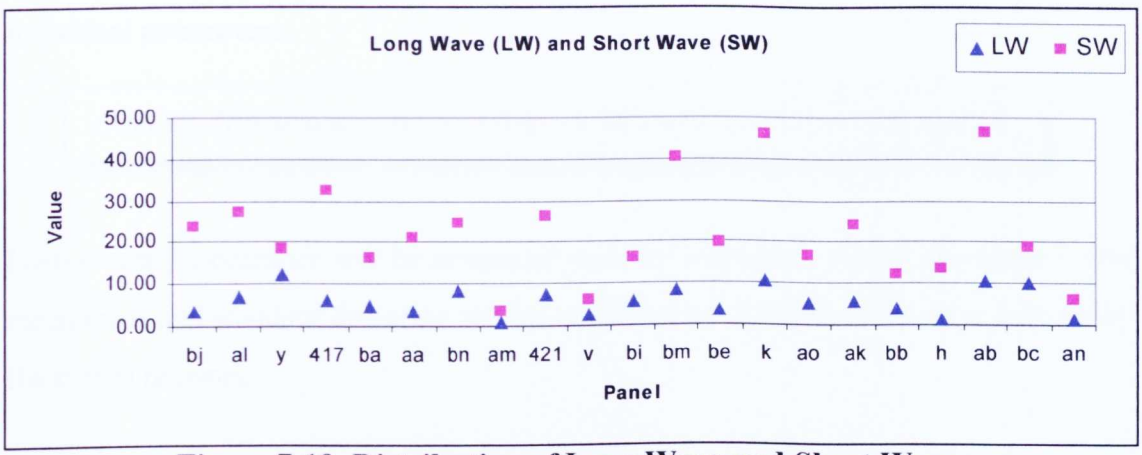

Figure 7-19 Distribution of Long Wave and Short Wave

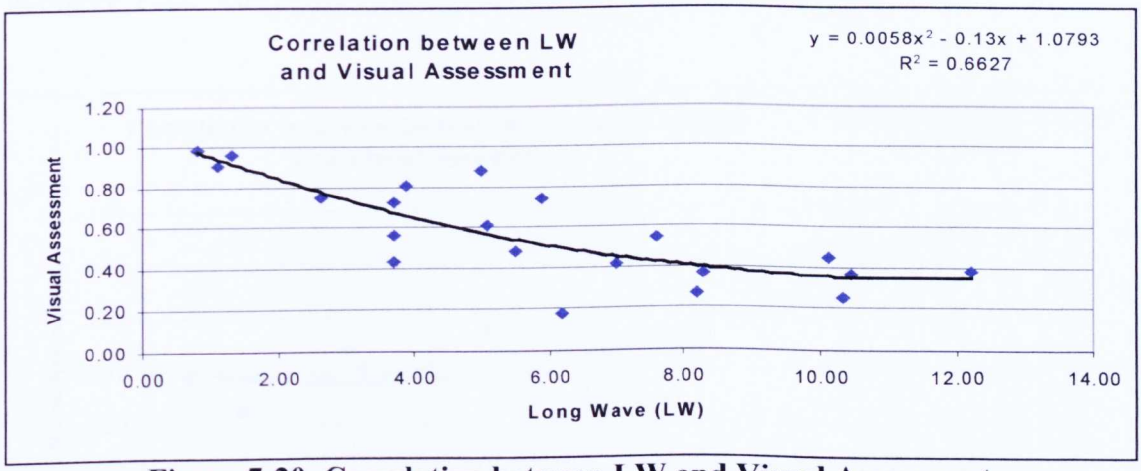

Figure 7-20 Correlation between LW and Visual Assessment

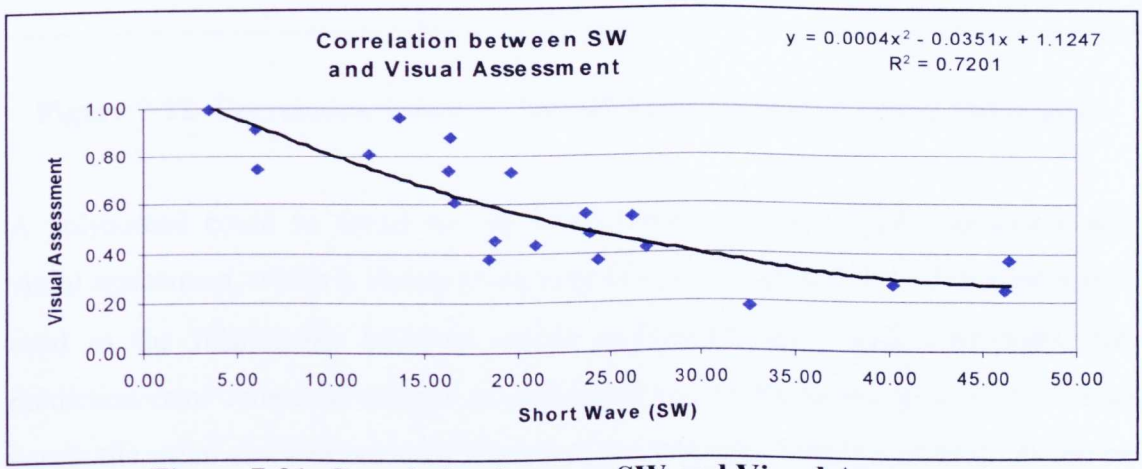

Figure 7-21 Correlation between SW and Visual Assessment

QMS provides us an overall appearance formula, which has a linear correlation with individual parameters.

$$Overall\ Appearance = 0.15 \times Gloss + 0.35 \times DORI + 0.50 \times OrangePeel$$

Here overall appearance will be compared with the reference, visual assessment. The mean error and standard deviation will be calculated to compare with those derived by the neural network.

The correlation between overall appearance (QMS) and visual assessment is depicted in Figure 7-22. The correlation coefficient is not high ($R^2 = 0.65$).

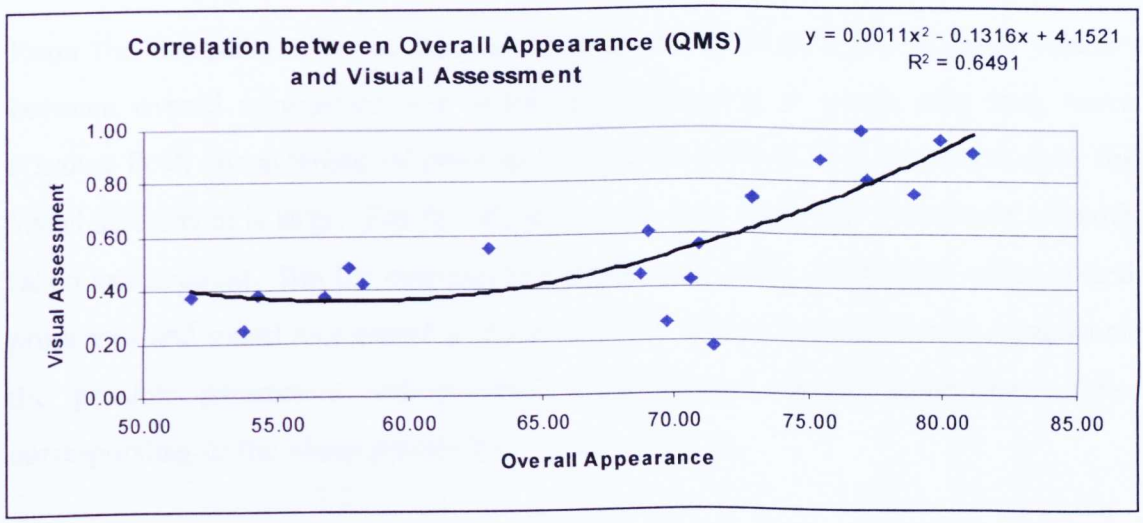

Figure 7-22 Correlation between Overall Appearance and Visual Assessment

A polynomial could be found for the relationship between overall appearance and visual assessment, which is shown in the right corner of Figure 7-22. If this formula is used as the relationship between overall appearance and visual assessment, the prediction error compared with visual assessment can be drawn in Figure 7-23. For all panels the mean absolute error is 28.6% and the standard deviation is 46.7. It can be seen that the mean absolute error and the standard deviation are much larger than those with the neural network model.

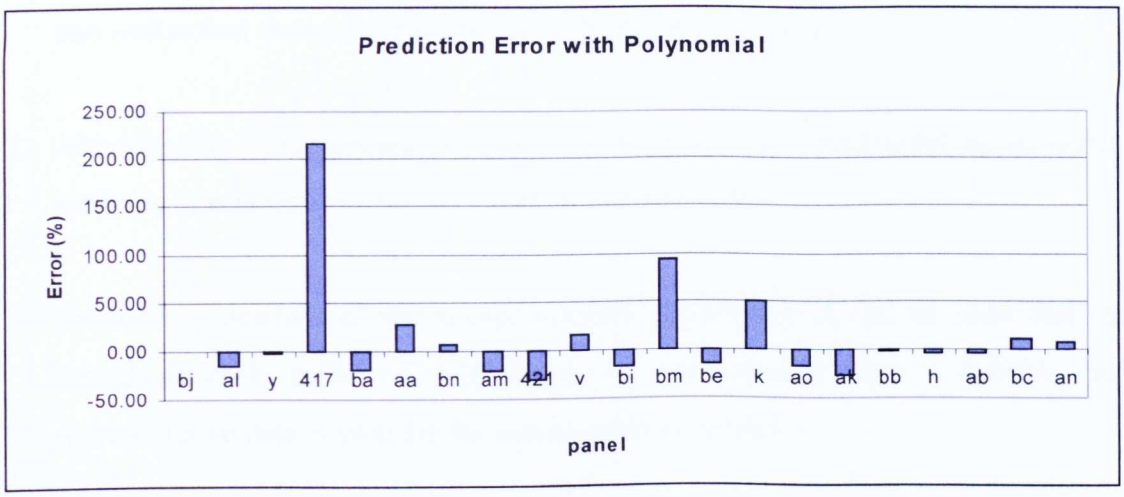

Figure 7-23 Prediction Error with Polynomial

From the comparison, it can be seen that as the QMS provides a linear relation between overall appearance and individual parameters, in which only long wave (Orange Peel) characteristic of paint surface is used and the final prediction error for visual assessment is large. For the Wavescan, the long wave and short wave are both taken into account. But the correlation between long wave, short wave, other optical properties and visual assessment is unknown. The neural network model contains all the possible parameters and provides a very good overall appearance index corresponding to the visual perception.

7.5. Conclusion

In this chapter, the paint appearance is successfully modeled using neural networks. The whole procedure for the neural network application has also been demonstrated. The comparison result shows the ability of the neural network to model the overall appearance with a high level of similarity to human visual perception. Based on the above discussion, the following conclusion can be drawn.

1. From the training and test results, it can be shown that the neural network model can well reflect the correlation between the input and output.

2. Although the paint appearance is difficult to model with traditional mathematical methods, it is comparatively easy with neural networks.

3. From the procedure of the neural network application, it can be seen that the neural network model is fully based on experimental data. Reliable and representative data is vital for the neural network model.

4. A neural network is an open system. If the environment that the neural network is applied to have been changed, the neural network can be easily retrained with new experimental data.

5. As the neural network is like a 'black box', the detailed operation of the neural network is unknown Caution needs to be exercised when using it.

Chapter 8

Modelling of Overall Appearance Using Fuzzy Logic

8.1. Introduction

In last chapter, the overall appearance was successfully modelled using a neural network. As pointed out in the conclusion, the nature of the processing inside a neural network is far from clear. A further more recent technique will be considered in this Chapter, known as Fuzzy Logic. Fuzzy Logic is a powerful problem-solving methodology used for many applications in embedded control and information processing. It provides a remarkably simple way to draw definite conclusions from vague, ambiguous or imprecise information. In this sense, fuzzy logic resembles human decision making with its ability to work from approximate data and find precise solutions. For example, when people visually assess gloss on the painted samples, normally they say the gloss is high or medium or low. Based on the comparison of all aspects of paint appearance and previous knowledge, a conclusion about which one is better can be made. By using a more natural rule-based approach which is closer to the real world, Fuzzy Logic can offer a superior performance and a better trade-off between system robustness and sensitivity, which results in the handling of non-linear models better than traditional methods.

Unlike classical logic which requires a deep understanding of a system, exact equations, and precise numeric values, Fuzzy Logic incorporates an alternative way of thinking, which allows the modelling of complex systems using a higher level of

abstraction originating from our knowledge and experience. An account of Fuzzy Logic theory can be found in reference [Dubois 1980]. This chapter will include a brief introduction on the concept of fuzzy logic, then concentrate on how to model overall appearance using Fuzzy Logic.

8.2. Fuzzy-Logic Modelled System

8.2.1. The Nature of Fuzzy Logic

Fuzzy Logic is concerned with the relative importance of precision, an activity that humans have been managing for a very long time. Fuzzy logic is a convenient way to map an input space to an output space in an efficient and rapid way. The primary mechanism for doing this is a list of 'if-then' statements called rules. All rules are evaluated in parallel, and the order of the rules is unimportant. The rules themselves are useful because they refer to variables and the adjectives that describe those variables. Fuzzy Logic starts with the concept of a fuzzy set, which is a set without a clearly defined boundary, and contain elements with only a partial degree of membership between 0 and 1. The following statement lays the foundations for fuzzy logic: *In fuzzy logic, the truth of any statement becomes a matter of degree* [Zadeh 1999].

The membership function is a curve that defines how each point in the input space is mapped to a membership value (or degree of membership), which is used to blur the discrete input into a fuzzy set. The typical process of a fuzzy logic model includes: (a) 'Fuzzification' where a crisp input is translated into a fuzzy set using a membership function, (b) Rule Evaluation, where the fuzzy outputs are computed in parallel with the specified rules based on the experience, and (c) 'Defuzzification' where the fuzzy output is translated to a crisp value. In section 8.2.3, the steps for fuzzy logic application in appearance measurement will be presented in detail.

8.2.2. Reasons for using Fuzzy Logic

Fuzzy Logic permits the description of complex systems using prior knowledge and experience in the form of simple rules. It does not require any system modelling or the use of equations governing the relationship between inputs and outputs. It provides an alternative solution to non-linear models handled by rules and membership functions. The inference process results in improved performance, simpler implementation and reduced design costs. In this case, particular observations about fuzzy logic are:

- Fuzzy logic can built on the experience of experts. As an overall appearance index is required to relate to human visual perception, human understanding on assessment of paint appearance should form the basis of the measurement system. Built on the experts' experience, the system may be more reliable and objective

- Fuzzy logic is an open, flexible system, which permits a change in the system performance with newly obtained knowledge.

- Fuzzy logic can model non-linear functions of arbitrary complexity. As this system is multi-input and non-linear, fuzzy logic can easily map the input and output.

- Fuzzy logic is conceptually easy to understand and use over traditional mathematical methods, because it is based on the natural language of human communication, which underpins many of the other advantages of fuzzy logic.

8.2.3. Modelling Overall Appearance Using Fuzzy Logic

To model overall appearance, first of all, a type of fuzzy inference should be chosen. The fuzzy inference is the process of formulating the mapping from a given input to

an output using fuzzy logic. The mapping then provides a basis from which decisions can be made. The process of fuzzy inference involves membership functions, fuzzy logic operators, and 'if-then' rules, which will be explained below. There are two types of fuzzy inference systems, Mamdani-type and Sugeno-type. These vary somewhat in the way outputs are determined [Mamdani 1975][Sugeno 1985]. In these two types, Mamdani's fuzzy inference method is the most commonly used. Ebrahim Mamdani proposed it in 1975 as an attempt to control a steam engine and boiler combination by synthesising a set of linguistic control rules obtained from experienced human operators. In our case, the Mamdani-type fuzzy inference is chosen to model the appearance measurement system (Figure 8-1). As orange peel (OP), metal texture (MT) and gloss are the most important parameters, to simplify the proposed system, these three parameters are defined as input and the Appearance Index (AI) is the output. Five typical steps to model overall appearance using fuzzy logic are presented below.

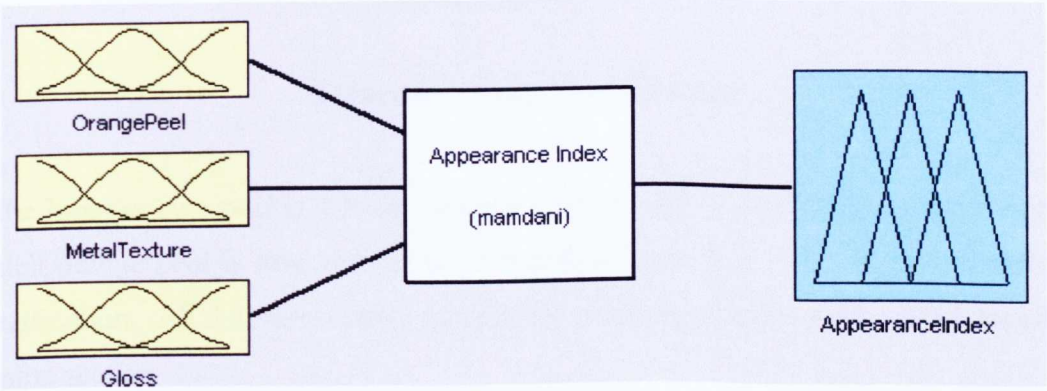

Figure 8-1. Mamdani model for Appearance Index

Step 1. 'Fuzzify' Inputs

The first step is to take the inputs and determine the degree to which they belong to each of the appropriate fuzzy sets via membership functions. The input is always a crisp numerical value limited to the universe of discourse of the input variable (in this

case the interval between 0 and 100) and the output is a fuzzy degree of membership in the qualifying linguistic set (always the interval between 0 and 1).

For example, the input, orange peel, is represented with three fuzzy linguistic sets: orange peel is low, orange peel is medium, orange peel is high. Then input, orange peel, can be fuzzified according to each of these linguistic sets and membership functions (Figure 8-2).

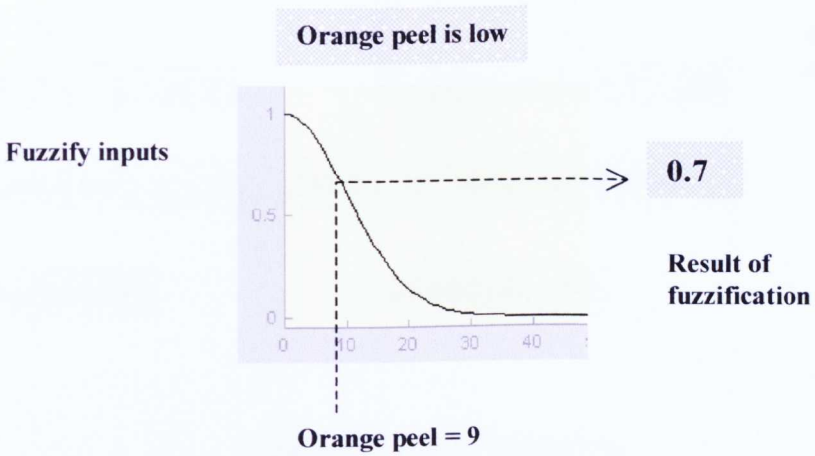

Figure 8-2 Input Fuzzification

If the input orange peel is 9 in the interval of 0 and 100 (crisp input), to the extent to which orange peel is low, the result of fuzzification is 0.7. This is the principle of fuzzification. All the membership functions to each input and output will be specified in next section.

Step 2. Apply Fuzzy Operator

If there is more than one input and the linguistic rules are applied to all of them, the fuzzy operator like AND or OR need to be used.

For example, in Figure 8-3, if the inputs: orange peel is 9 and metal texture is 6, which are both applied to the rules: orange peel is low and metal texture is low. In this case, the result of the fuzzy operator (AND) is 0.7.

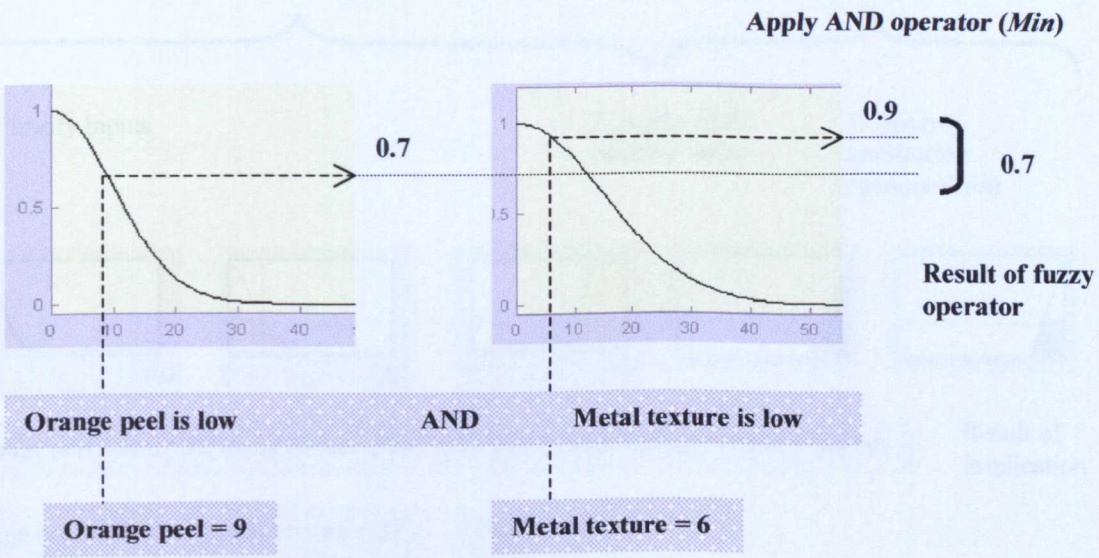

Figure 8-3 Fuzzy operation

Step 3. Apply the Implication Method

Before applying the implication method, every rule has a weight (a number between 0 and 1), which is applied to the number given by the antecedent. Generally this weight is 1. The input for the implication process is a single number given by the antecedent, and the output is a fuzzy set. The Implication is implemented for each rule. Two methods are used, *AND* method (*min*), which truncates the output fuzzy set and *product* method, which scales the output fuzzy set. For example, in figure 8-4, there are three inputs, orange peel, metal texture and gloss. Based on the rule: *If* ***orange peel*** *is* ***low*** *AND* ***metal texture*** *is* ***low*** *AND* ***gloss*** *is* ***high*** *then* ***appearance*** *is* ***perfect.***, The output of the antecedent is 0.4, after applying the implication operator (*min*), the result of implication is the fuzzy set, which is the area being truncated (on the right).

The definition of the membership functions for each input and output is described in detail in section 8.2.4.

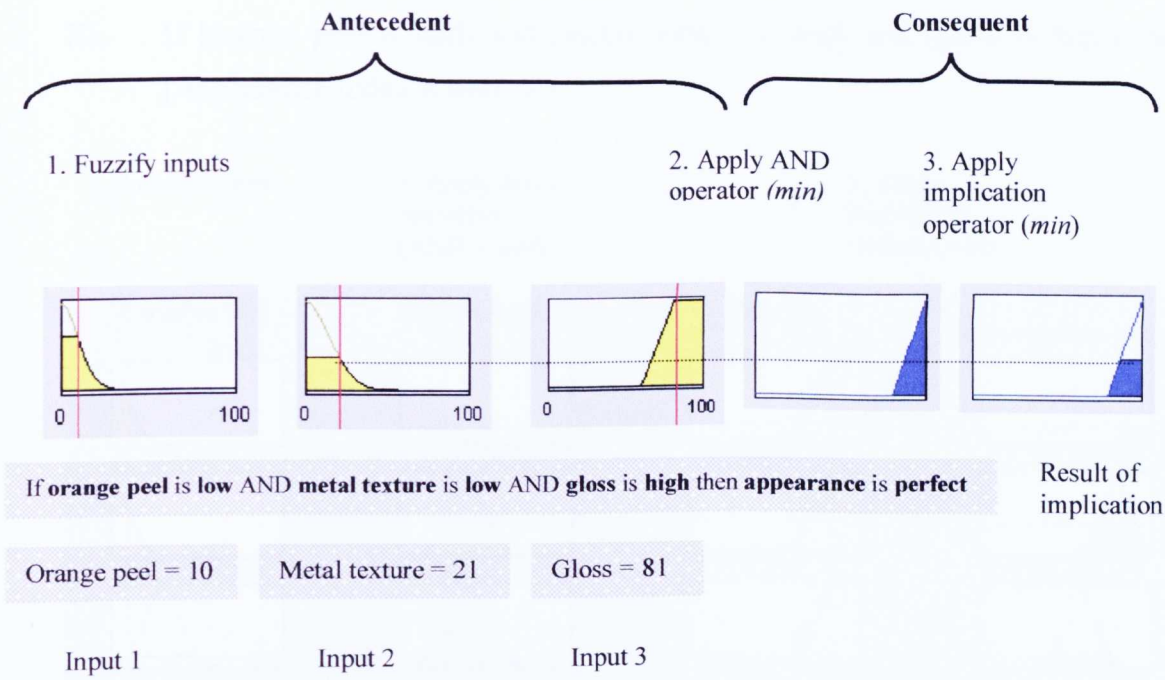

Figure 8-4 Fuzzy implication method

Step 4. Aggregate All outputs

Normally the decisions are based on all the rules applied. Aggregation is the process by which the fuzzy sets that represent the outputs of each rule are combined into a single fuzzy set. The input of the aggregation process is the list of truncated output functions returned by the implication process for each rule. The output of the aggregation process is one fuzzy set for each output variable.

There are three methods: *max* (maximum), *probor* (probabilistic or), and *sum*. An example is given in Figure 8-5. The fuzzy reasoning is based on three rules:

I. If [orange peel is low] and [metal texture is low] and [gloss is high] then [Appearance Index is perfect]

II. If [orange peel is low] and [metal texture is mid] and [gloss is high] then [Appearance Index is good]

III. If [orange peel is mid] and [metal texture is mid] and [gloss is high] then [Appearance Index is average)

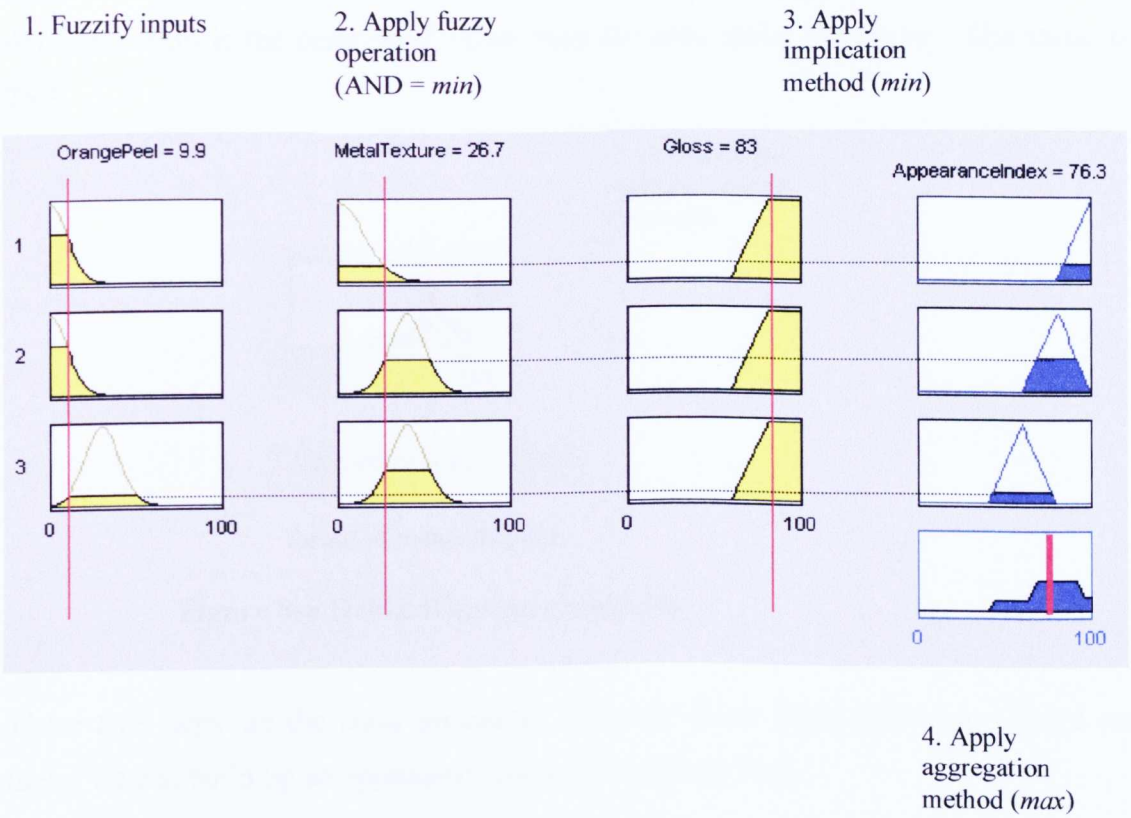

Figure 8-5 Aggregation of fuzzy sets

The output of the implication method (*min*) for each rule is a truncated triangle. Applying the aggregation method (*max*) to them, the result of aggregation is the area of a polygon shown in the bottom-right corner.

Step 5. Defuzzify

The input for the defuzzification process is a fuzzy set (the aggregate of the output fuzzy sets) and the output is a single number. The aggregate of a fuzzy set

encompasses a range of output values, and must be defuzzified in order to resolve a single output value from the set.

The most popular method is centroid calculation, which returns the centre of gravity of the area under the curve. The other methods are bisector, middle of maximum, largest of maximum, and smallest of maximum. In Figure 8-6, the result of defuzzification is the centroided value from the area under the curve. The value is 76.3.

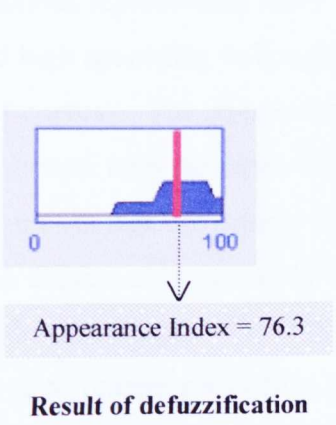

Figure 8-6 Defuzzification (centroid)

These five steps are the basic procedure for using fuzzy logic inference. Based on these, we can build up an appearance model using fuzzy logic.

8.2.4. Membership Functions

To fuzzify the input, the membership functions for the input and output need to be defined. Normally membership function is formed from the statistic result of visual assessment and instrument. In this case, a lot of data is needed to find out which distribution it is to the linguistic statement. Another way to define the membership function is the experience. Then the membership function can be tuned by the output of the model. The following membership functions are mainly based on the experience and partial statistic data. They are only one of the choices for the input and output.

The most commonly used membership function is a Gaussian distribution function [Moore 1998]:

$$f(x)=\frac{1}{\sigma\sqrt{2\pi}}e^{-\frac{1}{2}(\frac{x-\mu}{\sigma})^2}$$

where: μ is the mean value and σ is the standard deviation

For the input, orange peel, for which the interval is limited between 0 to 100, there are three Gaussian functions representing three statements of orange peel quality, which are low, middle and high according to human visual perception (in Figure 8-7 with the marks on the top of curves). The parameters of the functions are listed in Table 8-1. For example, the function with the mark 'Low' corresponds to the statement 'orange peel is low', which means that the orange peel effect is small. If the measured value is 0 (input x=0), the degree, corresponding to the statement of orange peel being low is maximum (fuzzification output =1); If the measured value is 10 (input x=10), the corresponding degree to orange peel being low is 0.606, the degree corresponding to the statement of orange peel being medium is 0.135, and the degree corresponding to the statement of orange peel being high is 0. So every input (measured orange peel value) corresponds to a certain degree of these three statements. This is the principle of fuzzifying the input into a fuzzy set.

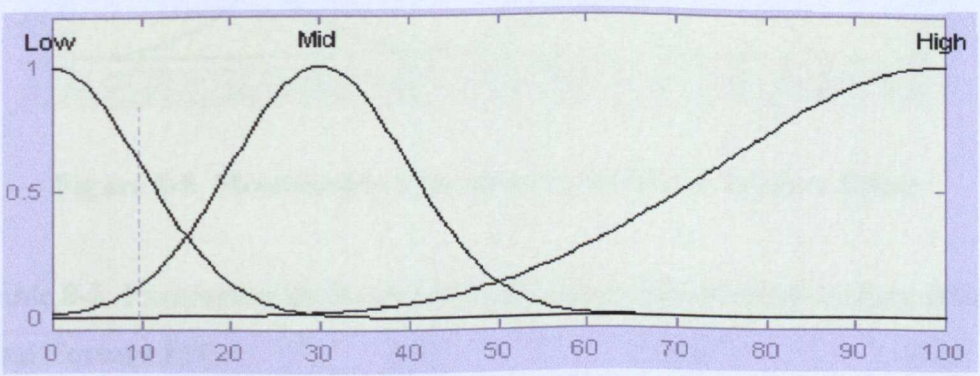

Figure 8-7 Membership functions of orange peel

Table 8-1 Parameters in Orange Peel membership functions

Orange Peel	Low	Mid	High
Mean μ	0	30	100
Standard deviation σ	10	10	25

The specification of the parameters (μ *and* σ) for each function depends on the statistical results from the measurement value corresponding to visual perception. For orange peel, if the measured value is 30, it has the maximum degree of the orange peel being medium. If it is less than 30, the degree of medium would decrease and the degree of low would increase; if it is more than 30, the degree of medium would decrease, but the degree of high would increase.

With a similar procedure, the membership functions can be defined for another input, metal texture effect, which also has three Gaussian functions with different parameters (see Figure 8-8 and Table 8-2).

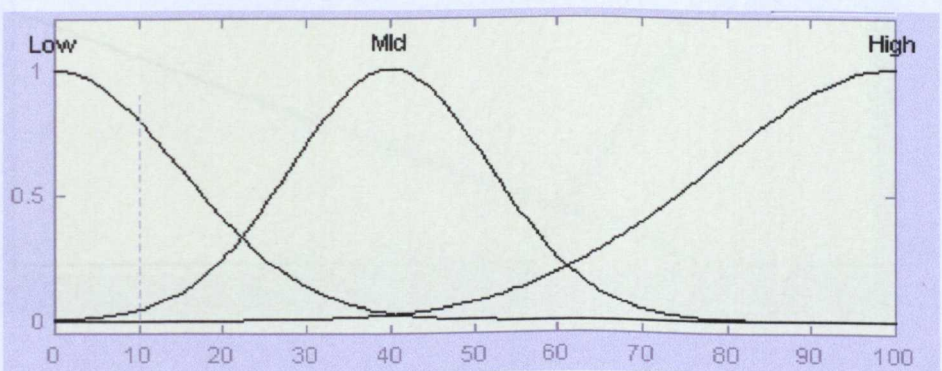

Figure 8-8 Membership Functions of the Metal Texture Effect

Table 8-2 Parameters in the membership functions of metal texture effect

Metal Texture Effect	**Low**	**Mid**	**High**
Mean μ	0	40	100
Standard deviation σ	15	12	22

As the measured value for the metal texture effect is larger than the orange peel corresponding to visual perception, the mean value of the membership function representing metal texture being medium is set to a value, 40. In this case, if the measured value for metal texture is 10 (input x=10), the degree of metal texture being low is 0.9459, the degree of metal texture being medium is 0.0561.

The membership functions for input, Gloss, are two functions, one is a triangular function representing the gloss being low, and the other is a trapezoidal function for gloss being high (Figure 8-9). As the measurement system is based on the reflected image, a certain level of gloss on the painted surface is essential for obtaining a clear image for measurement. Some experience has been obtained from experiments that if the gloss is larger than 80, there is no effect on overall appearance. If the gloss is between 60 to 80, the appearance drops quickly. If the gloss is less than 60, the appearance cannot properly be measured.

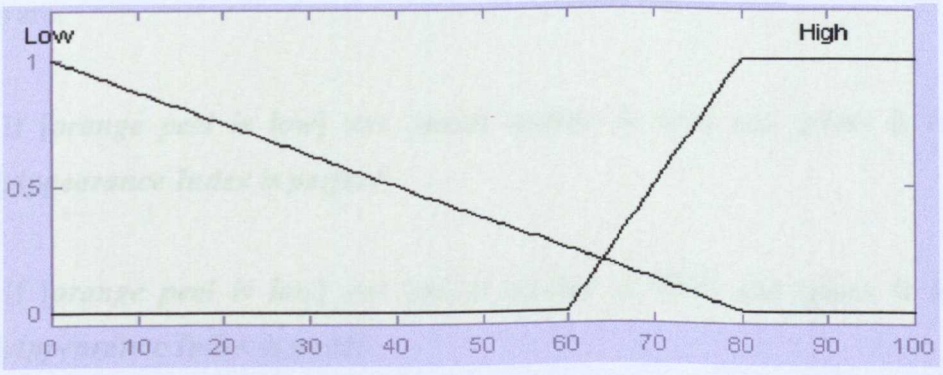

Figure 8-9 Membership Functions of Gloss

The output, appearance index, is defined with four membership functions corresponding to four levels of visual perception, which are the appearance being Perfect, Good, Average, and Poor (Figure 8-10). They are all triangular functions located in different positions of the appearance index axis to represent different levels of visual quality of the paint surface.

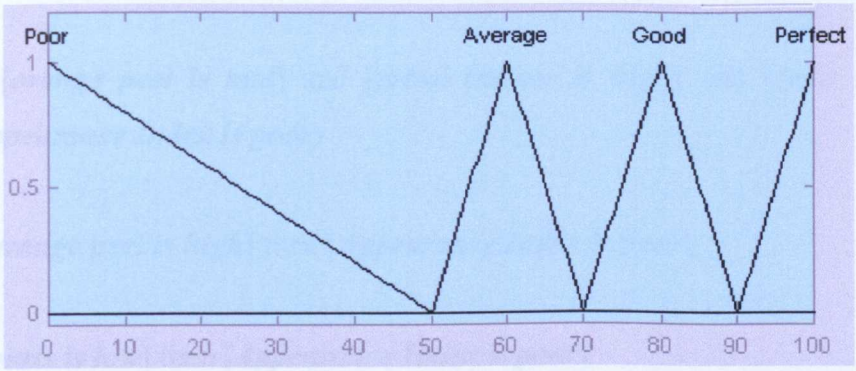

Figure 8-10 Membership Functions of the Appearance Index

8.2.5. Rules and Process

The Fuzzy logic model is fully based on the rules. Sometimes it is called rule-based fuzzy reasoning. To evaluate the overall appearance, eight rules are defined, which are mainly based on previous knowledge and expertise in this area. The complete rules are:

1. If [***orange peel is low***] and [***metal texture is low***] and [***gloss is high***] then [***Appearance Index is perfect***]

2. If [***orange peel is low***] and [***metal texture is Mid***] and [***gloss is high***] then [***Appearance Index is good***]

3. If [***orange peel is low***] and [***metal texture is high***] and [***gloss is high***] then [***Appearance Index is average***]

4. If [***orange peel is mid***] and [***metal texture is low***] and [***gloss is high***] then [***Appearance Index is good***]

5. If [***orange peel is mid***] and [***metal texture is mid***] and [***gloss is high***] then [***Appearance Index is average***]

6. If [***orange peel is mid***] and [***metal texture is high***] and [gloss is high] then [***Appearance Index is poor***)

7. If [***orange peel is high***] then [***Appearance Index is poor***]

8. If [***gloss is low***] then [***Appearance Index is poor***]

With these eight rules the process of how this fuzzy logic system works is shown in Figure 8-11. The defuzzification method used is the centroid calculation.

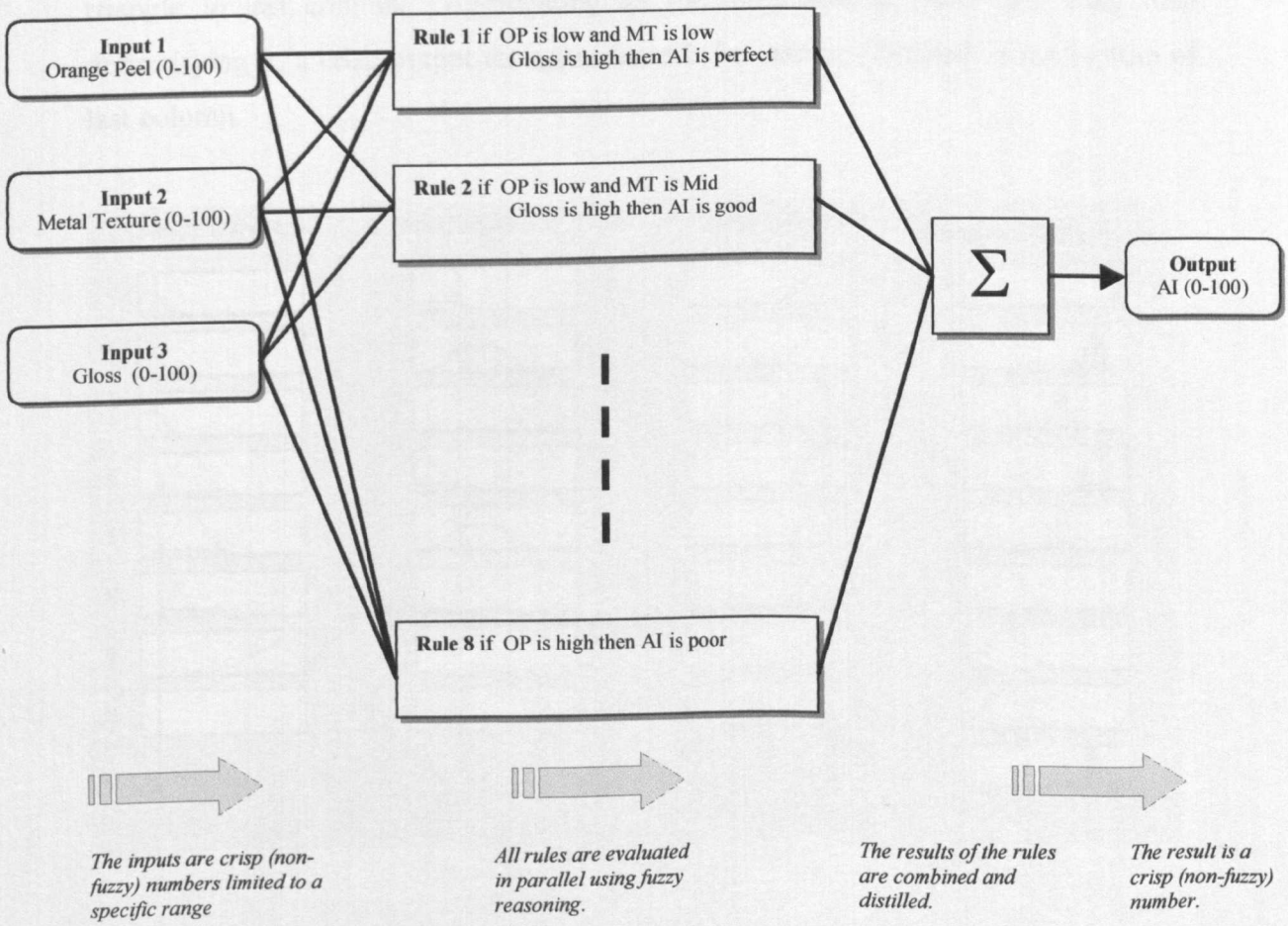

Figure 8-11. Process of fuzzy logic reasoning

8.2.6. Fuzzy Logic Model Interface

An interface programme for the fuzzy logic model has been developed with MATLAB (see Figure 8-12). Based on these eight rules, the whole procedure of fuzzy reasoning can be clearly illustrated. In Figure 8-12, the first column of the figure is the number of the rules. The orange peel, metal texture and gloss can be measured with the computer-interfaced measurement system, 'Smart Appearance', which is an integrated system with the measurement principle derived from Chapter 5 & 6 (details see Chapter 9). The model inputs are crisp values, indicated by red vertical lines. For the first rule, If [***orange peel is low***] and [***metal texture is low***] and [***gloss is high***] then [***Appearance Index is perfect***], the implication result is truncated triangle in last column. Aggregating all the contributions from each rule, then defuzzifying it, a crisp output for appearance index can be obtained in the bottom of last column.

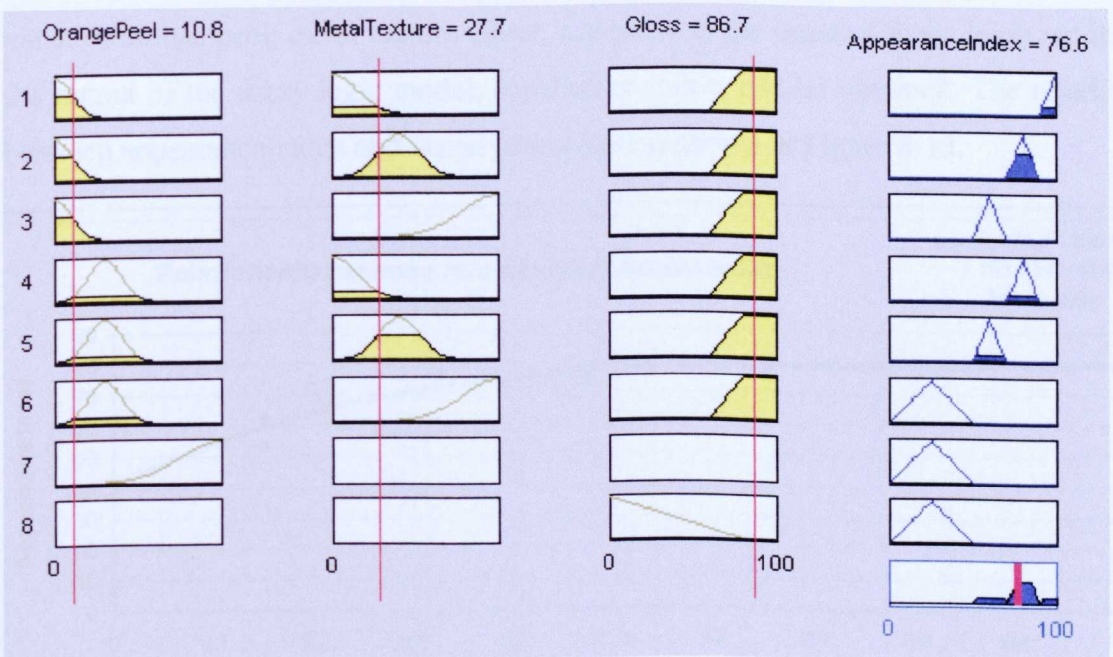

Figure 8-12. Interface of fuzzy logic model

For example, if the orange peel is 10.8, metal texture is 27.7 and gloss is 86.7. After the whole procedure of fuzzy reasoning, the defuzzified output, appearance index is 76.6.

8.3. Result and Conclusion

8.3.1. Correlation with Visual Assessment

To test the model performance, the correlation between appearance index (output of fuzzy logic model) and human visual assessment must be checked. There are ten samples of steel panels available. Using the visual assessment procedure and statistical method described in chapter 3, a set of visual assessment values can be assigned to these panels. The orange peel, metal texture effect and gloss were measured using the measurement system, 'Smart Appearance'. Taking the measured value of orange peel, metal texture effect, and gloss as the input of fuzzy logic model, the output of the fuzzy logic model, appearance index, can be obtained. The relation between appearance index and visual assessment is shown in Figure 8-13.

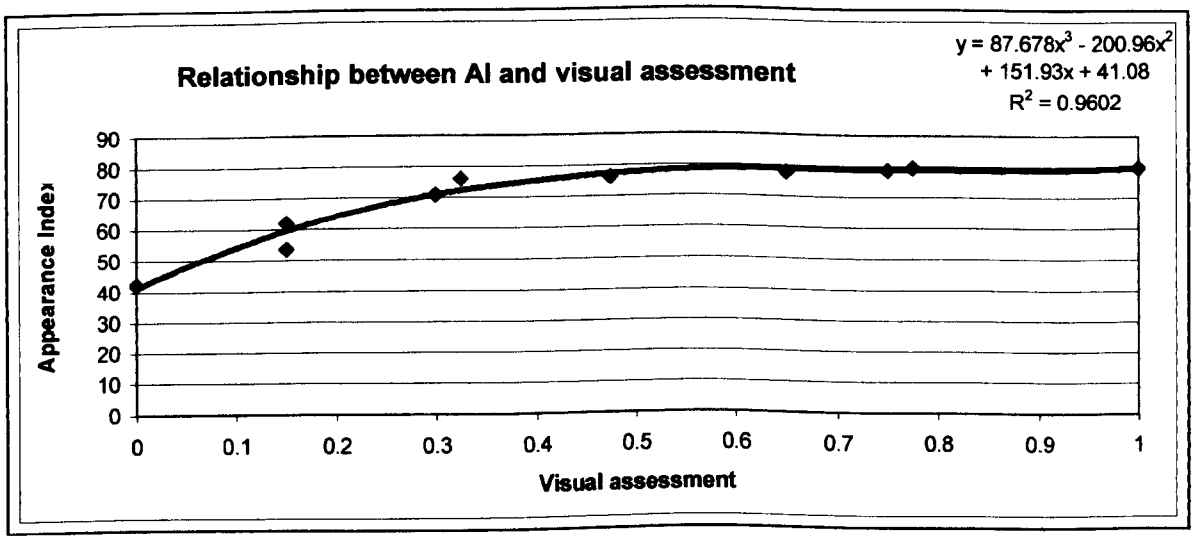

Figure 8-13. Correlation between AI and visual assessment

The correlation coefficient between AI and visual assessment is 0.84, which means that high correlation exists between them. For some panels the AI does not show its discriminate ability corresponding to the visual assessment. Further tuning is needed for membership functions and rules to improve its performance.

8.3.2. Appearance Index Surface

Unlike the neural network model, the fuzzy logic model can be well understood and the correlation between output and input can be clearly described. For example, if the gloss is fixed at 85, the appearance index surface via Metal Texture (x axis) and Orange Peel (y axis) can be drawn in Figure 8-14. The correlation between appearance index, orange peel, and metal texture can be visualised.

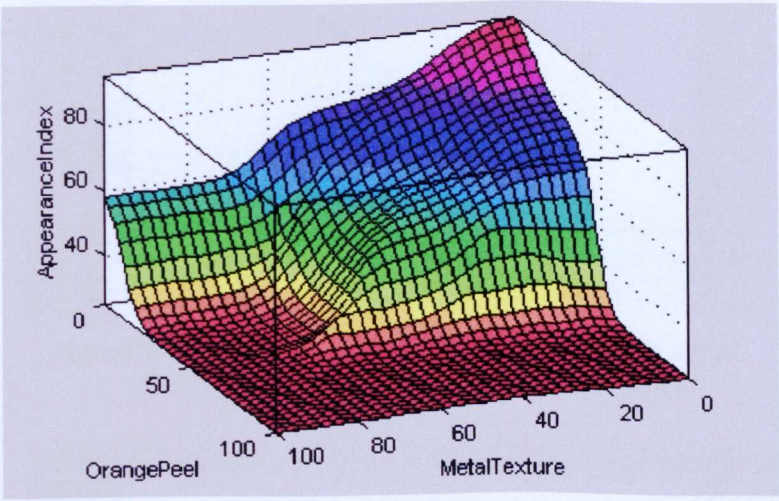

Figure 8-14 Appearance Index Surface at Gloss = 85

Based on this surface, the correlation between appearance index and individual parameters can be further indicated under certain conditions. For example, if the metal texture effect is set to 10, the correlation between AI and orange peel can be displayed in Figure 8-15. It is the surface profile at metal texture = 10. From Figure 8-15, it can be seen that AI drops nearly linearly from 92 to 70 when orange peel is between 0 and 40; when orange peel is between 40 to 60, AI drops quickly from 25. In the same way, the surface profile of AI via metal texture can be drawn when

orange peel is 5 and gloss is 85 in Figure 8-15, which indicates that the AI goes down linearly with the increase of the metal texture effect.

If the orange peel and metal texture are both small (=10), the AI via gloss can be drawn in Figure 8-17, which shows that AI drops down every quickly when gloss decreases from 80 to 60. If gloss is above 80, there is no effect to AI.

The AI surface can provide us full information about the correlation between input and output, which can reflect all the rules applied on it. From the introduction above, it can be seen that the fuzzy logic model can be easily adjusted with improvements in human experience.

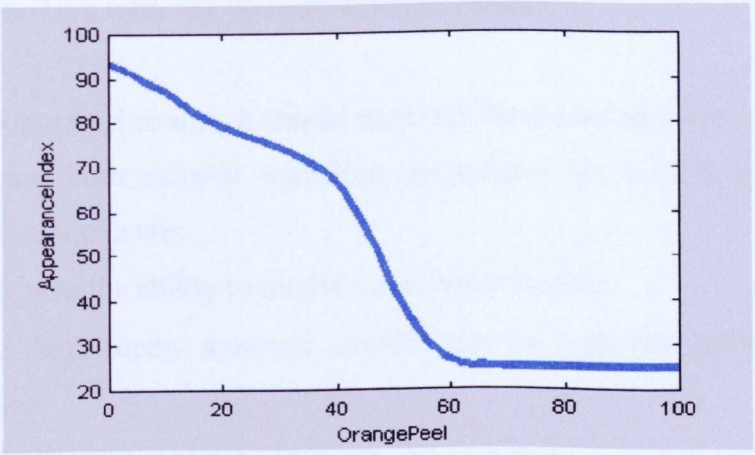

Figure 8-15 Appearance Index via Orange Peel at Metal Texture =10 and Gloss=85

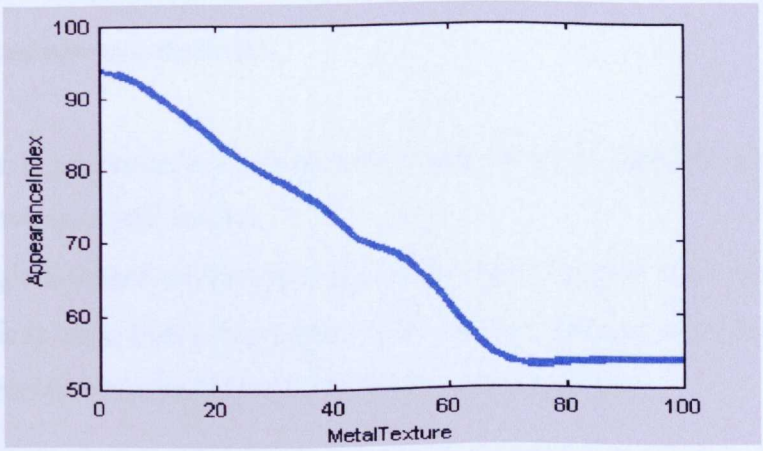

Figure 8-16 Appearance Index via Metal Texture at Orange Peel = 5 and Gloss = 85

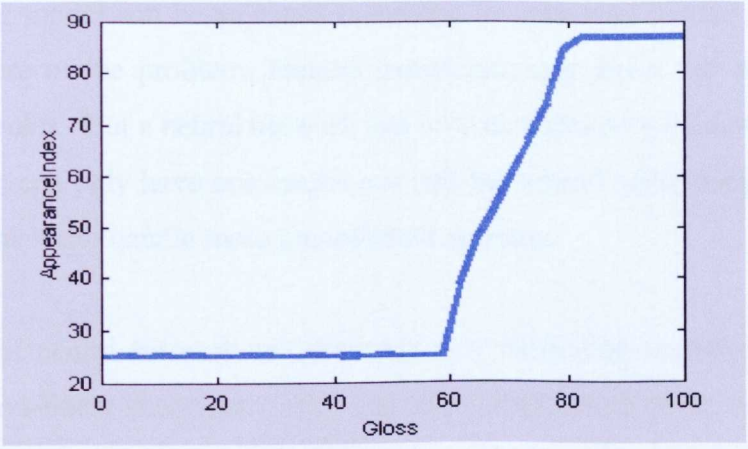

Figure 8-17 Appearance Index via Gloss at Orange Peel =10 and Metal Texture = 10

8.3.3. Comparison with the Neural Network Model

From the experimental results, it can be seen that the neural network model and fuzzy logic model are both suitable modelling techniques for overall appearance. The advantages in common are:

- They both have the ability to model a non-linear system.
- They are both open systems, which can be adjusted with the changed environment.
- They are both easily set up and used by the end-user.
- They are both achieved at low cost.

The differences between them are:

- The fuzzy logic procedure can be fully known. But the detailed processing of the neural network is still unclear.
- Fuzzy logic is based on human experience, but the neural network is fully based on historical data. Fuzzy logic can be set up from human experience. A Neural network has to be trained with sufficient experimental data.

- Fuzzy logic model can be adjusted according to improved human understanding of the nature of the problem. Human experience can direct the adjustments by tuning the rules. But a neural network can only be adjusted with new data.
- Fuzzy logic can only have one output per unit but neural networks can have more outputs, which can handle more complicated systems.

Fuzzy logic and neural network are relatively new modelling techniques, which are powerful for non-linear situations. They can complement each other, or be combined together to deal with more complicated systems.

8.3.4. Conclusion

The following conclusion can be drawn:

- Fuzzy logic is a powerful modelling tool to map any non-linear system. The preliminary result has shown that overall appearance can be modelled well with fuzzy logic.
- Fuzzy logic is an easy-to-use and open system, which is fully based on human experience.
- As fuzzy logic is fully based on human understanding and experience, if the nature of the problem is too complicated to describe with human linguistic rules, fuzzy logic cannot work properly. Fuzzy logic is suitable for systems having one output.

A new type of fuzzy logic interface has been developed [Jang 1991][Jang 1993], in which the learning ability has been developed to automatically adjust the membership functions and rules in a similar manner to neural networks. Further work may be undertaken along these lines.

Chapter 9

'Smart Appearance' -An Intelligent Measurement System for Paint Appearance

9.1. Introduction

In previous chapters, the measurement of paint appearance has been described. To integrate all the characteristics into one measurement system, an image-processing based measurement system prototype has been built, which has been named –'Smart Appearance'. With this system, the orange peel, metal texture effect, gloss, haze and contrast can be measured by using image signal processing techniques. In this chapter, details on how it works and how it is used in practice will be described.

9. 2. 'Smart Appearance' – An Intelligent Measurement System for Paint Appearance

The system is expected not only to measure the individual parameters on the paint surface, but also to provide an overall appearance index corresponding to human visual assessment. With the built-in neural network model, this system should simulate human perception processes. The measurement system has been preliminarily set up with an illumination system, image acquisition system, signal processing system and neural network system (see 9-1). In the following section, more details about each system will be presented.

Figure 9-1 'Smart Appearance' - An intelligent measurement system

9.2.1. Illumination System

As the measurements are based on the image acquired from a painted surface, the illumination system is a critical aspect in the measurement system. Choosing an appropriate lighting arrangement can result in increased accuracy, system reliability, and response time. To increase the measurement accuracy, the illumination system must provide an image with the greatest possible texture contrast whereby the areas of interest stand out against the otherwise featureless background. The image should make it easy for the measurement system to extract all the information required to complete the tasks [Mruatore, 1999]. The lighting should produce clear images which permits the orange peel and texture effect to be easily observed and extracted. At the same time, the light intensity should be adjusted to make the gloss and DOI measurement to be determined easily and accurately.

To simulate the conventional environment for human visual assessment, a fluorescent lamp is chosen as the light source in the illumination system, in which there are two 15W fluorescent tubes (Fig. 9-2). The arm has a parallel movement of 105^0 in the

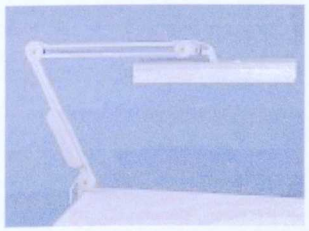

vertical and 360^0 in the horizontal planes. Changes of lighting angle and distance are easy to achieve.

The lighting pattern consists of light and dark strips with sharp edges, which makes the measurement of edge distortion much easier (see Fig. 9-3). As the maximum long wave effect to be measured is 10mm, the width of the dark strips should be larger than 20mm (in this case both sides have the maximum image distortion). The light strip between two blocks should also be larger than 20mm.

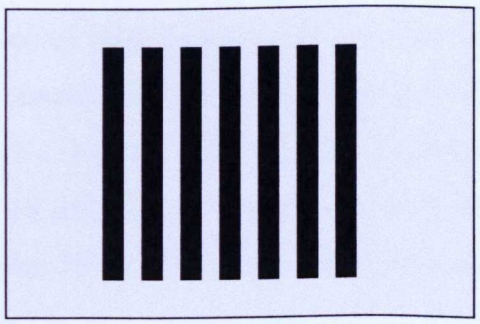

Figure 9-3 Light Pattern

The intensity of the light source is fixed in this system, but the light intensity of the reflected image on the surface is related to the distance between light source and the object and the aperture of the camera. As a general criterion, the maximum light intensity of the reflected image should correspond to less than 256 grey levels.

As shown in Figure 9-4, the distance between the light source (and camera) and the object surface is fixed. In this case, the light intensity is related only to the camera's aperture.

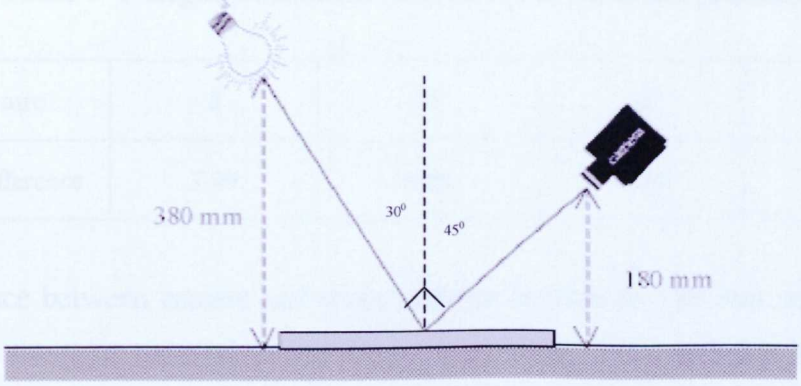

Figure 9-4 Illumination System

Figure 9-5 shows one light bar profile at different apertures in the above scene. The light intensity at f/no 8 or 11 is too high and the image profile is truncated at a grey level of 256. This is unsuitable for measuring the gloss. When the light intensity is truncated, the difference of light intensity between the pixel and its neighbours also decreases and it is not suitable for measuring orange peel and metal texture effect. The light intensity difference calculated with Equation (5-24) is shown in Table 9-1. The image profiles at f/no 16 and 22 give larger differences than those for f/no 8 and 11. The image profiles in f/no 16 and 22 are suitable for the measurement of the gloss and the metal texture effect.

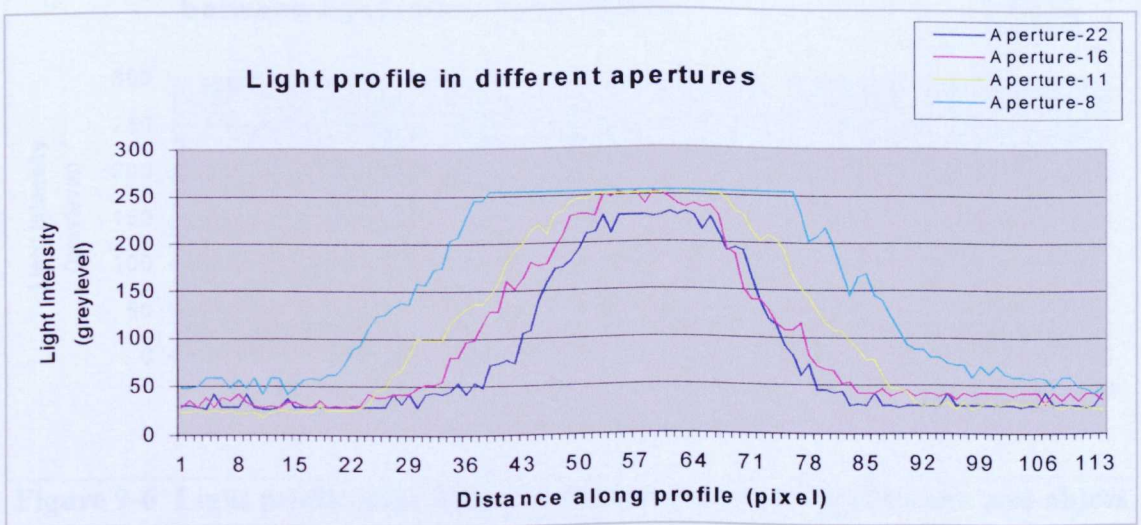

Figure 9-5 Light profile for different apertures

Table 9-1 Light Difference for different camera apertures

Aperture	8	11	16	22
Light difference	3.99	4.00	4.20	4.19

If the distance between camera and object surface is fixed to 180 mm and the f/no is kept to 16, the light intensity of the image is related to the distance between light source and object surface. Figure 9-6 shows the light profile for different distances between light source and object surface (to show them clearly, the light profiles at distances of 300mm, 400mm and 500mm are moved about 40 pixels along the x axis). All the light intensities are lower than the maximum grey level of 256, but the light profile with distances of 100mm or 200mm is nearly rectangular in shape. This makes the measurement of orange peel and metal texture effects difficult. For the light profiles with distances of 300mm, 400mm and 500mm, the light profiles are not much different and are suitable for the measurement of orange peel and metal texture effects. This measurement system is not sensitive to the distance change between light source and object surface in the range 300mm –500mm.

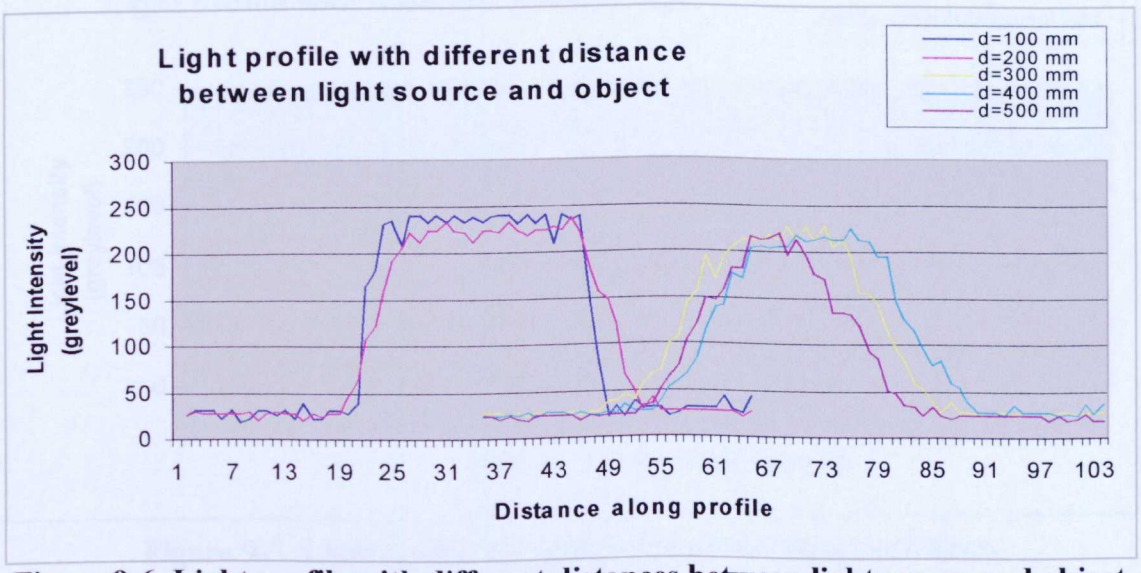

Figure 9-6 Light profile with different distances between light source and object

Another important issue is the influence of ambient light. All the ambient light should be prevented from entering the measurement system. To test the effects of the ambient light, there are three situations; the first is that there is no ambient light at all, the second is that there is ambient fluorescent light from the ceiling of the Lab (the reflected tube cannot be seen on the surface by the camera), the third is that there is both ambient fluorescent light from ceiling and sun light from the window of the laboratory. Figure 8-7 gives the image profiles in the three situations. From the image profiles, there is not too much difference between them. To further identify the difference between these situations, the orange peel and metal texture effect have been calculated respectively on these three situations. The results are listed in Table 9-2. The orange peel and metal texture effect is quite similar for these three situations. That means that the system is not sensitive to the ambient light interference at this level. The reason is that the light intensity of the desired image is almost 100 times higher than the ambient light (see Figure 9-7).

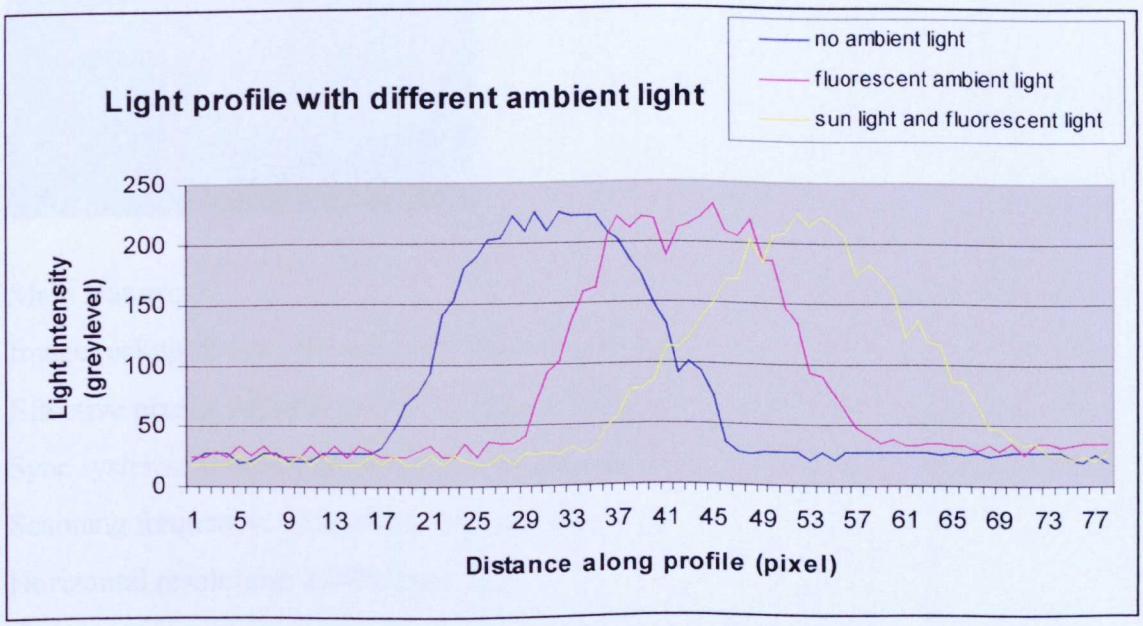

Figure 9-7 Light profile for different ambient light conditions

Table 9-2 Parameter Measurement in Different Conditions

	Condition	Orange Peel	Metal Texture Effect
1	No ambient light	9.3	36
2	Fluorescent ambient light	9.4	35
3	Sun light and fluorescent light	9.1	35

9.2.2. Image Acquisition System

The image acquisition system includes camera, frame grabber, computer and associated interface software.

Camera: JVC colour video camera, TK-C1380

Main feature:

Image pickup device: *½-inch, interline-transfer CCD*

Effective pixels: *440,000 pixels [752(H) × 582(V)]*

Sync systems: *internal, external, power sync*

Scanning frequency: *15.625kHz (H), 50.0(V)*

Horizontal resolution: *470TV lines (H)*

Video S/N: *48 dB*

Video Output: *composite video signal (BNC), Y/C (4-pin)*

Frame grabber: DATA TRASLATION® - DT 3153

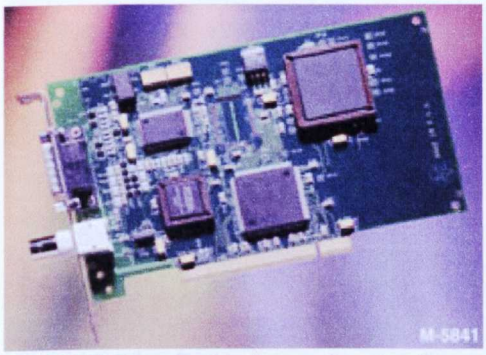

The DT3153 is a flexible, low-cost composite color frame grabber for the PCI bus.

Main feature:

Video Input: *Three multiplexed NTSC/PAL inputs or one Y/C (S-Video) and two NTSC/PAL inputs; 16-bit YCr Cb Digitization; 640 x 480 (NTSC) or 768 x 576 (PAL) spatial resolution; can be saved in 32-bit RGB or YUV format.*

Processing: *Real-time linear phase interpolation scaling and image clipping.*

General Purpose Inputs/Outputs: *Four bi-directional TTL-level input/outputs.*

Memory: *No onboard memory; uses PC system RAM for image storage.*

Display: *No onboard display; uses PC system display card for display and DDI for live, on-destructive overlays.*

Computer: PC Pentium II 266 MMX

PCI Bus, 256 Mbytes of RAM, Windows NT 4.0.

Image acquisition interface software:

A software package has been provided along with frame grabber to acquire the image immediately. Figure 9-8 shows the window of this package.

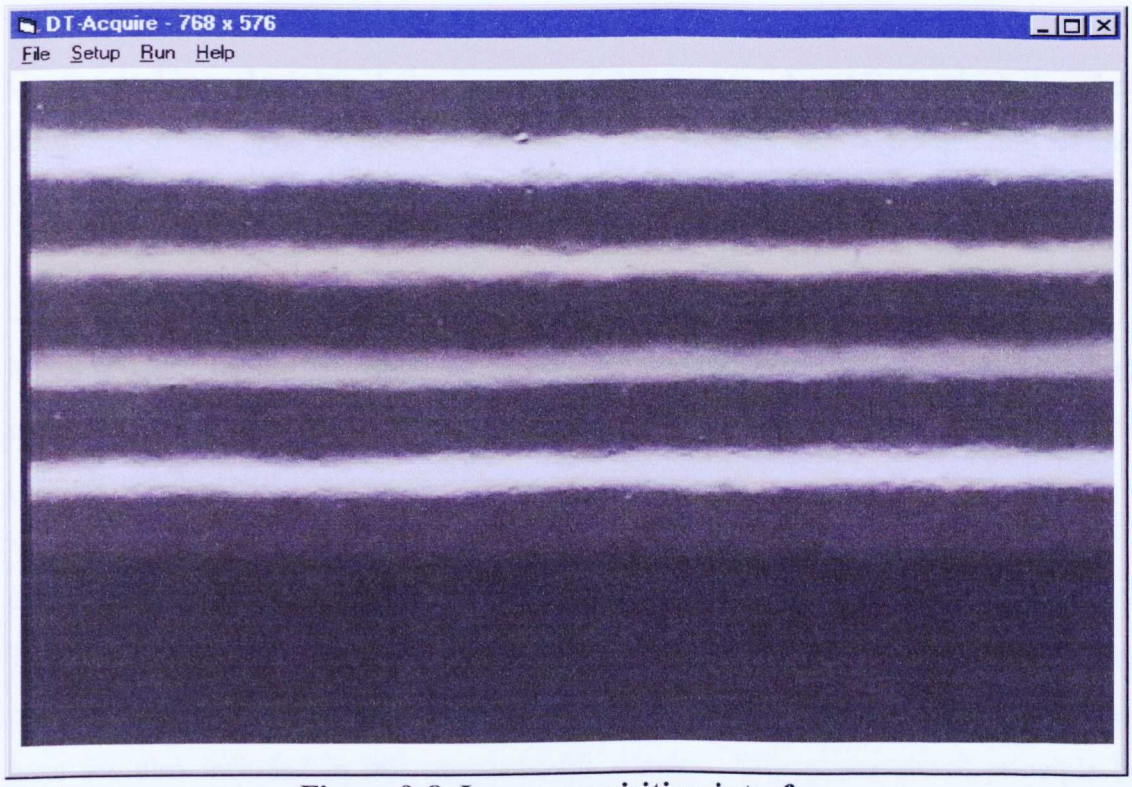

Figure 9-8 Image acquisition interface

The image can be saved in several popular formats, like *.BMP; *.EPS; *.JPG; *.PCX; *.PNG; *.PSD; *.TGA; *.TIF; *.WMF.

9.2.3. Signal Processing System

A computer-based signal processing system has been set up with MATLAB® tools. A set of programmes has been developed to perform the different measurements as described in previous chapters. They include:

- Separation of orange peel and metal texture effect.

In Chapter 5, the painted surface is categorised into three cases: orange peel dominated surface; orange peel and metal texture co-occurrence surface; and metal texture effect dominated surface Using a signal processing technique such as FFT or Filtering, the orange peel and metal texture can be separated.

- Evaluation of orange peel.

Orange peel is evaluated with the (Equation 5-28) for case A and B, in which the edge distortion of the light image is evaluated by the average standard deviation of the filtered image profiles.

- Evaluation of metal texture effect

Metal texture effect is evaluated in three ways, average standard deviation on filtered image profiles (Equation 5-23); light intensity difference on unfiltered image profiles (Equation 5-24); and texture contrast (Equation 6-2).

- Measurement of other optical properties

To measure as many parameters as possible and provide more information to the neural network model to assess the overall appearance, the measurement of gloss and haze are also included in this measurement system. The measurement principle is similar to the instrument QMS described in Chapter 2. They are not measured according to the definitions in Equation (2-1) and (2-2). They are based on the image acquired with the reflected fluorescent tube.

Gloss Measurement:

The gloss is determined by measuring the average difference between the light intensity of the reflected image and the light intensity of the surrounding area. This produces a figure, which is similar to, but not identical to specular gloss measurements (Fig. 9-9), but it is equivalent to visual perception. It is more helpful to assess the overall appearance as an important parameter. To measure the gloss accurately, the maximum light intensity on a standard sample (black glass) should be less than 256 grey levels. The final value is normalised to a range of 0 to 100, 100 is the maximum value.

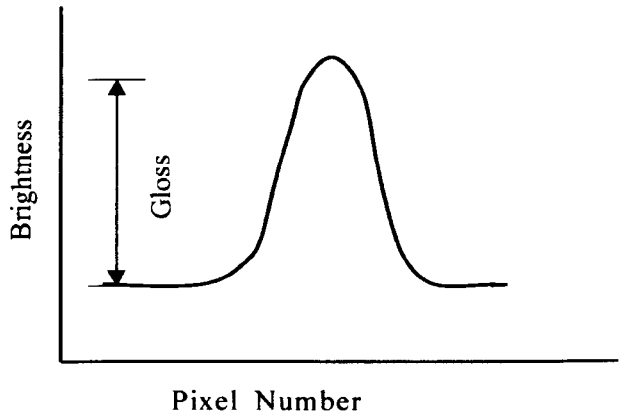

Figure 9-9 Gloss Measurement using 'Smart Appearance'

Haze Measurement:

The haze is determined by measuring the rate at which the image changes from dark to bright at the edge of the reflected image (Figure 9-10). Actually it is similar to the measurement for DOI (distinctness of image). The measurement of haze yields the clarity of the image. The final value also ranges from 0 to 100, 100 being the maximum value.

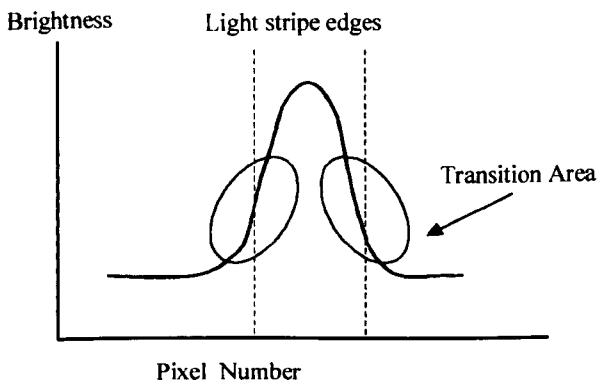

Figure 9-10 Haze Measurement in Smart Appearance

9.2.4. Neural Network System

To assess the overall appearance on the painted surface, a neural network model has been set up to link the overall appearance and all the measurable parameters. With the

trained neural network model, the measurement system can directly produce an overall appearance index using the measured individual parameters (see Chapter 7).

9.2.5. Software Package

A software package has been developed as an interface for the measurement system – Smart Appearance (see Figures 9-11). With this software package, the image can be displayed in the left-hand area, and the individual parameters, like orange peel, metal Texture Effect, Gloss, Haze, and Contrast can be calculated separately. Using these measurement results as the inputs of the neural network model, the overall appearance can also be evaluated with a trained neural network model.

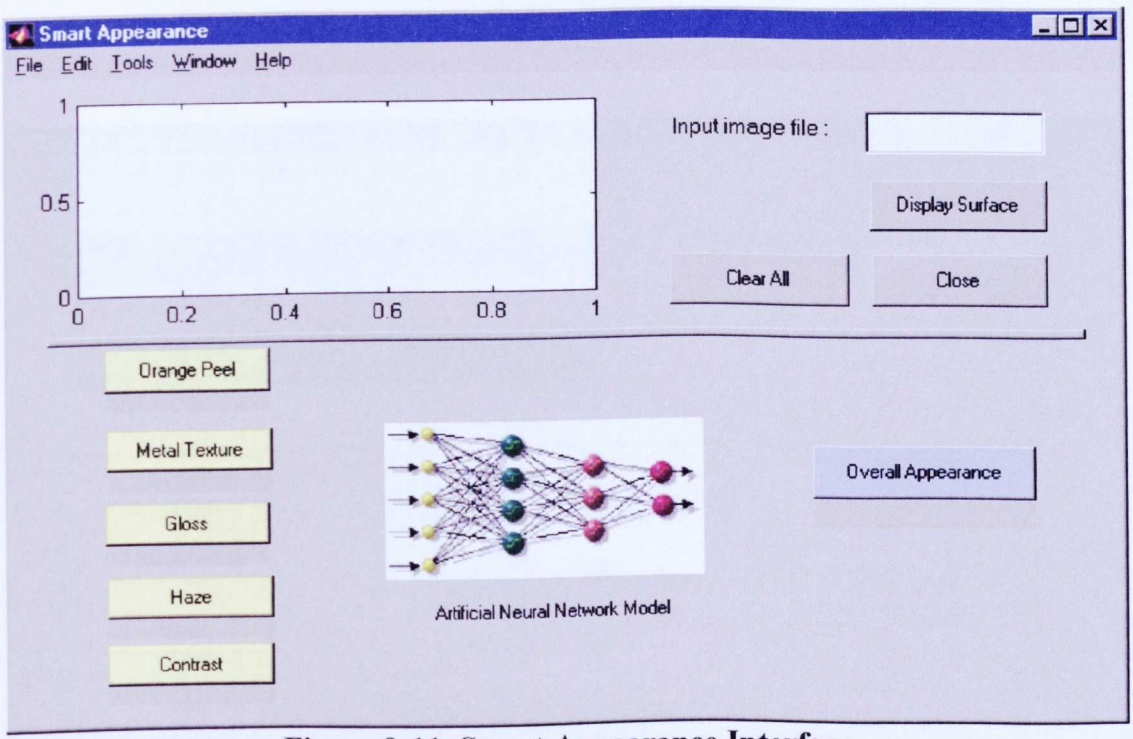

Figure 9-11 Smart Appearance Interface

So far the package is only a demonstration version, which is quite easy to use. The image acquisition is achieved through a separate programme (to be combined into this package in due course). First, the file name needs to be typed into the Input image file

area, then, by clicking the Display Surface button, the image will be displayed in the top-left area (see Figure 9-12).

In the second half of the window, there are six buttons representing each individual parameter. By clicking the Orange Peel button or the Metal Texture button, the orange peel and metal texture can be calculated at the same time and the results are displayed in the shadow of each button. To calculate gloss, haze and contrast, by simply clicking the buttons for Gloss, Haze or Contrast, these three parameters will be presented at the same time in their shadow areas. Using these five parameters as the inputs of the neural network model, the overall appearance can be evaluated with a trained neural network model by just clicking the Overall Appearance button. The overall appearance is evaluated with the overall index from 0 to 1, index 1 representing the best overall appearance.

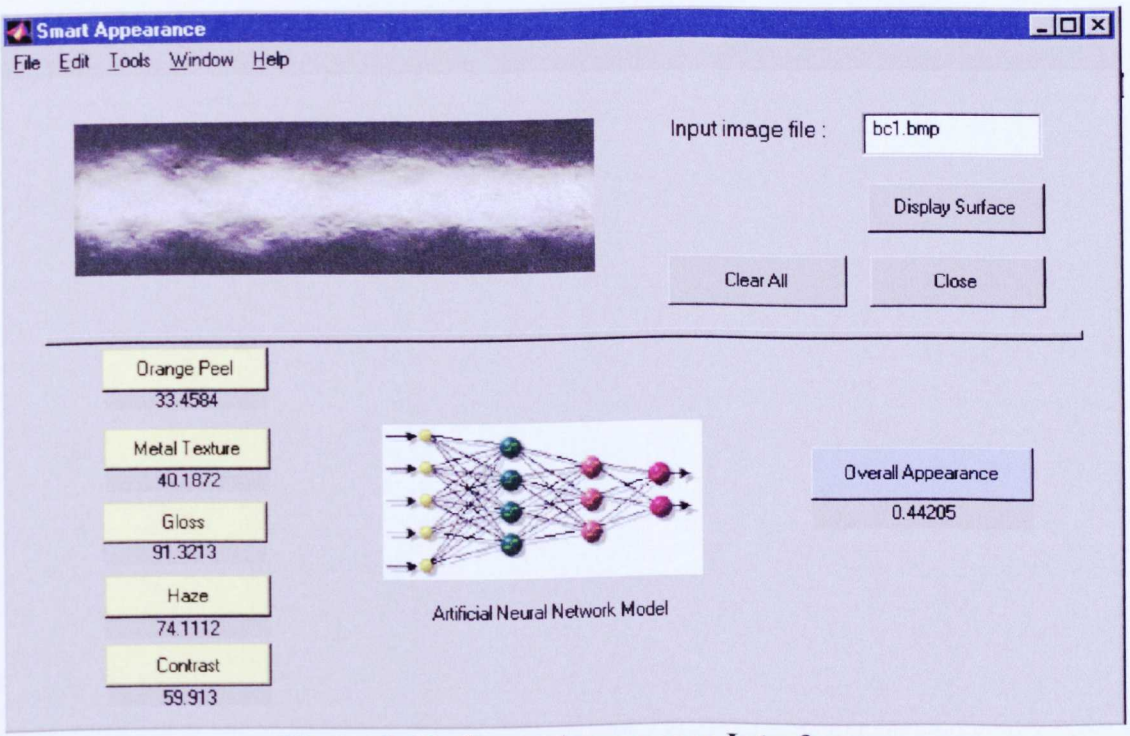

Figure 9-12 Smart Appearance Interface

9.3. *Conclusions*

Although the measurement system – 'Smart Appearance'- is still in its initial version, it has been proved that it can effectively evaluate the orange peel and metal texture effect respectively, and also other optical properties of the painted surface .The result shown in Chapter 7 demonstrated that the overall appearance index has a good correlation with human visual perception. With the system described, it is easy to measure each parameter and the overall appearance. Potentially, it can be developed into a commercial instrument.

Chapter 10

Conclusions

10.1. Summary

This thesis includes a literature survey in the area of appearance measurement by visual assessment, a round robin test procedure, image processing, digital signal processing, artificial neural networks, fuzzy logic, instrumentation and interface programming.

1. First of all, the 'state of the art' in the area of appearance measurement was presented, which summarised the concept of appearance, models, attributes and definitions. As this area is very specialised, some of the most important measurement methods and instruments are described. A significant conclusion is that there is no standard measurement framework, even for the most popular parameter, orange peel. Correlation between overall appearance and measurable parameters needed to be modelled with more powerful modelling tools.

2. As visual assessment has an important role in appearance measurement, optimisation of the visual assessment procedure and statistical methods to reduce the subjective error were found to be essential. A standard procedure and statistical methods were presented to carry out visual assessments on the testing panels. The statistical result shows that this method is objective and effective in presenting visual assessment results even if the number of observers is small.

3. To identify the parameters and instruments used in the automotive industry, a round robin test was launched to perform visual assessment and instrument measurements on a set of panels within the consortium of partners. A summary of the correlation between these parameters and visual assessment provided the basis of the further work. Orange peel and metal texture effects needed to be evaluated separately; the overall appearance needs to be modelled with more powerful modelling tools.

4. To separate orange peel and metal texture effects, the quality of paint appearance is categorised into three cases comprising different degrees of orange peel and metal texture. The time-domain signal processing techniques, FFT and filtering were used on the image profiles of the reflected fluorescent tube image on the panels. The orange peel and metal texture effects could be separated according to the FFT and filtering results.

5. The orange peel was evaluated on the distorted edges along the reflected fluorescent tube image after 2-D image filtering to remove the metal texture effect. The final value was found to be proportional to the standard deviation of the distorted image edge.

6. The metal texture effect was evaluated on the image profiles across the reflected fluorescent tube. It was evaluated using the standard deviation of filtered profiles or the light intensity difference between pixels of the unfiltered profiles. Both gave a good correlation with visual texture assessment.

7. The technique for texture pattern recognition was used to evaluate the texture effect when a fine texture comparison was needed. A set of computable textural parameters based on grey-tone spatial-dependence matrices, which directly corresponding to visual perception, were employed to evaluate the metal texture effect on paint appearance. The preliminary experimental results showed that this method could evaluate the metal texture effect, especially for very fine comparisons.

8. To resolve the overall appearance modelling problem, a novel and more powerful modelling tool, artificial neural networks, was introduced to model the overall appearance. The test results showed that the neural network model was able to reflect the correlation between overall appearance and the major parameters measured from a painted surface.

9. As an alternative, another modelling tool, fuzzy logic, was also presented as a non-linear model to link the overall appearance and individual parameters. Human understanding and expertise could be built into the measurement system. This model also provided a good correlation between overall appearance and visual perception.

10. Based on the studies in the area of appearance measurement, an integrated measurement system, 'Smart Appearance', was developed using the image processing techniques and the artificial neural network model. With this system, the orange peel and metal texture could be evaluated separately and the other parameters like gloss and haze could also be obtained from the image. Taking the parameters as the input, the overall appearance was presented with a trained neural network.

10.2. Contributions to Knowledge

According to the work summarised above, this thesis makes the following contributions to the scientific area of appearance measurement.

1. Summary of the state of the art in the area of appearance measurement.
2. Presentation of a standard procedure and statistical method to obtain objective results from visual assessment.
3. Identification of the parameters used in the automotive industry revealing their correlation with visual perception.
4. Separation of orange peel and metal texture effects using image processing.

5. Evaluation of orange peel and metal texture effects using image processing.
6. Comparison of the texture effect with a texture pattern recognition technique.
7. Modelling of overall appearance using artificial neural networks.
8. Modelling of overall appearance using fuzzy logic methods.
9. Development of an integrated measurement system, 'Smart Appearance', to achieve more objective results correlating well with human perception.

Five papers are directly derived from this research work. Four of them have been published. One has been submitted. They are:

[1]. H. Kang, C. Butler, Q. Yang, F. Sacerdotti, F. Benati, *Modelling of Paint Appearance Using Artificial Neural Network,* submitted to SPIE's International Symposium on Intelligent Systems for Advanced Manufacturing, Boston, Massachusetts, USA, November 2000.

[2]. H. Kang, C. Butler, Q. Yang, F. Sacerdotti, F. Benati, *Appearance Measurement System Using Fuzzy Logic,* Proceedings of IEEE Instrumentation and Measurement Technology Conference, *IMTC '2000*, Baltimore, Maryland, USA, May, 2000.

[3]. H. Kang, C. Butler, Q. Yang, F. Sacerdotti, F. Benati, *Visual Assessment of Paint Appearance on Car Body Surface,* Proceedings of X. International Colloquium on Surfaces, Chemnitz, Germany, January 2000.

[4]. H. Kang, C. Butler and Q. Yang, *Evaluation of Metal Texture Effect on Paint Appearance,* SPIE's International Symposium on Intelligent Systems for Advanced Manufacturing, Boston, Massachusetts, USA, September 1999.

[5]. H. Kang, C. Butler and Q. Yang, *Measurement of Paint Appearance Using Image Processing System,* Proceedings of IEEE International Workshop on Intelligent Signal Processing, Budapest, Hungary, September 1999.

10.3. Further Work

Appearance measurement is a complex subject despite many years of investigation. According to this study, the following work is indicated to further develop appearance measurement and to meet industrial requirements.

- Colour measurement

  As indicated in Chapter 2, colour is an important attribute of paint appearance. It changes according to different viewing parameters such as, lighting conditions, light sources, background colours, and luminance levels. This makes colour appearance assessment more difficult. In this study, only gloss is taken into account. In the future, colour quality could be evaluated using a range of view angles and luminance levels. Appearance measurement would be more complete with the characteristics of colour and gloss. Comparing a panel with a given shade or a reference panel across a wide range of illumination conditions is the main task for colour appearance assessment.

- Modelling

  The neural network and fuzzy logic models are both preliminary models set up for modelling overall appearance. More data is needed to train and test the models to yield a robust system. Further architectures and algorithms should be investigated.

- Defects detection.

  This is another aspect of appearance measurement. Defects should be evaluated in some way when assessing the quality of appearance. Typically, defects could come from the environment such as dust, the painting control procedures, paint equipment condition, substrate condition and so on. In some cases, small defects are expected not to affect the overall measurement result when we concentrate on the quality of paint such as gloss and orange peel.

- Instrumentation

  To meet the requirements from the automotive industry, a stand-alone instrument and an on-line measurement system needs to be developed. These are substantial challenges.

For a stand-alone instrument, important issues are the size of components, low power consumption and the discrimination ability of the camera over a short distance. Figure 10-1 shows the proposed framework of a stand-alone system instrument.

In this system, the size of lighting system, camera and power supply must be small. The microprocessor (possibly a DSP chip) should be powerful enough to control the lighting, camera, power supply and display (LCD). The microprocessor should have the ability to capture the image, perform signal / image processing functions, and run neural network algorithms. The CPU speed should be high enough to provide a measurement result rapidly.

For on-line measurement equipment, a framework is suggested in Figure 10-2. There is a multi-channel image acquisition system to obtain images from different positions of the car body at the same time. The image data can be transferred through an Intranet. As this measurement system is in an open environment, the key issue is to prevent interference from other light sources or noise.

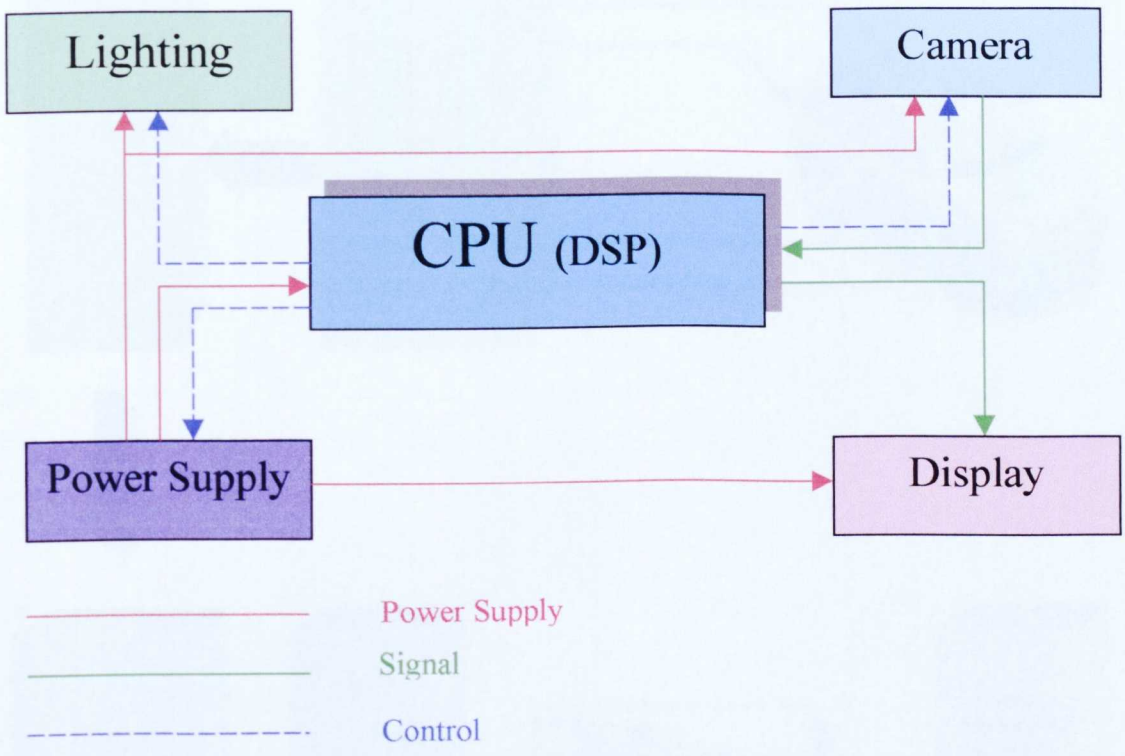

Figure 10-1 Framework of a stand-alone instrument

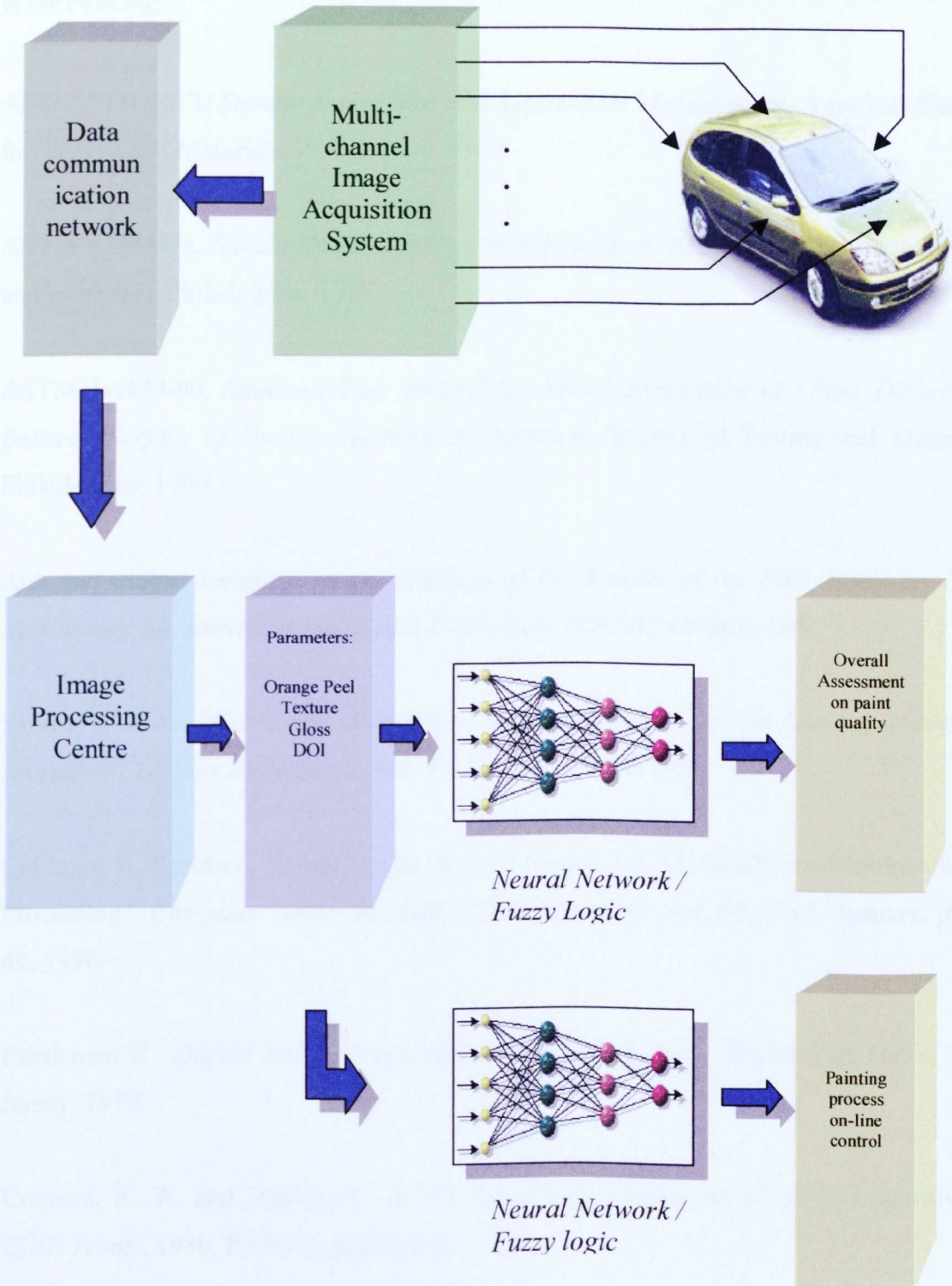

Figure 10-2 Framework of on-line measurement system

References:

ASTM E12, *ASTM Standards on Color and Appearance Measurement*, American Society for Testing and Materials, Philadelphia, 1984

ASTM E284-95a, *Standards Terminology of Appearance*, American Society for Testing and Materials, Philadelphia, 1995

ASTM D4449-90, *Standard Test Method for Visual Evaluation of Gloss Differences Between Surface of Similar Appearance,* American Society of Testing and Materials, Philadelphia, 1990.

Autosurf project technical report, *Analysis of the Results of the R&R Study on Paint Appearance Measurement and Visual Evaluation, VOLDL0000601, 1998.*

Billmeyer F.W., "Color and Appearance Characterization for the Coating Industry", Journal *of Coatings Technology*, Vol. 57, No. 722, March 1985

Califano, A. Kjeldsen, R. and Molle, R. M., "Data- and Model-Driven Multiresolution Processing", *Computer Vision and Image Understanding*, Vol. 63, No.1, January, pp27-49, 1996.

Castleman K. *Digital Image Processing,* Prentice-Hall, Inc., Englewwod Cliffs, New Jersey, 1979.

Conners, R. W. and Harlow, C. A. "A theoretical comparison of texture algorithms", *IEEE Trans.*, 1980, PAMI-2, pp204-222.

Crochiere, R.E., and L.R. Rabiner. *Multi-Rate Signal Processing*. Prentice Hall Inc., Englewood, Cliffs, NJ, 1983.

Dagnall H. *Exploring Surface Texture,* Rank Taylor Hobson, 1980.

DARPA Neural Network Study, Lexington, MA: M.I.T. Lincoln Laboratory, 1988.

Davies E. R. *Machine Vision – Theory, Algorithms and Practicalities*, 2nd Edition, Academic Press, London, 1997.

Demuth H. and Beale M. *Neural Network Toolbox, User's Guide,* The MathWorks, Inc. MA, 1998.

Dubois, D.and Prade H., *Fuzzy Sets and Systems: Theory and Applications*, Academic Press, New York, 1980.

Gonzalez R. C. and Woods R. E. *Digital Image Processing,* Addison-Wesley Publishing Co. Inc. MA, 1992.

Guthrie J. T. and Weakey A. P., "Assessment of the Orange-Peel Defect in Automotive Coatings", *Surface Coatings International* 1996 (2).

Halden M., "Characterization of Steel Sheet Surfaces in Order to Predict Surface Appearance after Painting", *IBEC'97, Automotive Body Painting*, pp115-120.

Hagan, M. T., and Menhaj M., "Training feedforward networks with the Marquardt algorithm," *IEEE Transactions on Neural Networks*, vol. 5, no. 6, pp. 989–993, 1994.

Hagan, M. T., Demuth H. B. and Beale M. H., *Neural Network Design*, Boston, MA: PWS Publishing, 1996.

Hammond III H. K. "Gloss", *ASTM Standardisation News*, Feb. 1987, pp36-40.

Haralick R. M., Shanmugam K., and Dinstein I., "Texture Features for Image Classification", *IEEE Trans. on System, man and Cybernetics*, Vol. SMC-3, No. 6, November 1973.

Henning B. Ad *Oculos: Digital Image Processing*, International Thomson Publishing, 1995.

Hunter, R. S., *The Modes of Appearance and Their Attributes*, Review and Evaluation of Appearance: Methods and Techniques, ASTM STP 914, J. J. Rennilson and W. N. Hale, Eds. , American Society for Testing and Materials, Philadelphia, 1986, pp.5-13.

Hunter, R. S., *The Measurement of Appearance*, John Wiley & Sons, New York, 1975.

Haykin, S. *Neural Networks, A comprehensive Foundation,* Macmillan College Publishing Company, Inc, New York, 1994.

ISO 2813: 1994(E), Third edition, *Paints and varnishes-Determination of specular gloss of non-metallic paint films at 20°, 60° and 85°.*

Jang, J. R., "Fuzzy Modeling Using Generalized Neural Networks and Kalman Filter Algorithm," *Proc. of the Ninth National Conf. on Artificial Intelligence (AAAI-91)*, pp. 762-767, July 1991.

Jang, J.-S. R., "ANFIS: Adaptive-Network-based Fuzzy Inference Systems," *IEEE Transactions on Systems, Man, and Cybernetics*, Vol. 23, No. 3, pp. 665-685, May 1993.

Judd, B. J., "A Five-attribute System of Describing Visual Appearance", *STP 297*, American Society for Testing and Materials, Philadelphia, 1961.

Kendall, M. *Kendall's Advanced theory of statistics,* 6th Edition, Edward Arnold, London, 1994.

Kendall, M. & J. D. Gibbons, *Rank Correlation Methods,* Fifth Edition, Edward Arnold, London, 1990.

Kigle-Boeckler G., "Surface smoothness and its influence on paint appearance—How to measure and control it", *ANTEC '96*, pp3433

Kiran M. B. and Ramamoorthy B. "Evaluation of Surface Roughness by Vision System", 7th Int. Conf. on Metrology and Properties of Engineering Surfaces, 1997, pp 288-293.

Kruskal, J. B. and Wish, M., *Multidimensional Scaling*, Sage Publications, Beverly Hills, CA, USA, 1981.

Kendall M. & Gibbons J. D., *Rank Correlation Methods,* Fifth Edition, Edward Arnold, London, 1990.

Lee, J. and Hsueh Y., "A new method for texture analysis using morphological gradient texture histograms", *Journal of the Chinese Institute of Engineers*, Vol. 19, No. 3, pp393-399, 1996.

Lee Y., Lee J. and Hsueh Y. "Fuzzy uncertainty texture spectrum for texture analysis", *Electronics Letters* 8th June 1995, Vol. 31, No. 12, pp959-960.

Luo R., "Color appearance assessment", *JSDC* Volume 112 March 1996

Lyons R. G., *Understanding Digital Signal Processing,* Addison-Wesley publishing Co. CA, 1997.

Mamdani E.H. and Assilian S., "An experiment in linguistic synthesis with a fuzzy logic controller", *International Journal of Man-Machine Studies*, Vol. 7, No. 1, pp. 1-13, 1975

Matlab, *Signal Processing Toolbox, User's Guide*, The Math Works Inc. 1998.

McCamy C. S. "Observation and Measurement of the Appearance of Metallic Materials. Part I. Macro Appearance", *Color Research and Application*, Vol. 21, No. 4, August 1996.

Montgomery D. C., *Design and Analysis of Experiments,* 3rd ed. John Wiley & Sons, Inc. New York, 1991.

Moore D. S. and McCabe G. P., *Introduction to the practice of statistics,* third Edition, W. H. Freeman and Company, New York, 1998.

Moroney, M. J., *Facts from Figures,* Second Edition, Penguin, London, 1990.

Muratore, J. A., "Illumination for Machine Vision", Dolan-Jenner Industries.1999.

O'Donnell, F. X. D. and Billmeyer, F. W., *Psychometric Scaling of Gloss*, Review and Evaluation of Appearance: Methods and Techniques, ASTM STP 914, J. J. Rennilson

and W. N. Hale, Eds. , American Society for Testing and Materials, Philadelphia, 1986, pp.14-32.

Osterhold M. "Characterization of surface structures by mechanical and optical Fourier spectra", Progress in Organic Coatings, 27 (1996) pp195-200.

Pourdeyhimi B. and Nayernouri A. "Evaluating Traffic Paint Degradation Using Image Analysis". Journal of Coatings Technology, Vol. 66, No. 834, July 1994.

Praschan E. A. "Automotive Coatings and the Optimal Testing Protocol", *ASTM Standardization News*, October 1995.

Puente Leon, F. "Image Processing Methods for the Macroscopic Acquisition of High-Quality Images of Surfaces and Tools", 7th Int. Conf. on Metrology and Properties of Engineering Surfaces, pp452-459, 1997.

QMS-BP, *Quality Measurement System for Coated Surfaces, User's manual*, Autospect Inc. 1996.

Reed T. D. and Hans Du Buf J. M. "A Review of Recent Texture Segmentation and Feature Extraction Techniques", *CVGIP: Image Understanding*, Vol. 57, No. 3, May 1993, pp359-372.

Rosenfeld, A., "Image analysis: Problems, Progress and Prospects", *Pattern Recognition*, Vol. 17, No.1, pp3-12, 1984.

Rumelhart, D. E., Hinton G. E., and Williams R. J., "Learning internal representations by error propagation", *Parallel Data Processing, vol.*1, Cambridge, MA: The M.I.T. Press, pp. 318-362, 1986.

Scheers J., Mare C. D. and Meseure K., "SIBETEX: Steel's Contribution to an Improved Paint Appearance For Outer Car Body Panels", *Automotive Body Painting, IBEC 1996.*

Scheers J. and Meseure K., "Assessment of Steel Surface Roughness and Waviness in Reflection with Paint Appearance", 7th Int. Conf. on Metrology and Properties of Engineering Surfaces, 1997 pp252-261.

Schiffman S., Reynolds M. and Young F., *INTRODUCTION TO MULTIDIMENSIONAL SCALING,* Theory, Methods, and Applications, Academic Press, Inc. New York, 1981.

Scott, P. "Foundation of topological characterization of surface texture", *7th Int. Conf. on Metrology and Properties of Engineering Surfaces*, 1997, pp162-169.

Smith, K. B. "A Sharp Look at Gloss", *Surface Coatings International* 1997 (12).

Summerscales E. "The Visual Assessment of Finish", 1980.

Suga, *Handy Image Clarity Meter, Model: HA-NSIC*, Suga Test Instruments Co. Ltd, 1985

Sugeno M., *Industrial applications of fuzzy control*, Elsevier Science Publication Company, 1985.

Tamura H., Mori S. and Yamawaki T., "Texture Features Corresponding to Visual Perception", *IEEE Trans. on System, Man and Cybernetics*, vol. SMC-8, No. 6, June 1978.

Tennant-Smith J. *BASIC statistics,* Butterworth & Co (Publishers) Ltd, England, 1985.

Wave-scan, *Operating Instructions, Mode d'emploi*, BYK, Gardner, 1992.

VisioPaint, *Paint Appearance Measurement System, User's manual*, Digital Surf Co, 1995.

Venkat Ramana, K. and Ramamoorthy, B., "Statistical methods to compare the texture features of machined surfaces", *Pattern Recognition*, Vol. 29, No. 9, pp1447-1459, 1996.

Whitehouse D. J., *Handbook of Surface Metrology*, Rank Taylor Hobson Ltd, 1994.

Zadeh L. A. *Fuzzy Logic Toolbox User's Guide*, The MathWorks, Inc. MA, 1999

Publications:

[1] H. Kang, C. Butler, Q. Yang, F. Sacerdotti, F. Benati, *Modeling of Paint Appearance Using Artificial Neural Network,* submitted to SPIE's International Symposium on Intelligent Systems for Advanced Manufacturing, Boston, Massachusetts, USA, November 2000.

[2] H. Kang, C. Butler, Q. Yang, F. Sacerdotti, F. Benati, *Appearance Measurement System Using Fuzzy Logic,* Proceedings of IEEE Instrumentation and Measurement Technology Conference, *IMTC '2000,* Baltimore, Maryland, USA, May, 2000.

[3] F. Benati, F. Sacerdotti, H. Kang, S. Gatti, *Development of a Hand-Held Burr Measurement System for Statistical Process Control of the Trimming Process,* Proceedings of IEEE Instrumentation and Measurement Technology Conference, *IMTC '2000,* Baltimore, Maryland, USA, May, 2000.

[4] H. Kang, Q. Yang, C. Butler, T. Xie, and F. Benati, *Optimization of Sensor Locations for Measurement of Flue Gas Flow in Industrial Ducts and Stacks Using Neural Networks,* IEEE Transactions on Instrumentation and Measurement, Vol. 49, No. 2, April 2000.

[5] F. Sacerdotti, B. Griffiths, F. Benati and H. Kang, *The variability of functional and amplitude three-dimensional roughness parameters for electron-beam and electro-discharged texture surfaces,* Measurement Science and Technology, Institute *of* **Physics**, vol. 11, No. 3, March 2000, pp171-177

[6] H. Kang, C. Butler, Q. Yang, F. Sacerdotti, F. Benati, *Visual Assessment of Paint Appearance on Car Body Surface,* Proceedings of X. International Colloquium on Surfaces, Chemnitz, Germany, January 2000.

[7] H. Kang, C. Butler and Q. Yang, *Evaluation of Metal Texture Effect on Paint Appearance,* SPIE's International Symposium on Intelligent Systems for Advanced Manufacturing, Boston, Massachusetts, USA, September 1999.

[8] H. Kang, C. Butler and Q. Yang, *Measurement of Paint Appearance Using Image Processing System,* Proceedings of IEEE International Workshop on Intelligent Signal Processing, Budapest, Hungary, September 1999.

[9] H. Kang, Q. Yang, C. Butler, T. Xie, and F. Benati, *Optimisation of Sensor Locations for Measurement of Flue Gas Flow in Industrial Ducts and Stacks Using Neural Networks,* Proceedings of the 16th IEEE Instrumentation and Measurement Technology Conference, IMTC 1999, Vol. 1, pp. 81-85.

[10] T. Xie, Q. Yang, B.E. Jones, H. Kang, and C. Butler, *Effects of the Size of the Measured Surface on the Performance of an Air Cone-Jet Sensor for In-Process Inspection,* Proceedings of the 16th IEEE Instrumentation and Measurement Technology Conference, IMTC 1999, Vol. 1, pp. 1358-1361.

[11] H. Kang, Q. Yang, and C. Butler, *Modeling and Measurement Accuracy Enhancement of Flue Gas Flow Using Neural Networks,* IEEE Transactions on Instrumentation and Measurement, Vol. 47, No. 5, October 1998, pp1379-1384.

[12] H. Kang, Q. Yang, C. Butler and J. Chen, *New Survivability Measure of Military Communication,* Proceedings of IEEE Military Communications Conference MILCOM 1998, Vol.1, pp 71-75.

[13] H. Kang, Q. Yang, and C. Butler, *Modeling and Measurement Accuracy Enhancement of Flue Gas Flow Using Neural Networks,* Proceedings of IEEE Instrumentation and Measurement Technology Conference, IMTC 1998, Vol. 2, pp. 930-934.

ANNEX Textural Features [Haralick, 1973]

Notation: $p(i,j) = \frac{P(i,j)}{R}$ is the *(i,j)*th entry in a normalised Grey-tone spatial-dependence matrix.

N_g is the number distinct grey levels in the quantified image.

$p_x(i) = \sum_{j=1}^{N_g} p(i,j)$ is the *i*th entry in the marginal-probability matrix obtained by summing the rows of *p(i,j)*.

$$p_y(j) = \sum_{i=1}^{N_g} p(i,j)$$

$$p_{x+y}(k) = \sum_{i=1}^{N_g} \sum_{\substack{j=1 \\ i+j=k}}^{N_g} p(i,j), \quad k=2, 3, \ldots, 2N_g.$$

$$p_{x-y}(k) = \sum_{i=1}^{N_g} \sum_{\substack{j=1 \\ |i-j|=k}}^{N_g} p(i,j), \quad k=0, 1, \ldots, 2N_g-1$$

Texture Features:

1) Angular Second Moment:

$$f_1 = \sum_{i=1}^{N_g} \sum_{j=1}^{N_g} \{p(i,j)\}^2$$

2) *Contrast:*

$$f_2 = \sum_{n=0}^{N_g-1} n^2 \left\{ \sum_{\substack{i=1 \\ |i-j|=n}}^{N_g} \sum_{j=1}^{N_g} p(i,j) \right\}$$

3) *Correlation:*

$$f_3 = \frac{\sum_{i=1}^{N_g} \sum_{j=1}^{N_g} (ij) p(i,j) - \mu_x \mu_y}{\sigma_x \sigma_y}$$

where μ_x, μ_y, σ_x, and σ_y are the means and standard deviations of p_x and p_y.

4) *Sum of Squares: Variance*

$$f_4 = \sum_{i=1}^{N_g} \sum_{j=1}^{N_g} (i-\mu)^2 p(i,j)$$

5) *Inverse Difference Moment:*

$$f_5 = \sum_{i=1}^{N_g} \sum_{j=1}^{N_g} \frac{1}{1+(i-j)^2} p(i,j)$$

6) *Sum Average*

$$f_6 = \sum_{i=2}^{2N_g} i\, p_{x+y}(i)$$

7) Sum Variance:

$$f_7 = \sum_{i=2}^{2N_g} (i - f_8)^2 p_{x+y}(i)$$

8) Sum Entropy:

$$f_8 = -\sum_{i=2}^{2N_g} p_{x+y}(i) \log\{p_{x+y}(i)\}$$

9) Entropy

$$f_9 = -\sum_{i=1}^{N_g} \sum_{j=1}^{N_g} p(i,j) \log(p_{x+y}(i,j))$$

10) Difference Variance:

$$f_{10} = \text{var}\,iance\,of\ p_{x+y}$$

11) Difference Entropy:

$$f_{11} = -\sum_{i=0}^{N_g-1} p_{x-y}(i) \log\{p_{x-y}(i)\}$$

12), 13) Information Measures of Correlation:

$$f_{12} = \frac{HXY - HXY1}{\max\{HX, HY\}}$$

$$f_{13} = (1 - \exp[-2.0(HXY2 - HXY)])^{\frac{1}{2}}$$

$$HXY = -\sum_{i=1}^{N_g}\sum_{j=1}^{N_g} p(i,j)\log(p(i,j))$$

where HX and HY are entropies of p_x and p_y, and

$$HXY1 = -\sum_{i=1}^{N_g}\sum_{j=1}^{N_g} p(i,j)\log\{p_x(i)p_y(j)\}$$

$$HXY2 = -\sum_{i=1}^{N_g}\sum_{j=1}^{N_g} p_s(i)p_y(j)\log\{p_x(i)p_y(j)\}$$

14) Maximal correlation Coefficient:

$$f_{14} = (Second\ largest\ eigenvalue\ of\ Q)^{\frac{1}{2}}$$

$$where \quad Q(i,j) = \sum_{k=1}^{N_g} \frac{p(i,k)p(j,k)}{p_x(i)p_y(k)}$$